Lecture 18

DTI Applications

DTI in Cerebral Neoplasm

Deviated

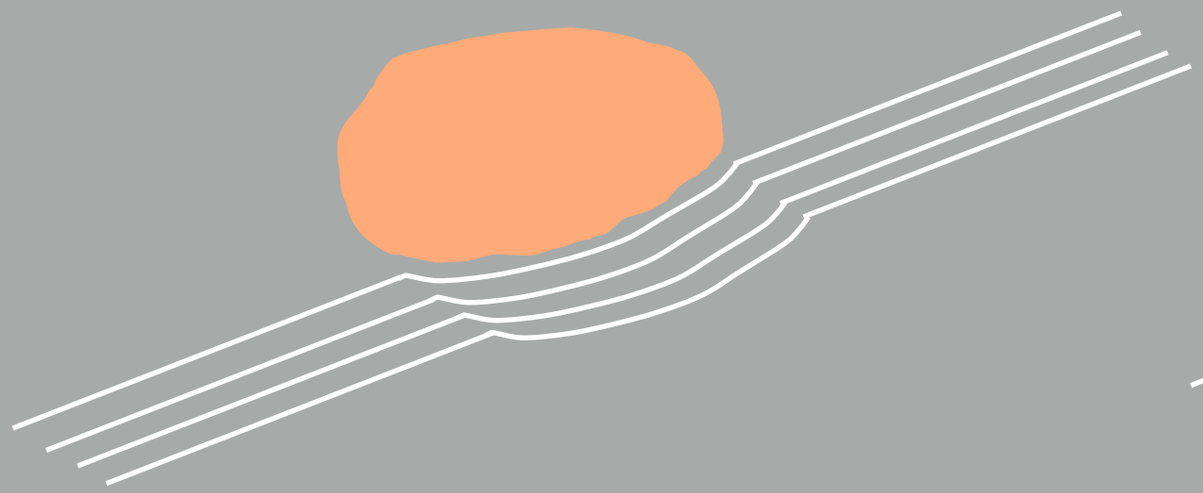

Infiltrated

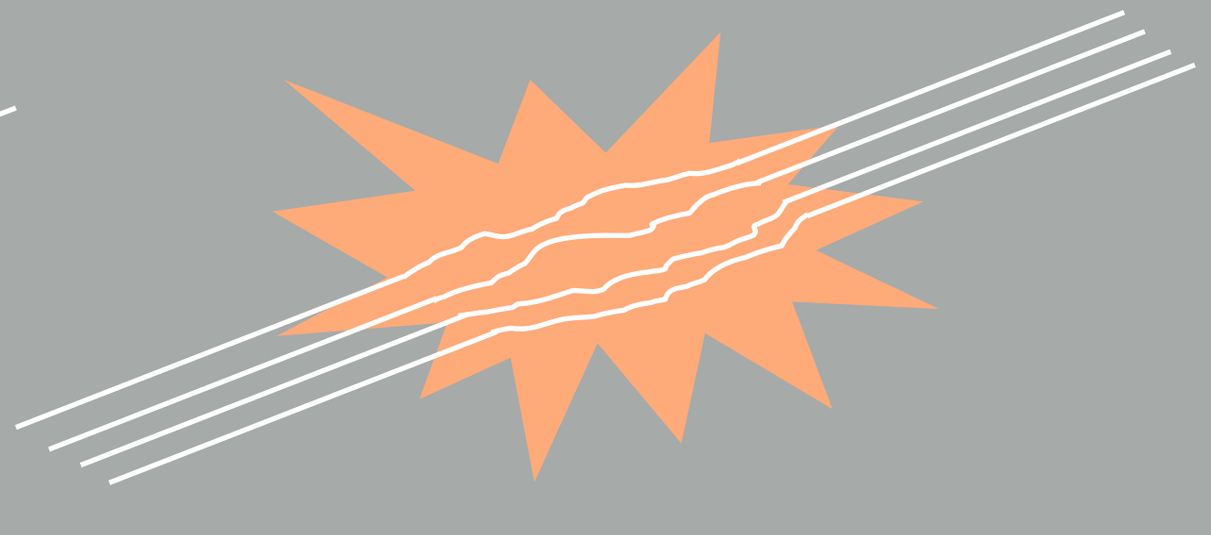

Edema

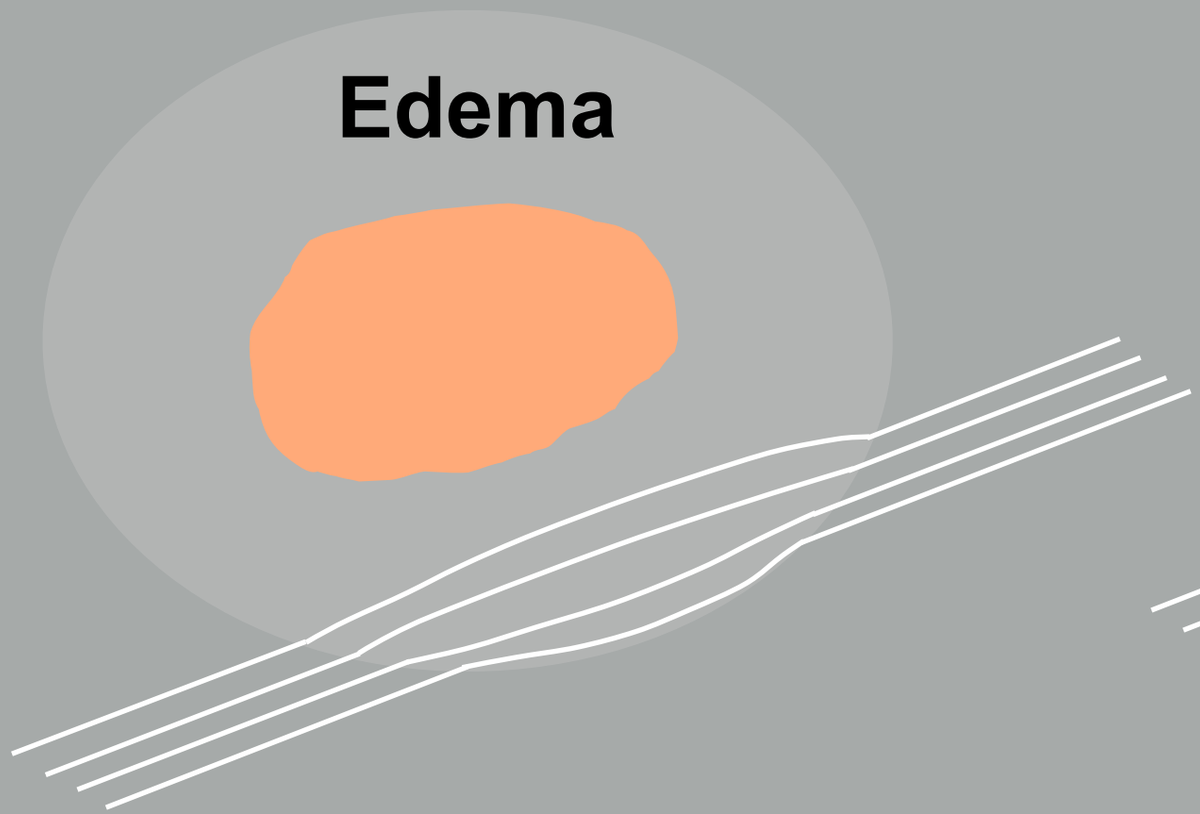

Destroyed

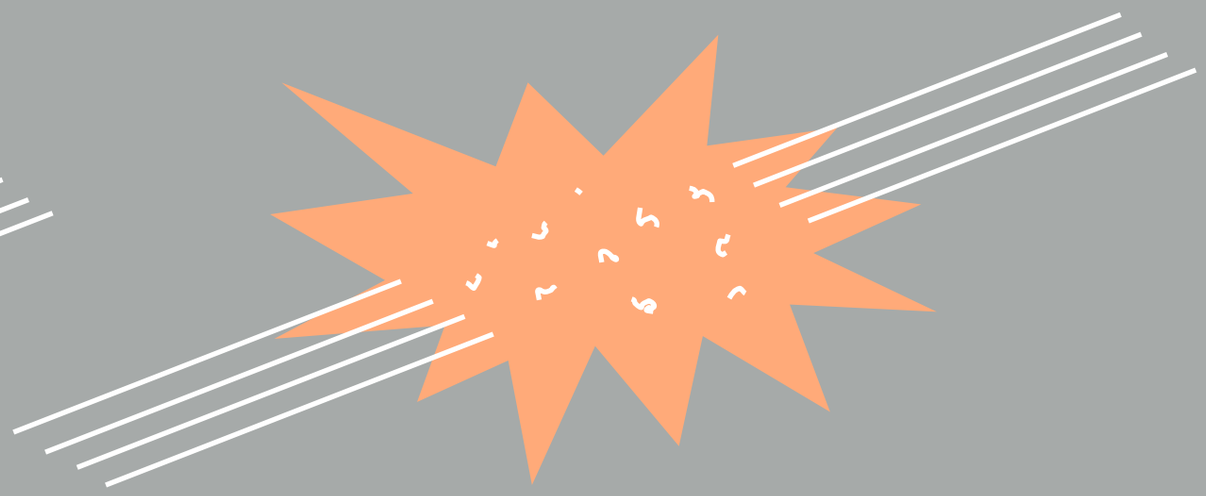

Pattern 1: Shift

Anisotropy: ~ Normal

Location / Organization: Abnormal

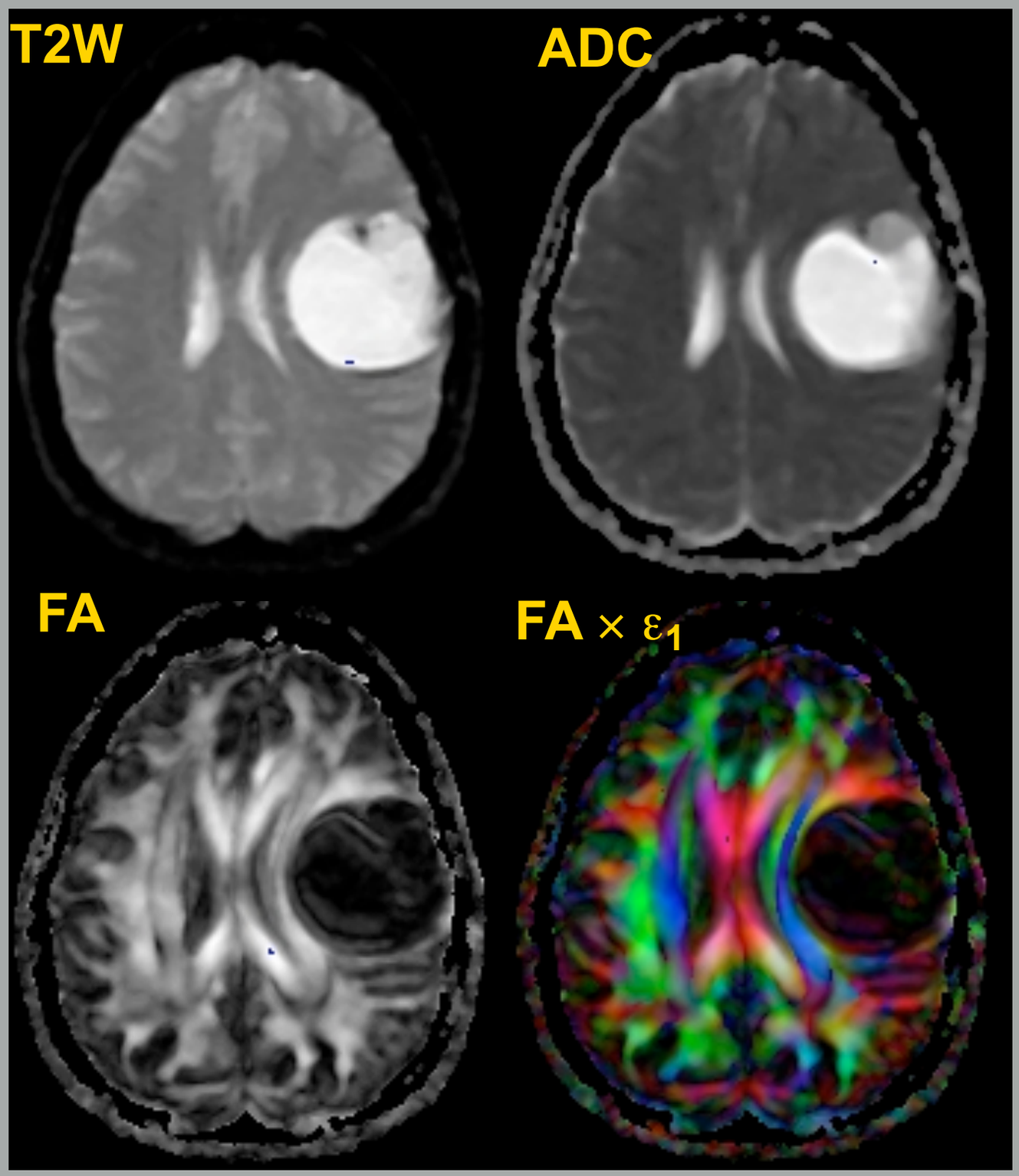

A.S. Field

Pattern 2: Edema

Anisotropy:

Decreased

Location / Organization:

Normal

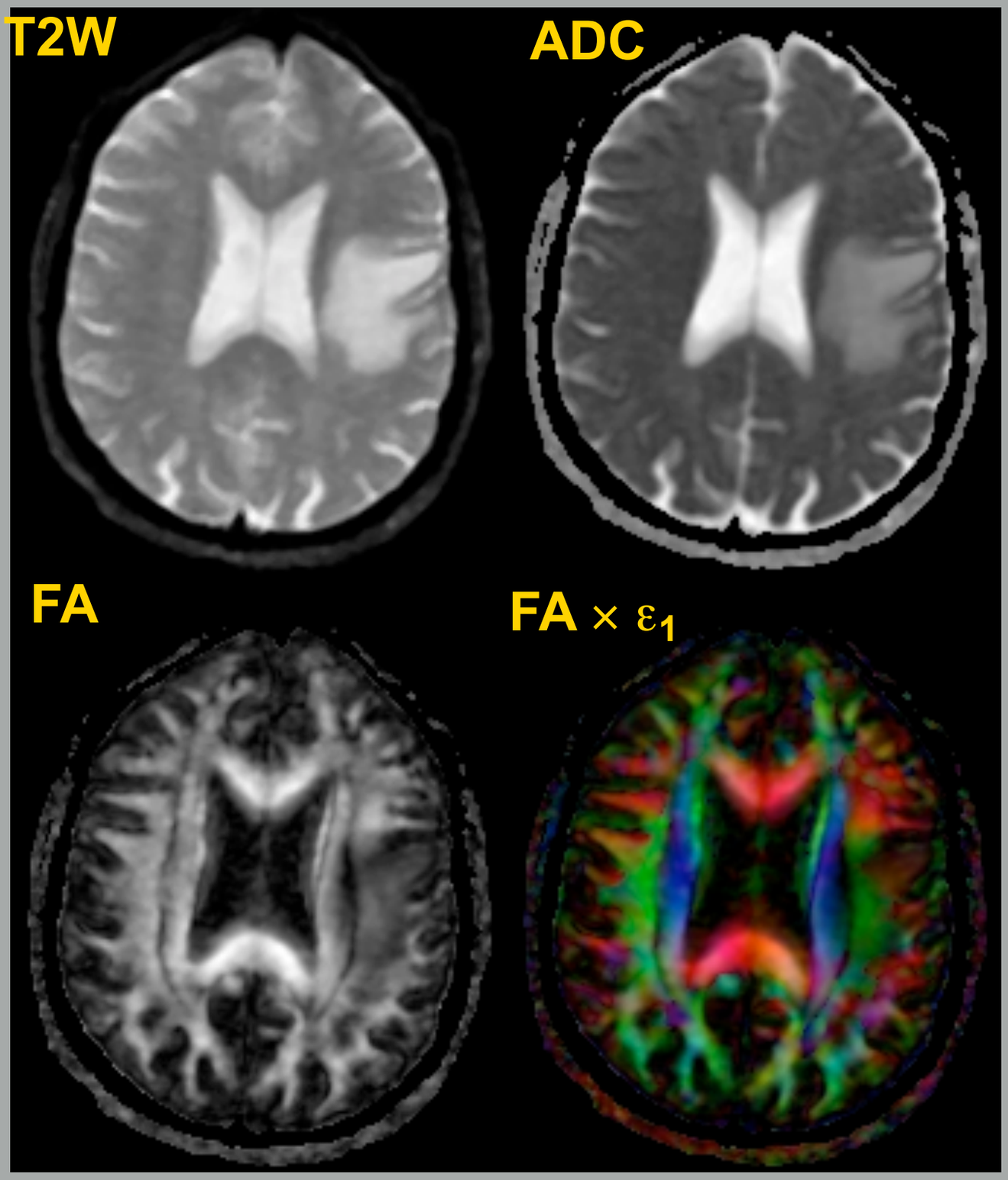

A.S. Field

Pattern 3: Invasion

Anisotropy:

Decreased

Location / Organization:

Abnormal

A.S. Field

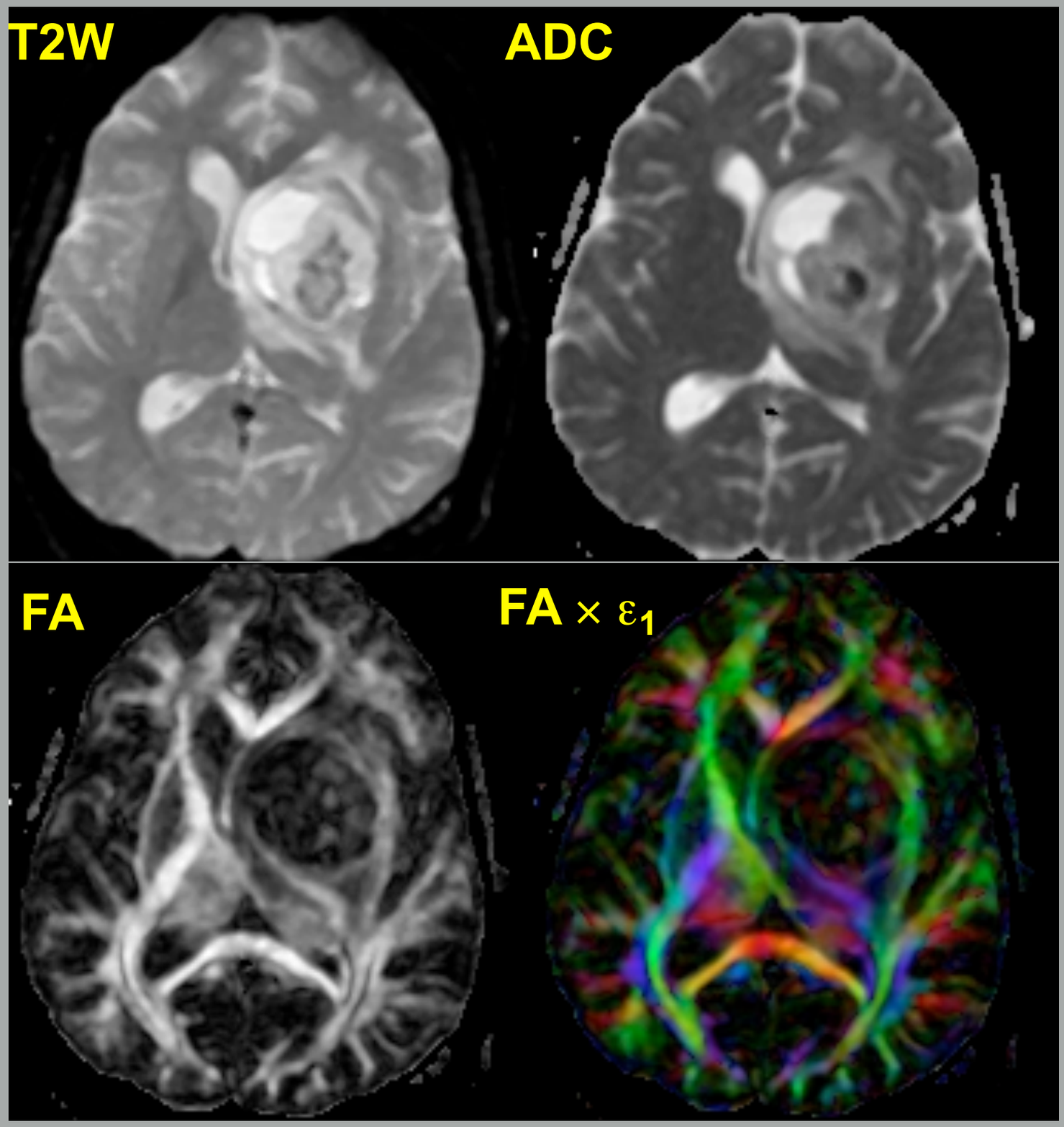

Pattern 4: Destruction

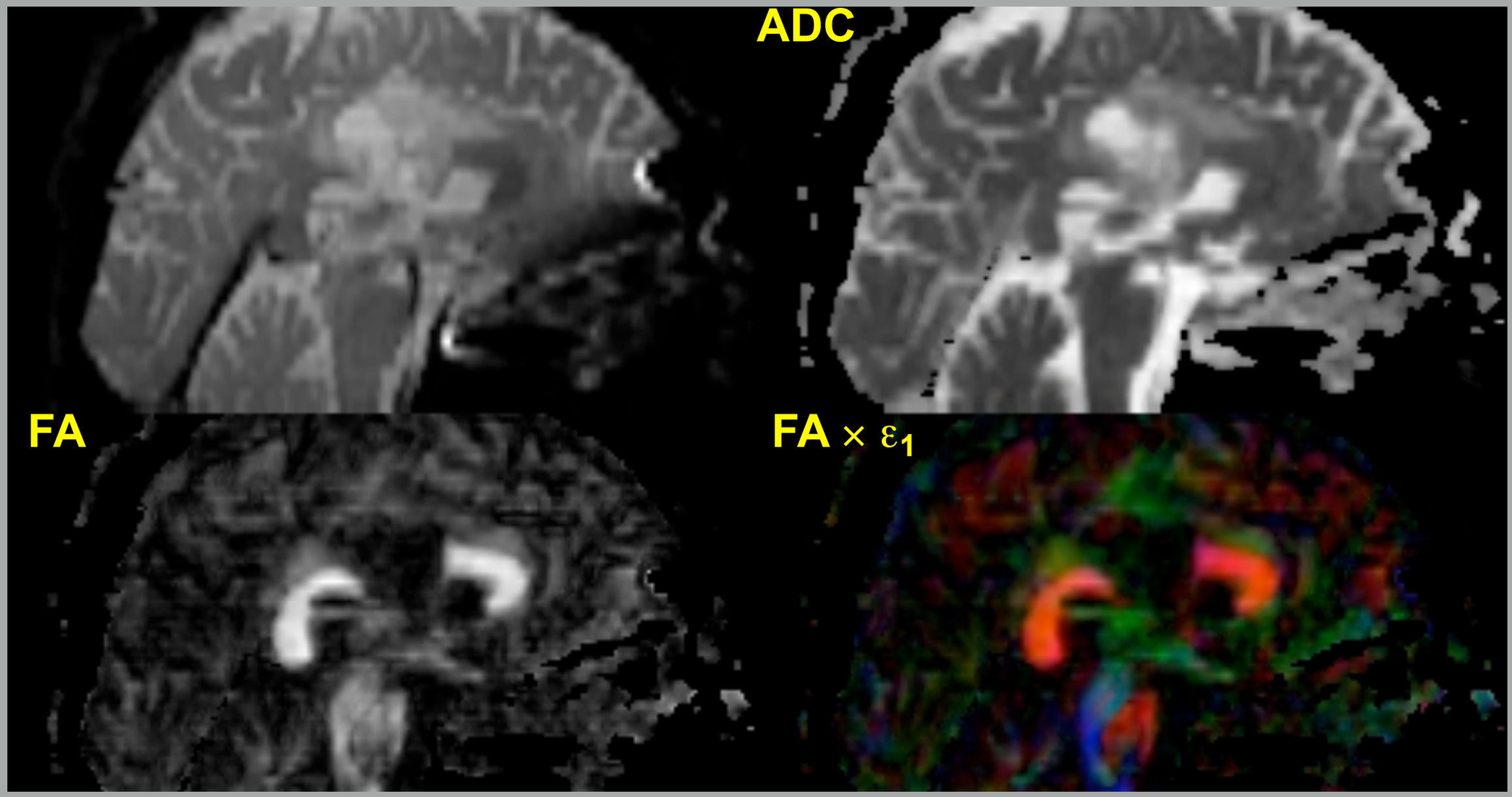

Anisotropy: ~ 0

Location / Organization: ??

A.S. Field

Pilocytic Astrocytoma

Preop

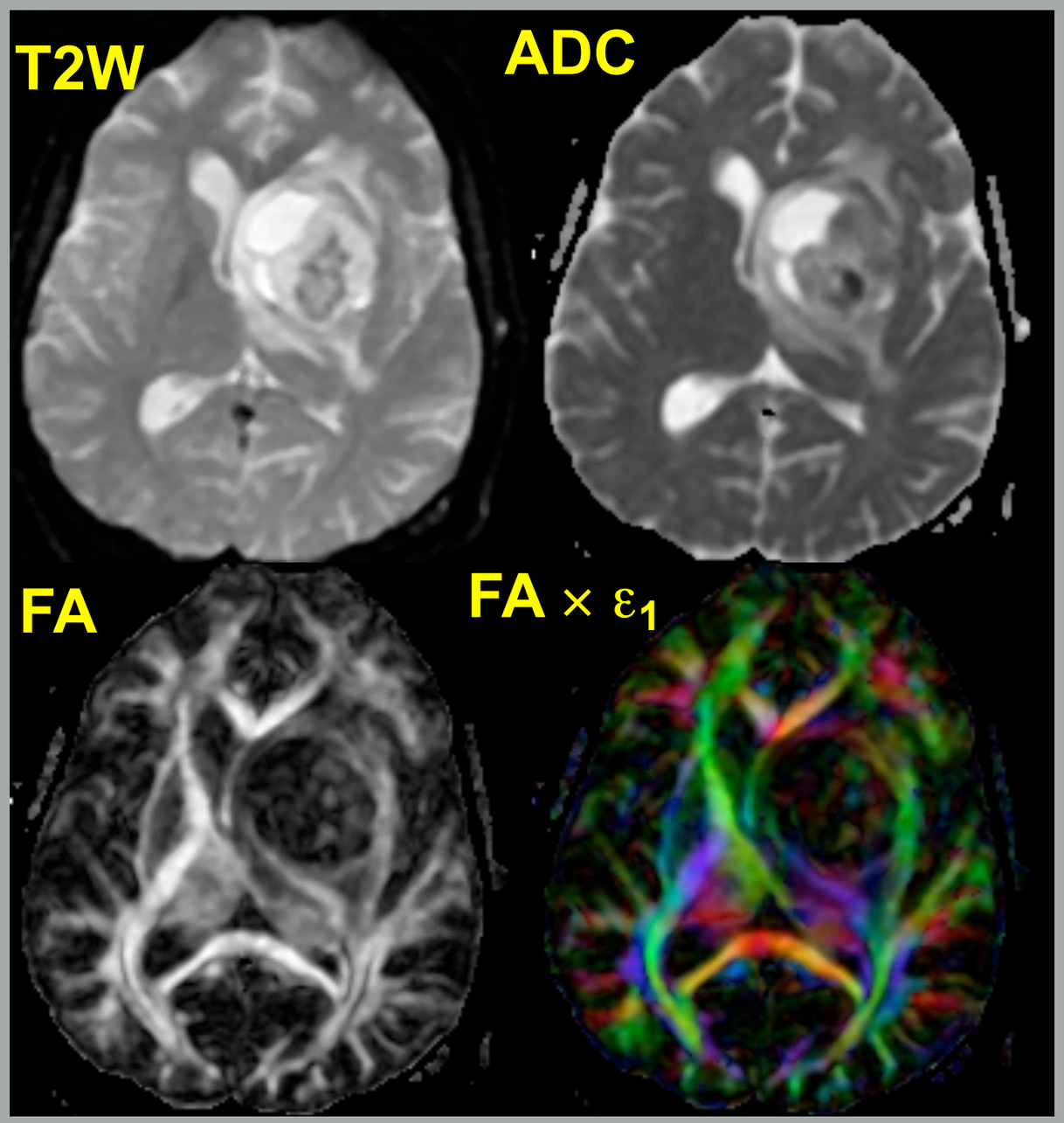

Postop

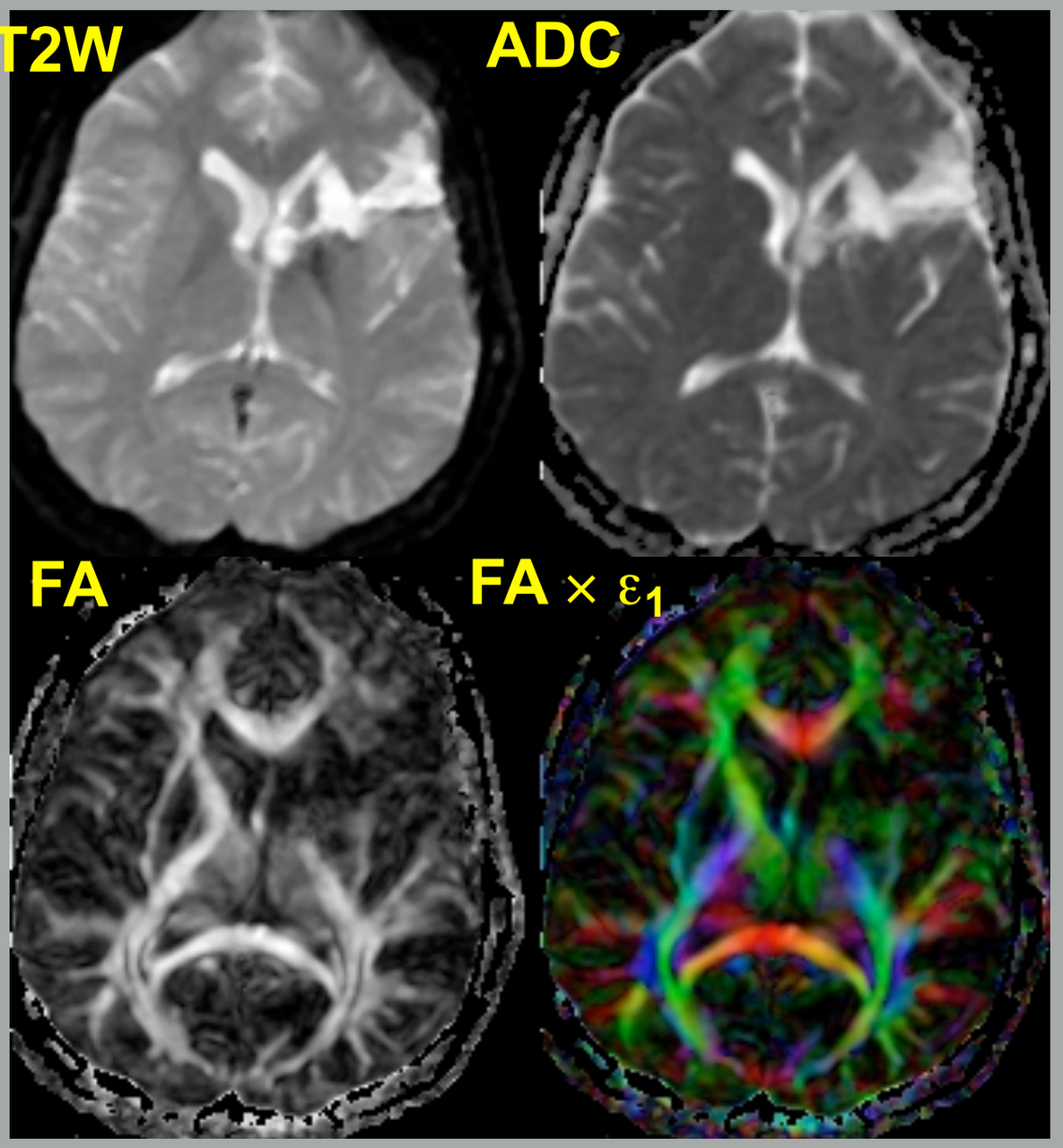

A.S. Field

DTI in Autism

White Matter Structure in Autism: Preliminary Evidence from Diffusion Tensor Imaging

Naama Barnea-Goraly, Hower Kwon, Vinod Menon, Stephan Eliez, Linda Lotspeich, and Allan L. Reiss

BIOL PSYCHIATRY 2004;55:323–326

DTI in Autism

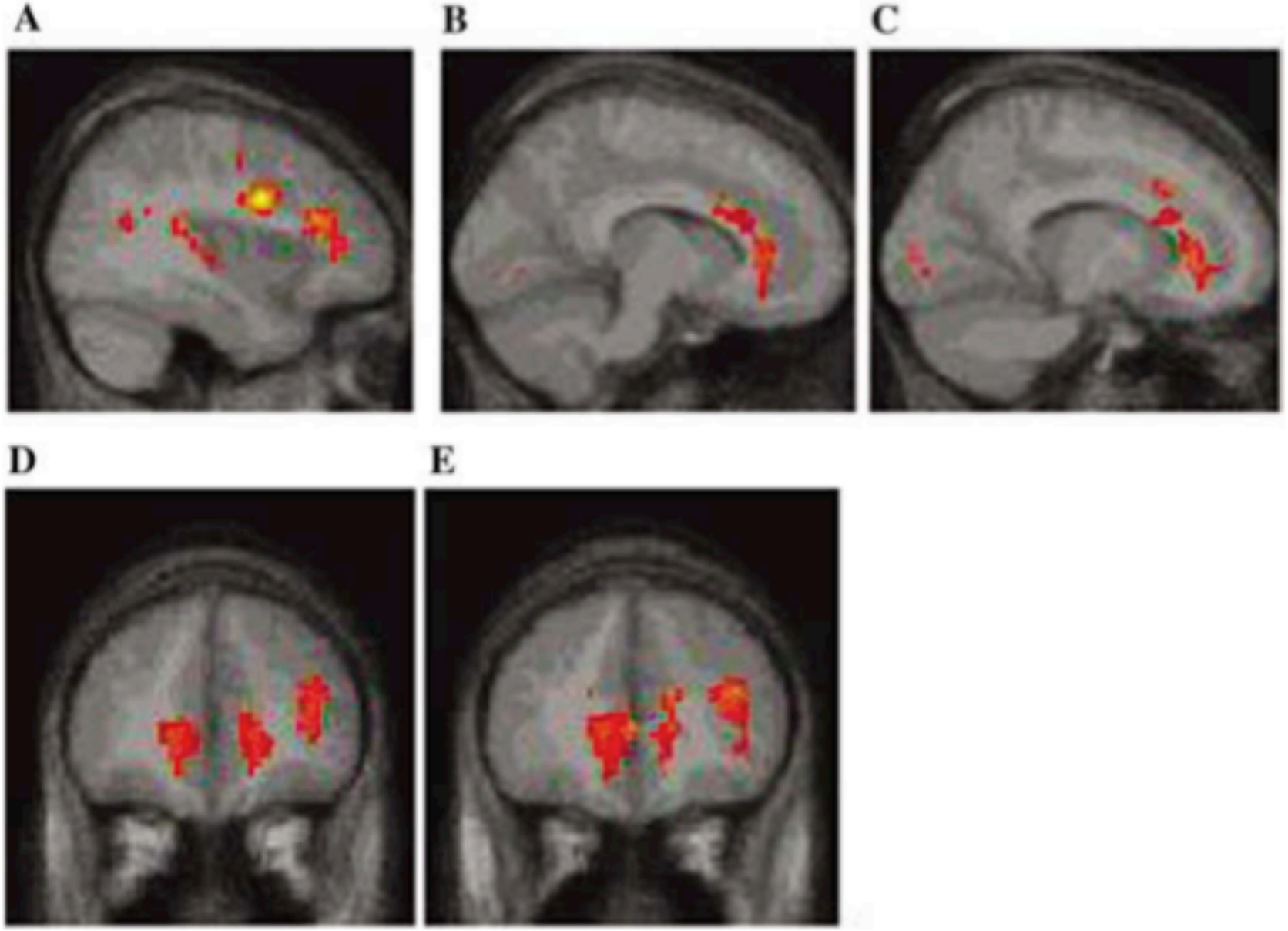

Regions of significant reduction in WM FA

DTI in Autism

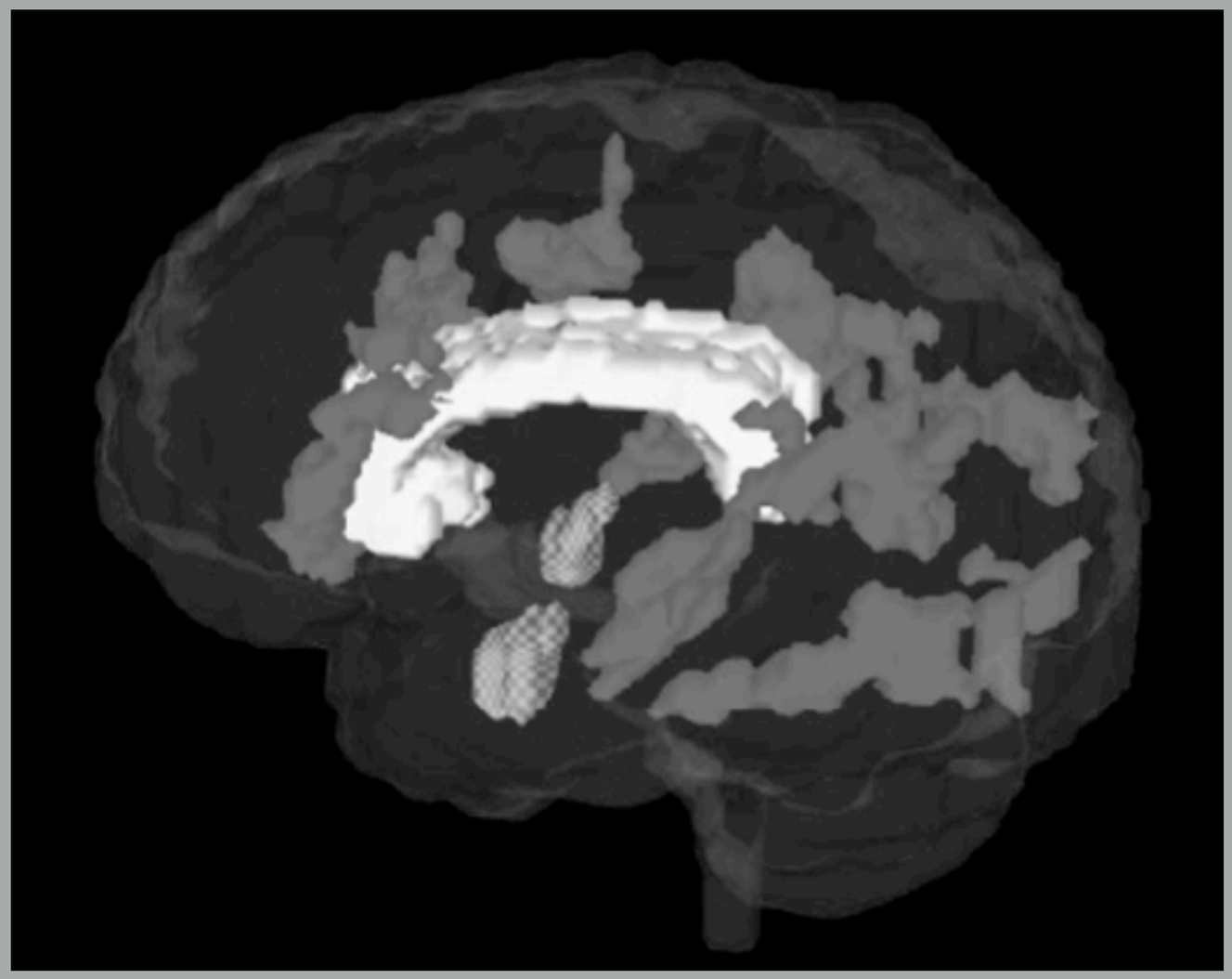

Figure 2. A three-dimensional representation of the aberrant white matter (dark gray) in relation to the corpus callosum (white), and the amygdala (checkered gray).

DTI in Alcoholism

ELSEVIER

EJR
EUROPEAN JOURNAL OF RADIOLOGY

European Journal of Radiology 45 (2003) 244–255

www.elsevier.com/locate/ejrad

Diffusion tensor imaging in normal aging and neuropsychiatric disorders

Edith V. Sullivan [a], Adolf Pfefferbaum [a,b,*]

[a] *Department of Psychiatry and Behavioral Sciences, Stanford University School of Medicine, Stanford, CA 94305, USA*
[b] *Neuroscience Program, SRI International, Center for Health Sciences (BN 168), 333 Ravenswood Avenue, Menlo Park, CA 94025, USA*

Received 9 October 2002; received in revised form 10 October 2002; accepted 11 October 2002

DTI in Alcoholism

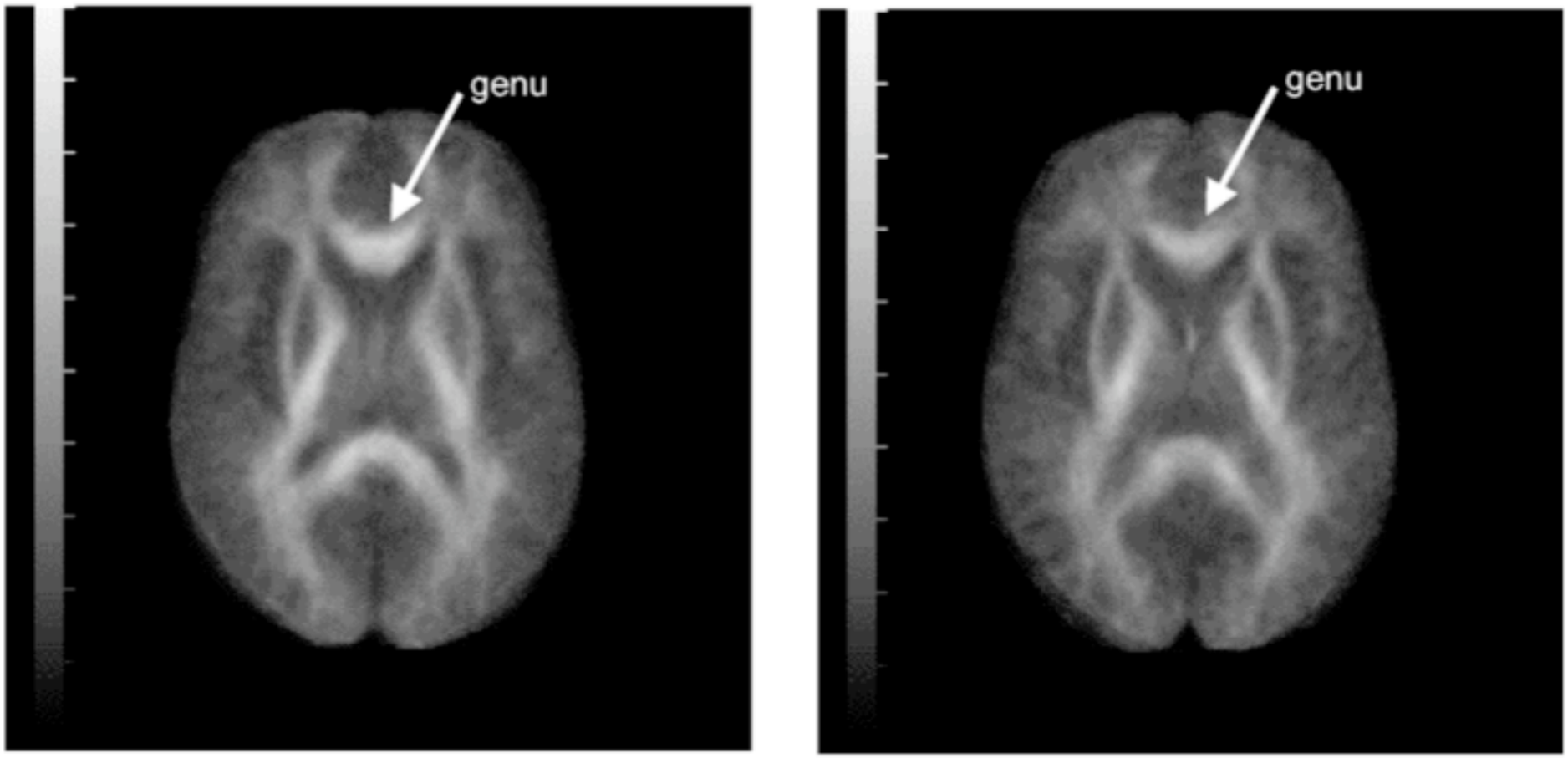

Fig. 2. Across-subject average FA maps of 10 healthy control men and 14 alcoholic men. The gray scale bar indicates the FA levels, which are generally lower in the alcoholic than control average.

DTI in Alcoholism

Neuropsychopharmacology (2005) 30, 423–432

www.neuropsychopharmacology.org

Disruption of Brain White Matter Microstructure by Excessive Intracellular and Extracellular Fluid in Alcoholism: Evidence from Diffusion Tensor Imaging

Adolf Pfefferbaum*[,1,2] and Edith V Sullivan[2]

[1]Neuroscience Program, SRI International, Stanford University School of Medicine, USA; [2]Department of Psychiatry and Behavioral Sciences, Stanford University School of Medicine, USA

DTI in Alcoholism

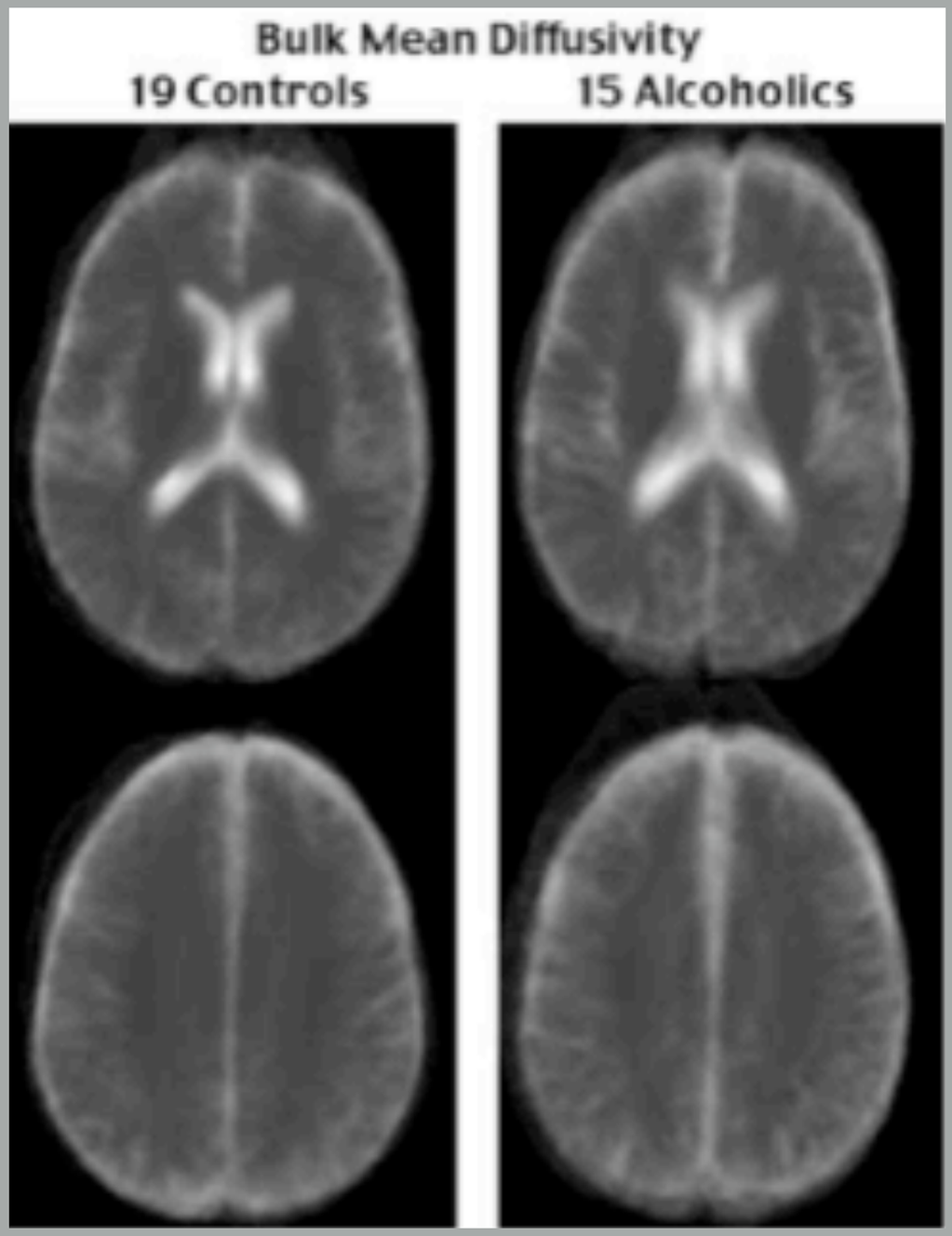

DTI in Alcoholism

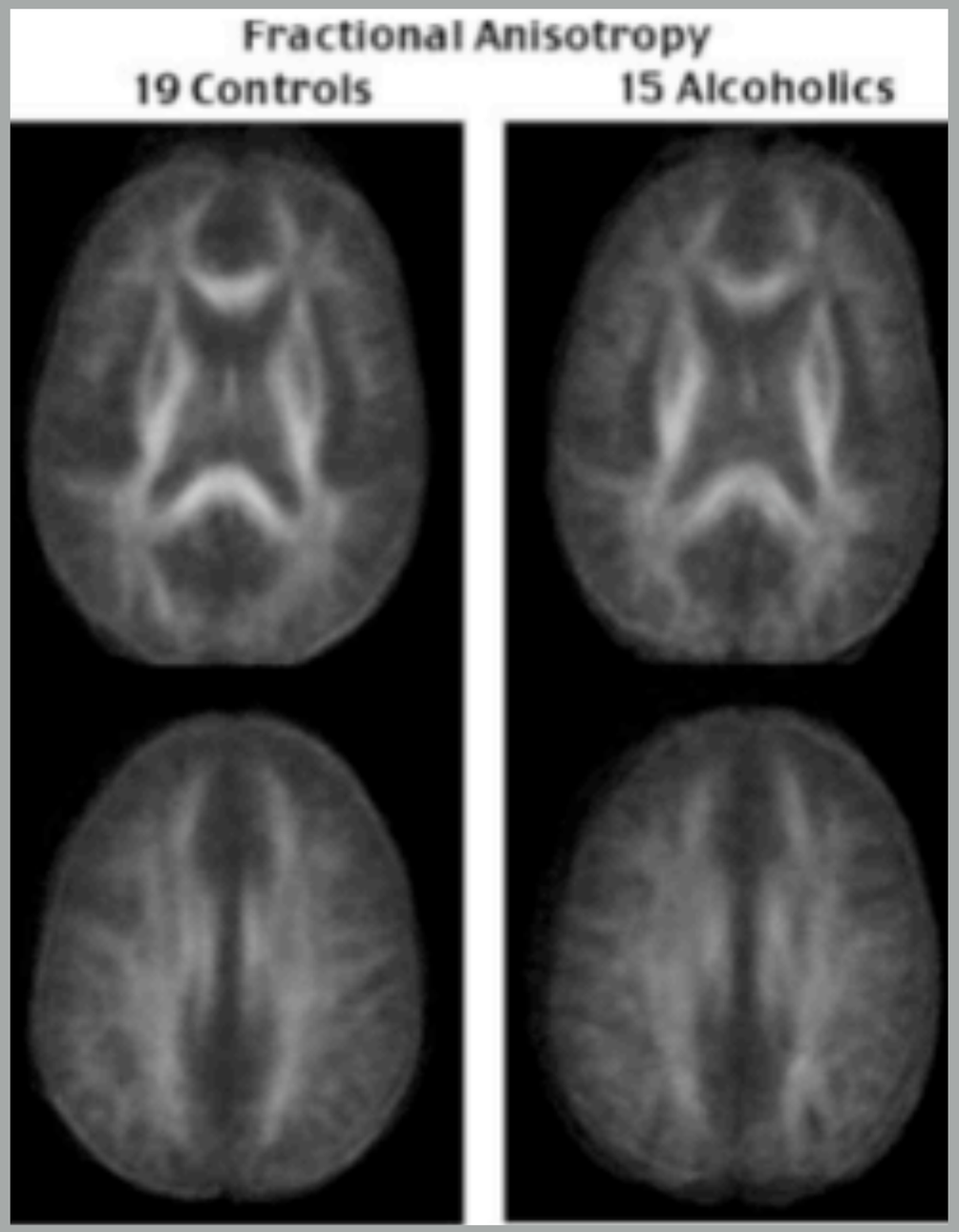

DTI in Alcoholism

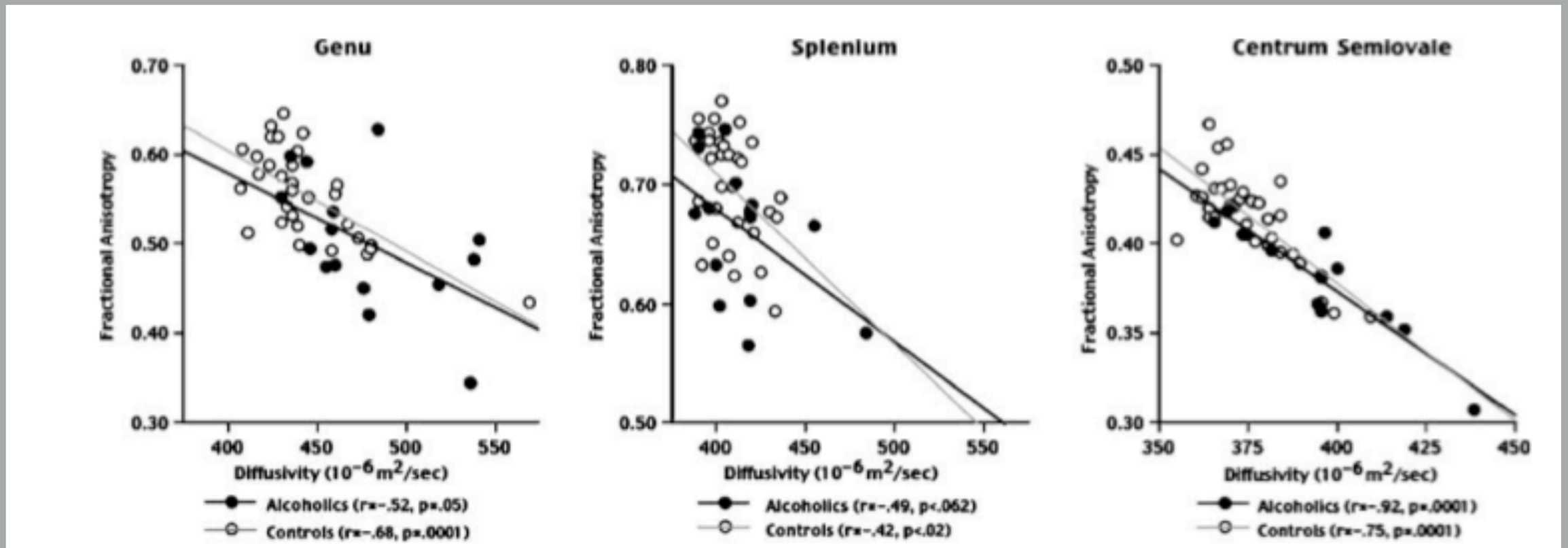

Figure 4 Lower FA and higher mean diffusivity were related to each other in controls and alcoholics.

DTI in Alcoholism

FA in binge drinkers

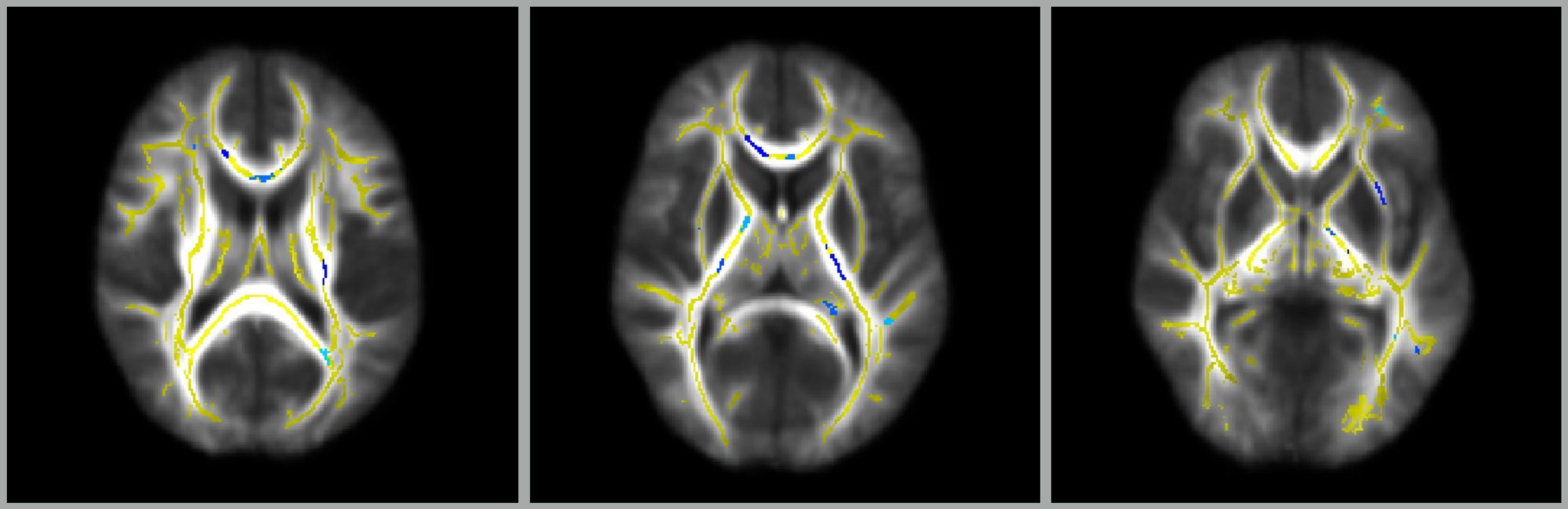

Binge drinkers lower than controls

McQueeny, et. al.

DTI in Marijuana Use

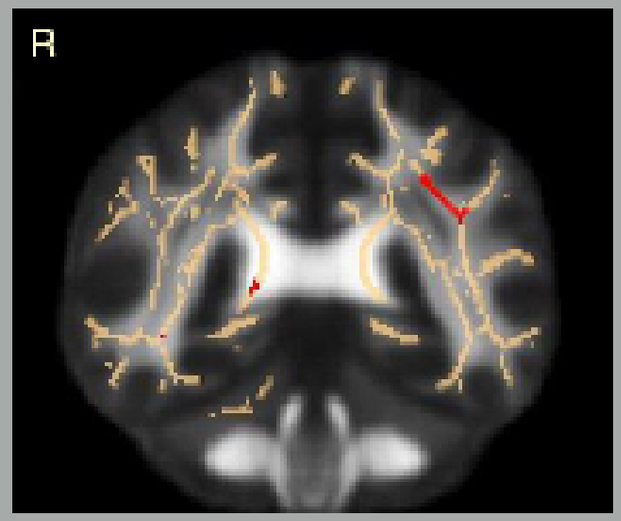

MJ<C
Left SLF
d=.08, 212 µl

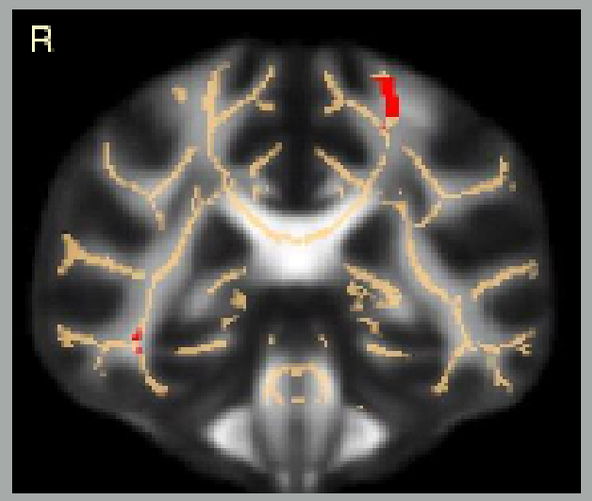

MJ<C
Left post-central
d=.9, 109 µl

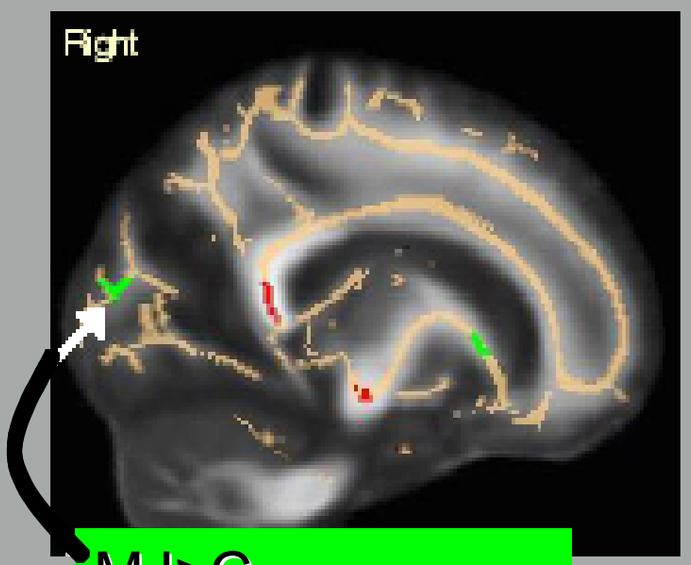

MJ>C
Left occipital
d=1.0, 95 µl

FA different in MJ users

Bava, et. al., *in preparation*

DTI in Aging

ELSEVIER

European Journal of Radiology 45 (2003) 244–255

EJR
EUROPEAN JOURNAL OF RADIOLOGY

www.elsevier.com/locate/ejrad

Diffusion tensor imaging in normal aging and neuropsychiatric disorders

Edith V. Sullivan [a], Adolf Pfefferbaum [a,b,*]

[a] *Department of Psychiatry and Behavioral Sciences, Stanford University School of Medicine, Stanford, CA 94305, USA*
[b] *Neuroscience Program, SRI International, Center for Health Sciences (BN 168), 333 Ravenswood Avenue, Menlo Park, CA 94025, USA*

Received 9 October 2002; received in revised form 10 October 2002; accepted 11 October 2002

DTI in Aging

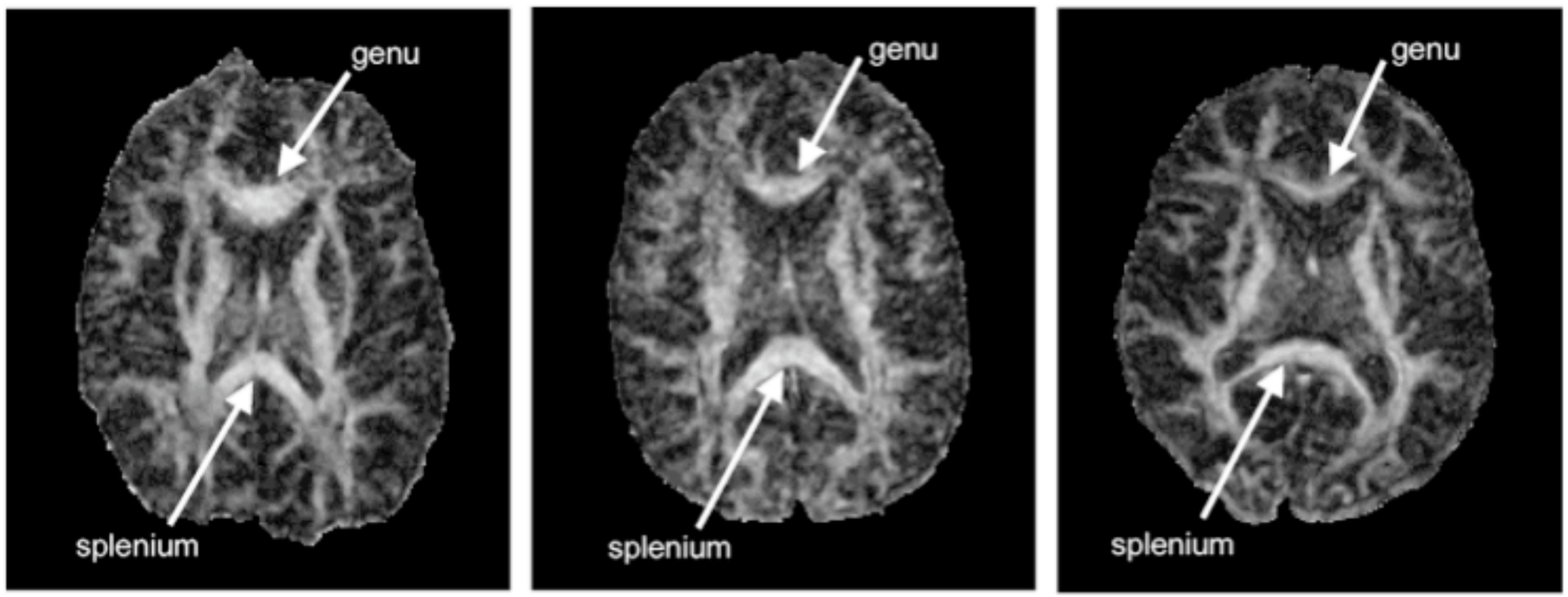

23 years old
genu FA = .633

45 years old
genu FA = .521

79 years old
genu FA = .466

DTI in Aging

ELSEVIER

Available online at www.sciencedirect.com

ScienceDirect

Neuroscience and Biobehavioral Reviews 30 (2006) 749–761

NEUROSCIENCE AND BIOBEHAVIORAL REVIEWS

www.elsevier.com/locate/neubiorev

Review

Diffusion tensor imaging and aging

Edith V. Sullivan[a,*], Adolf Pfefferbaum[a,b]

[a]*Department of Psychiatry and Behavioral Sciences, Stanford University School of Medicine, 401 Quarry Road, Stanford, CA 94305, USA*
[b]*Neuroscience Program, SRI International, Menlo Park, CA, USA*

DTI in Aging

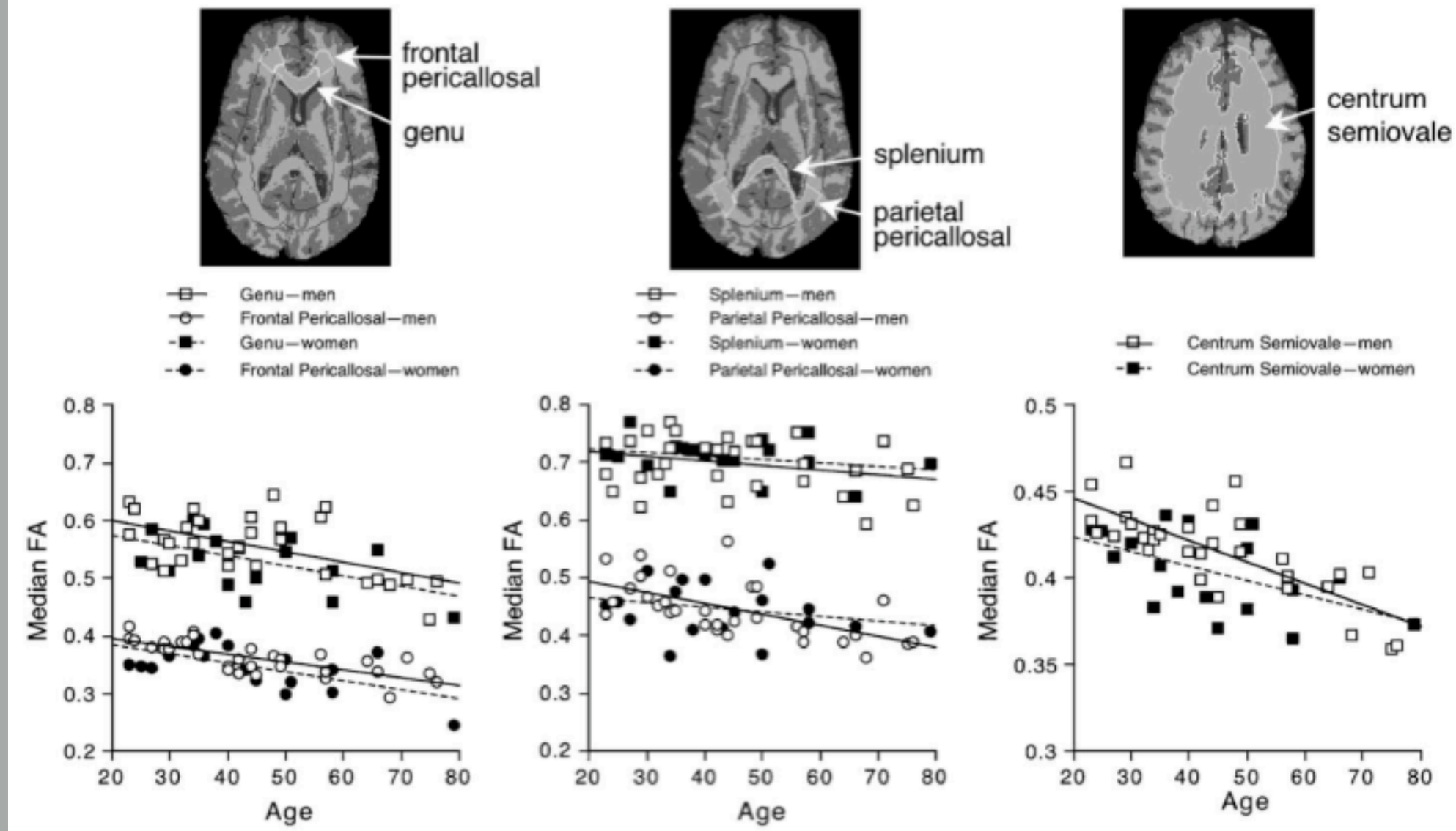

Fig. 2. Healthy men and women showed equivalent and significant decreases in FA with advancing age, which was greater in the genu than the splenium and greatest in the centrum semiovale. Modified from (Sullivan et al., 2001b).

DTI in Aging

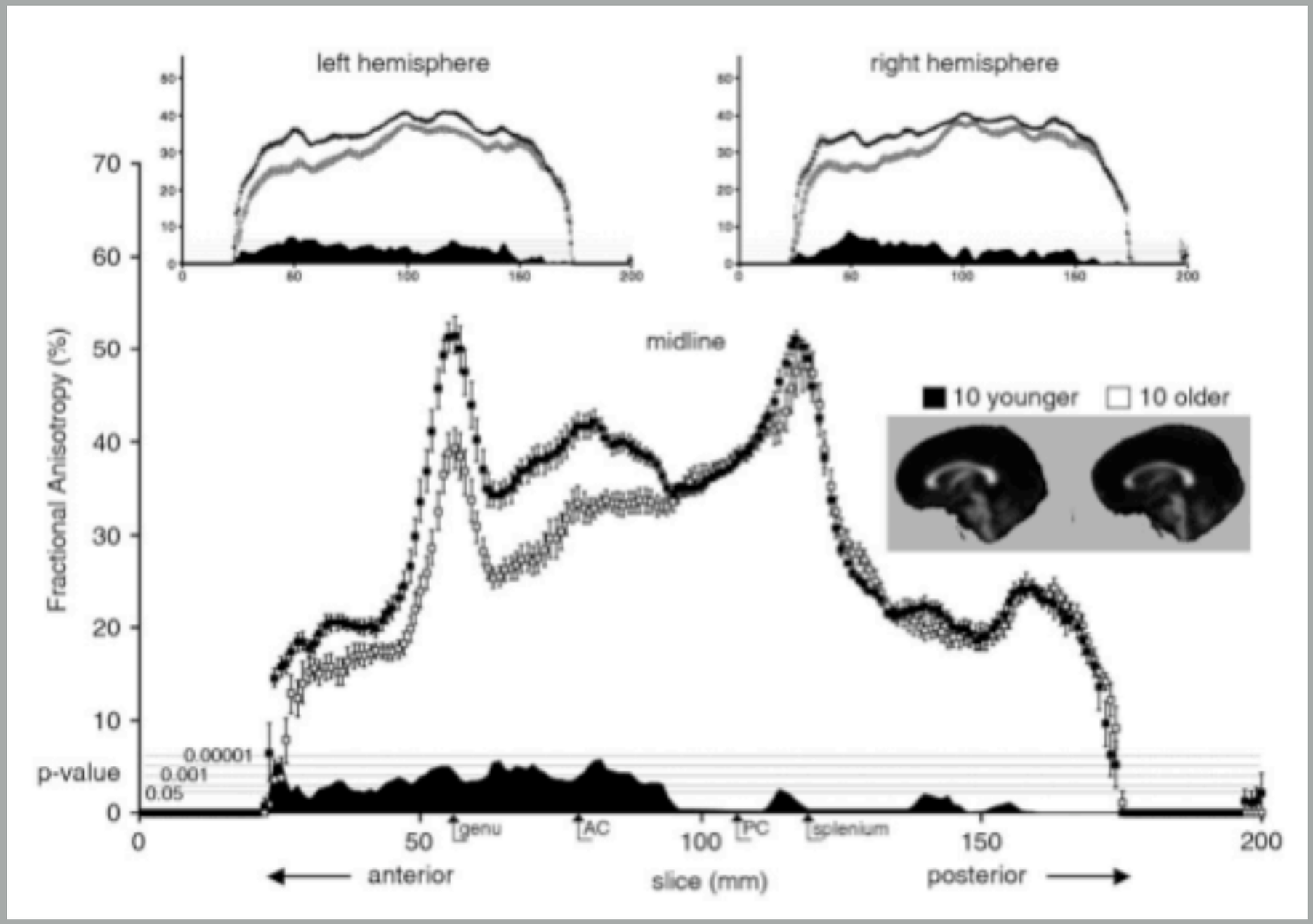
left hemisphere
right hemisphere
midline
10 younger
10 older
Fractional Anisotropy (%)
p-value
0.00001
0.001
0.05
genu
AC
PC
splenium
anterior
slice (mm)
posterior

DTI in Aging

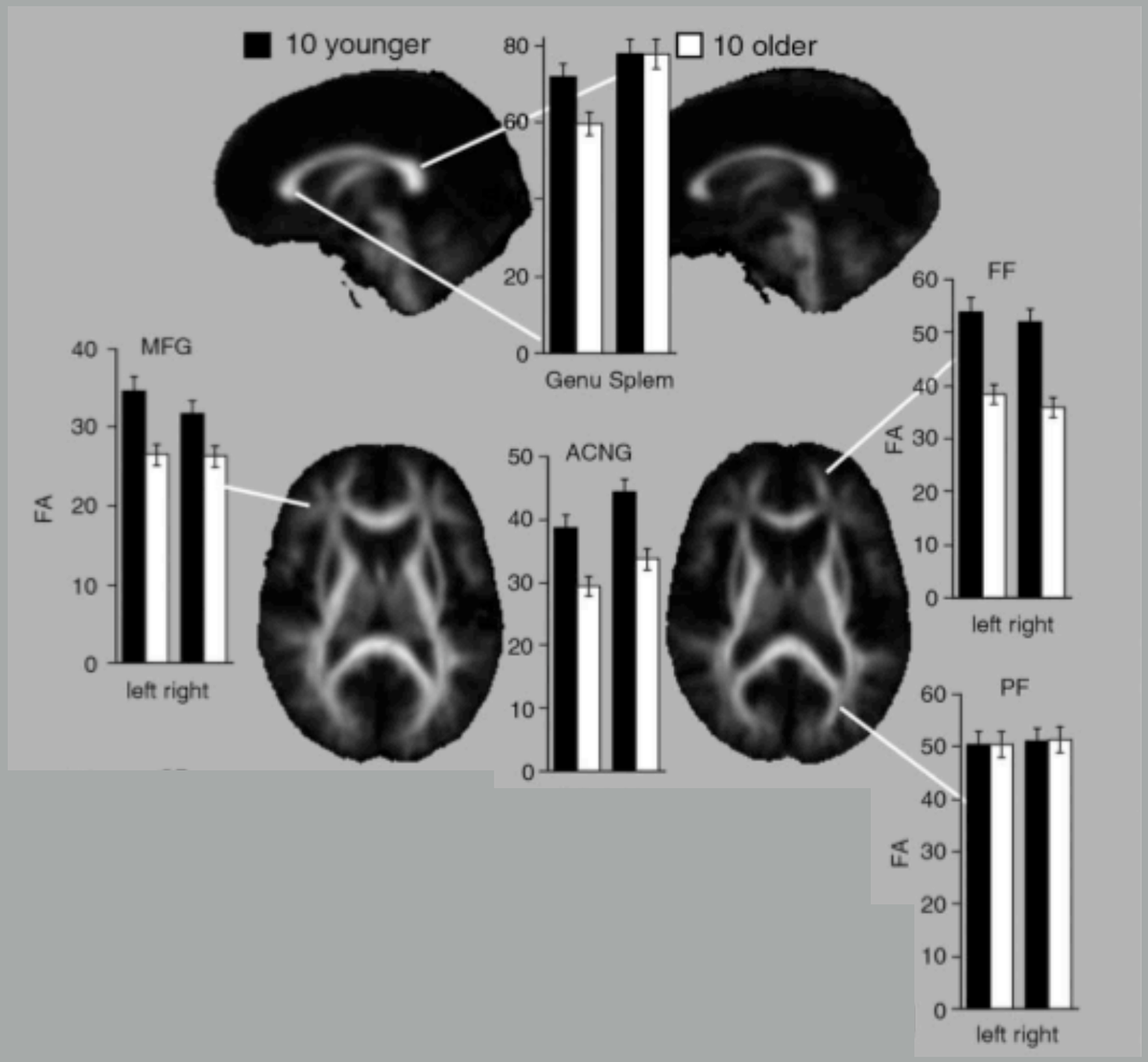

DTI and Connectivity

Large-scale model of mammalian thalamocortical systems

Eugene M. Izhikevich and Gerald M. Edelman*

The Neurosciences Institute, 10640 John Jay Hopkins Drive, San Diego, CA 92121

PNAS | **March 4, 2008** | vol. 105 | no. 9 | **3593–3598**

DTI and Connectivity

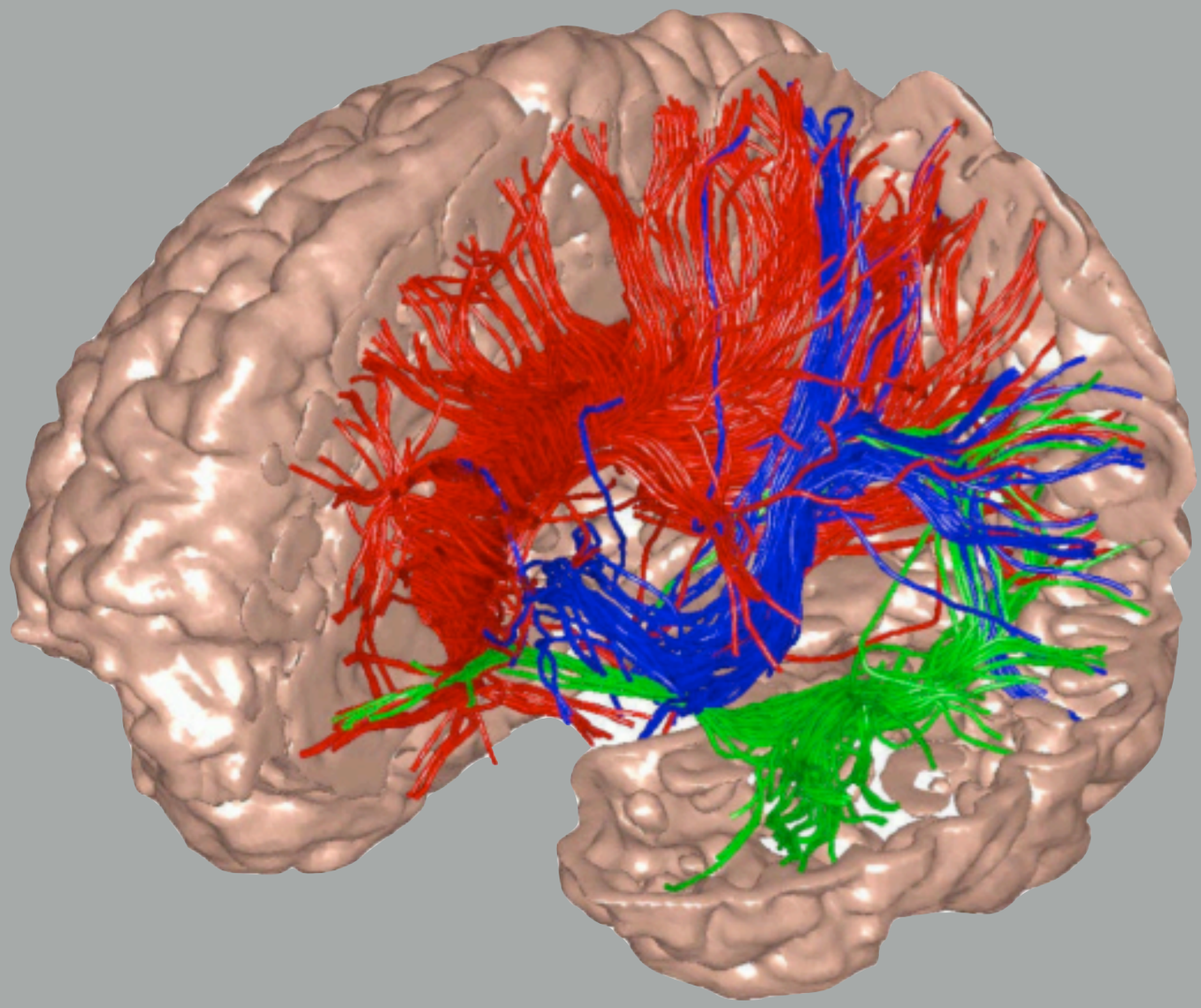

DTI and Connectivity

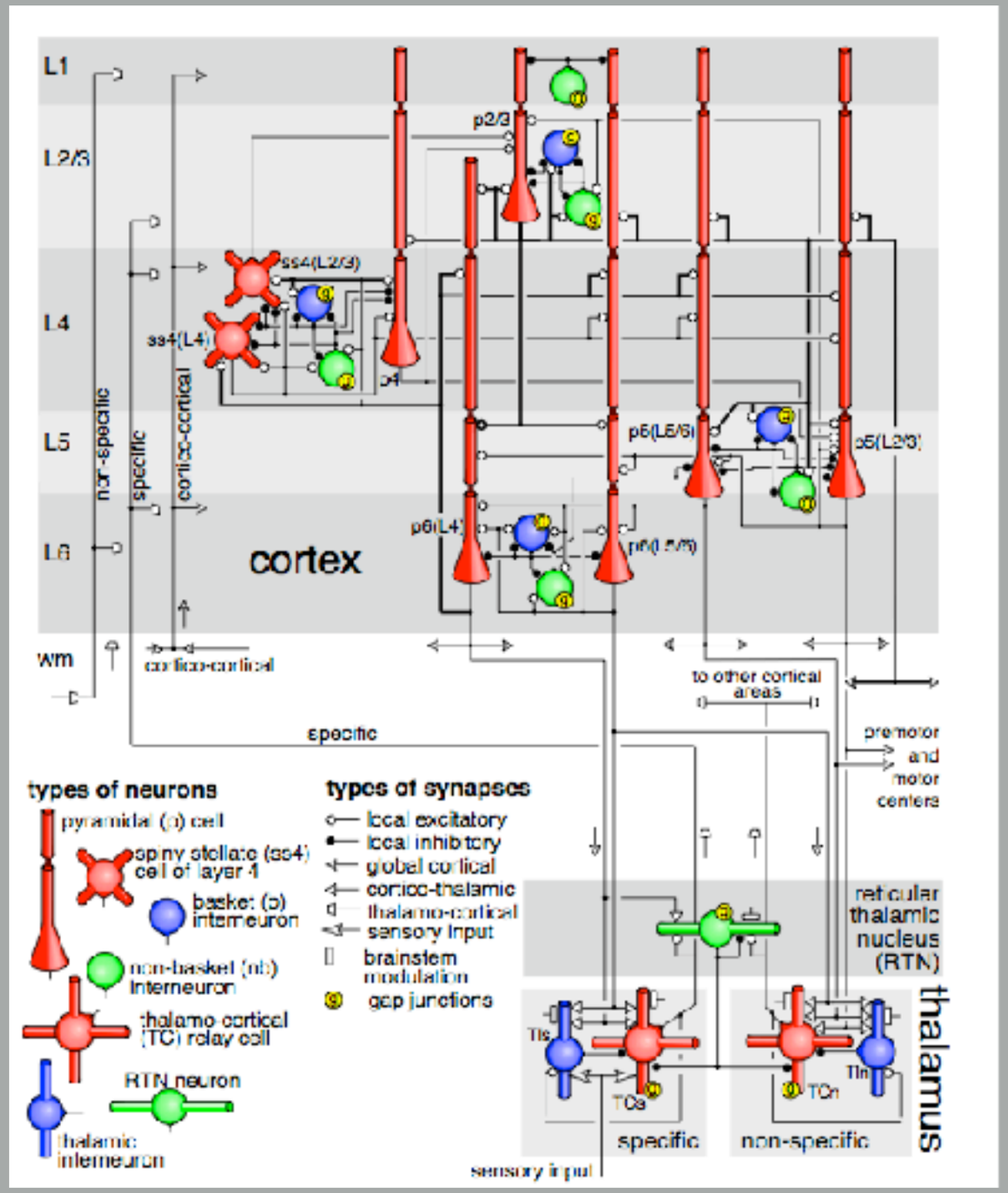

DTI and Connectivity

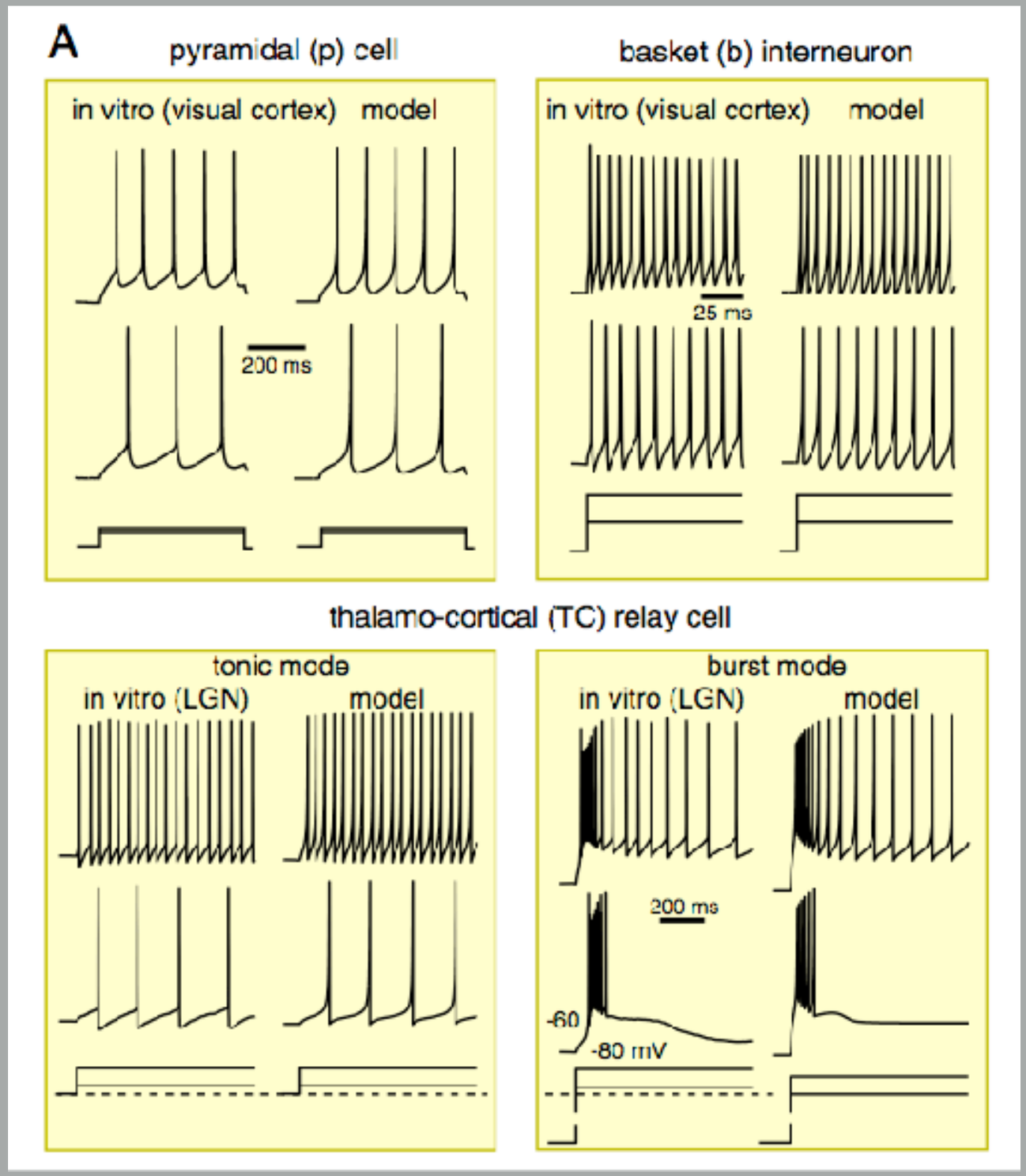

DTI and Connectivity

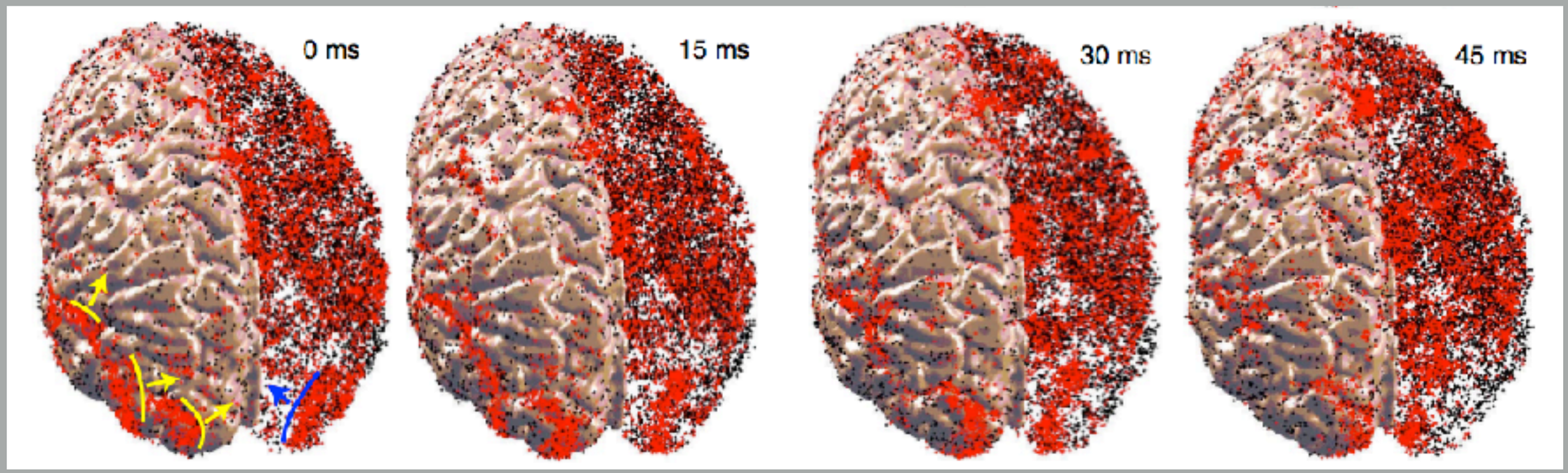

Propagation waves in the brain

red = excitatory neurons
black = inhibitory neurons

DTI and Connectivity

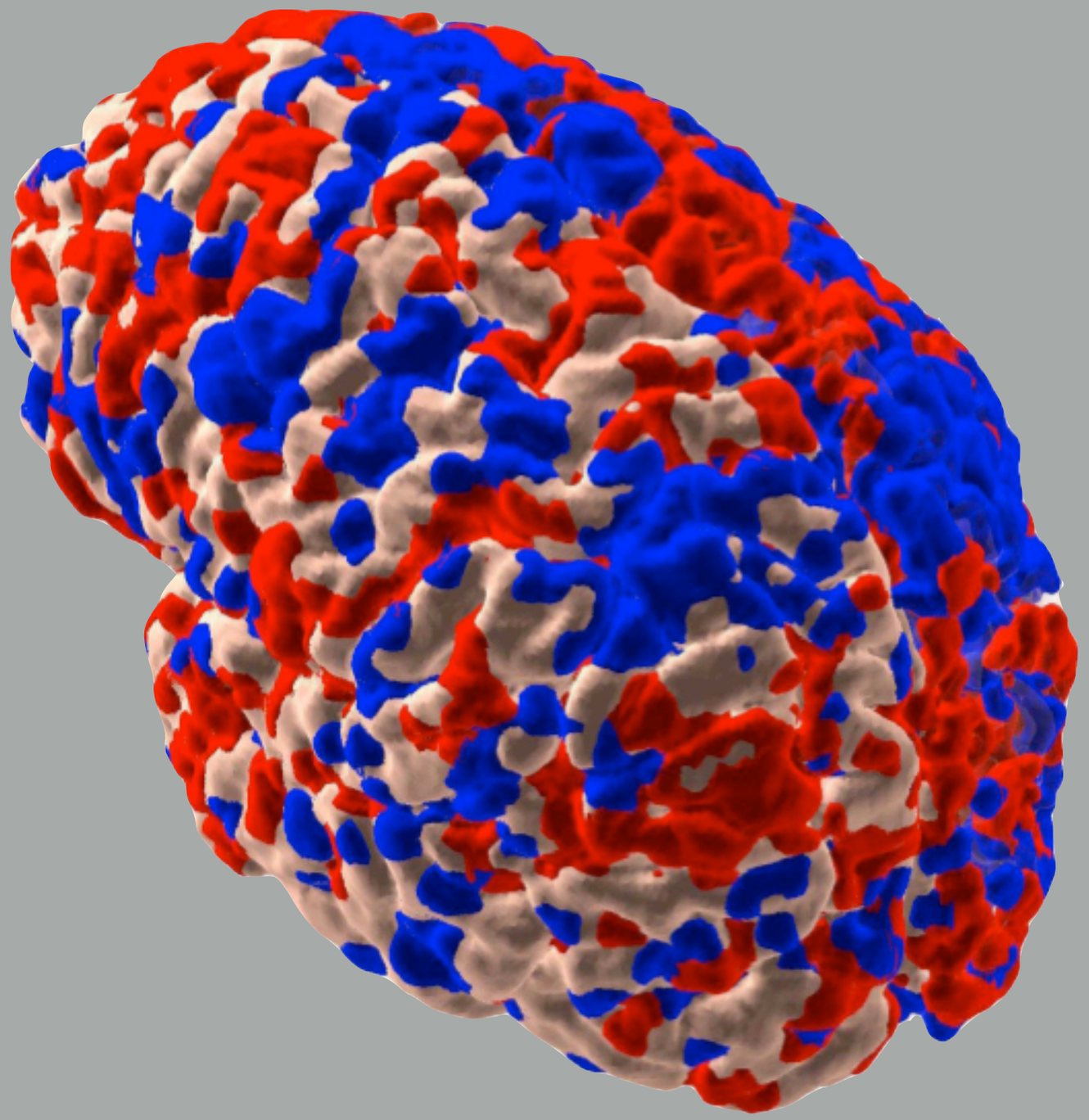

Correlations of fMRI signal in posterior cingulate and other regions

red = positive

blue = negative

Brainstem effects in traumatic brain injury

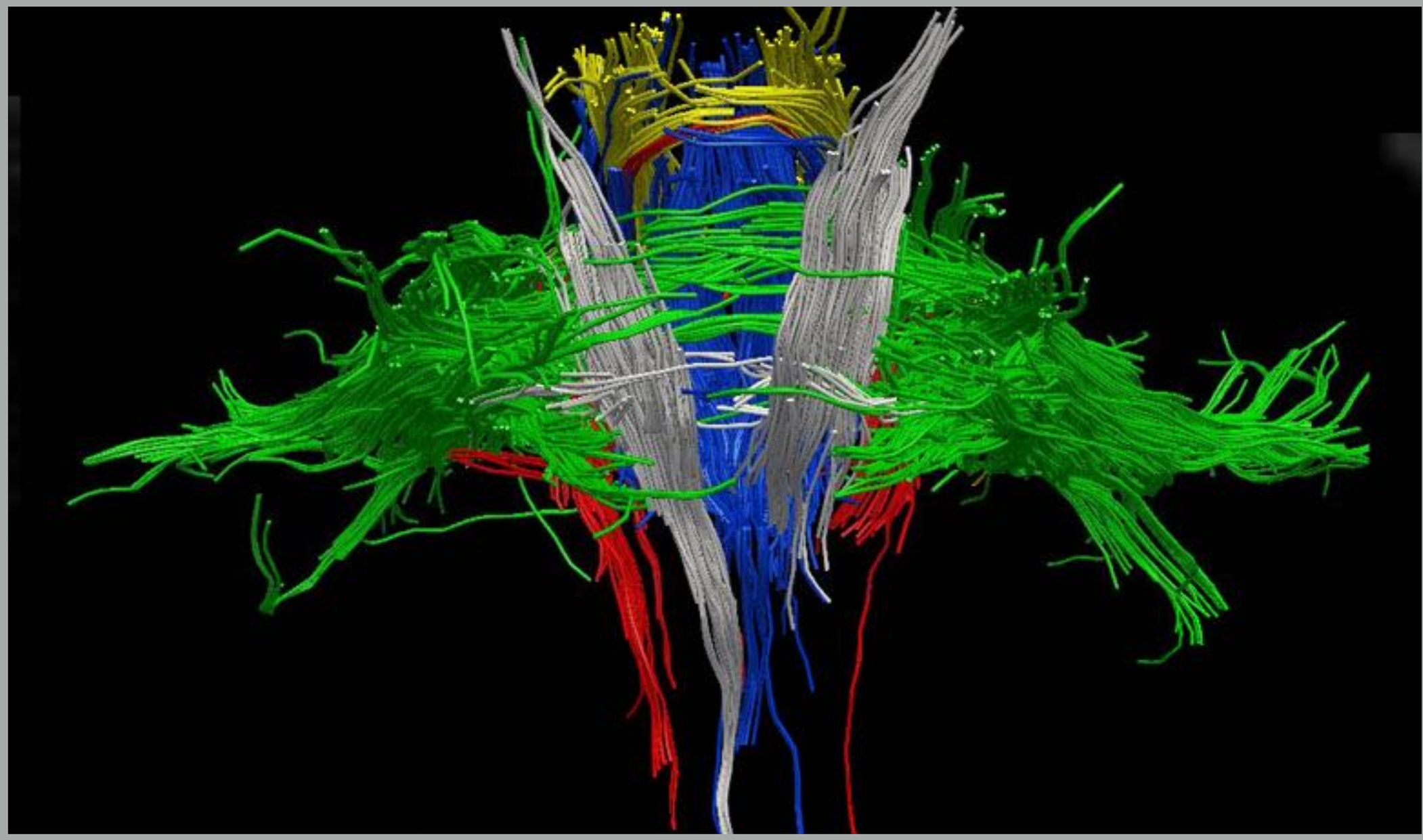

Lisa Delano Wood and Mark Bondi
Dept of Psychology, VA San Diego

Spinal Cord Injury
(Rat Model at 7T)

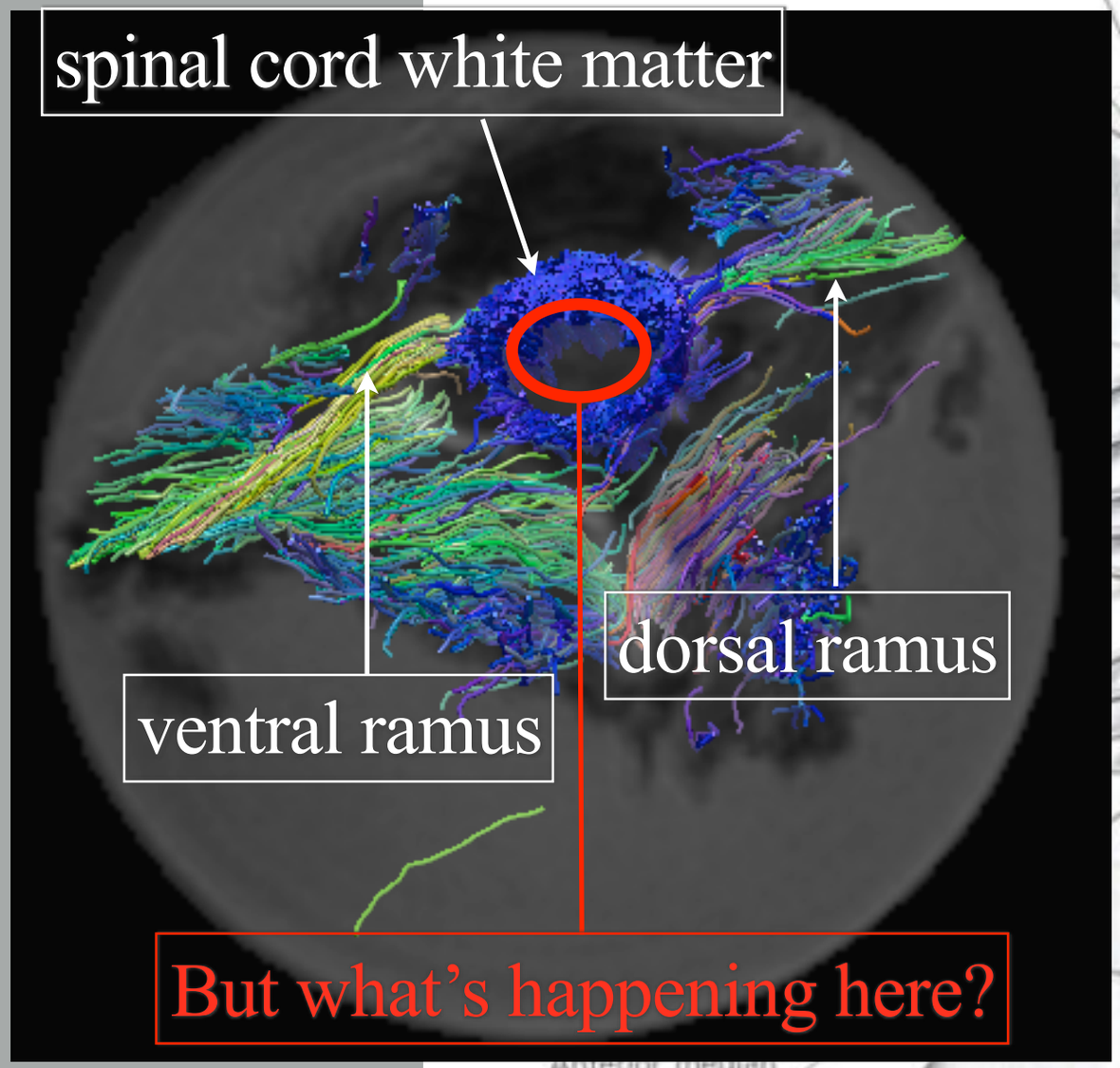

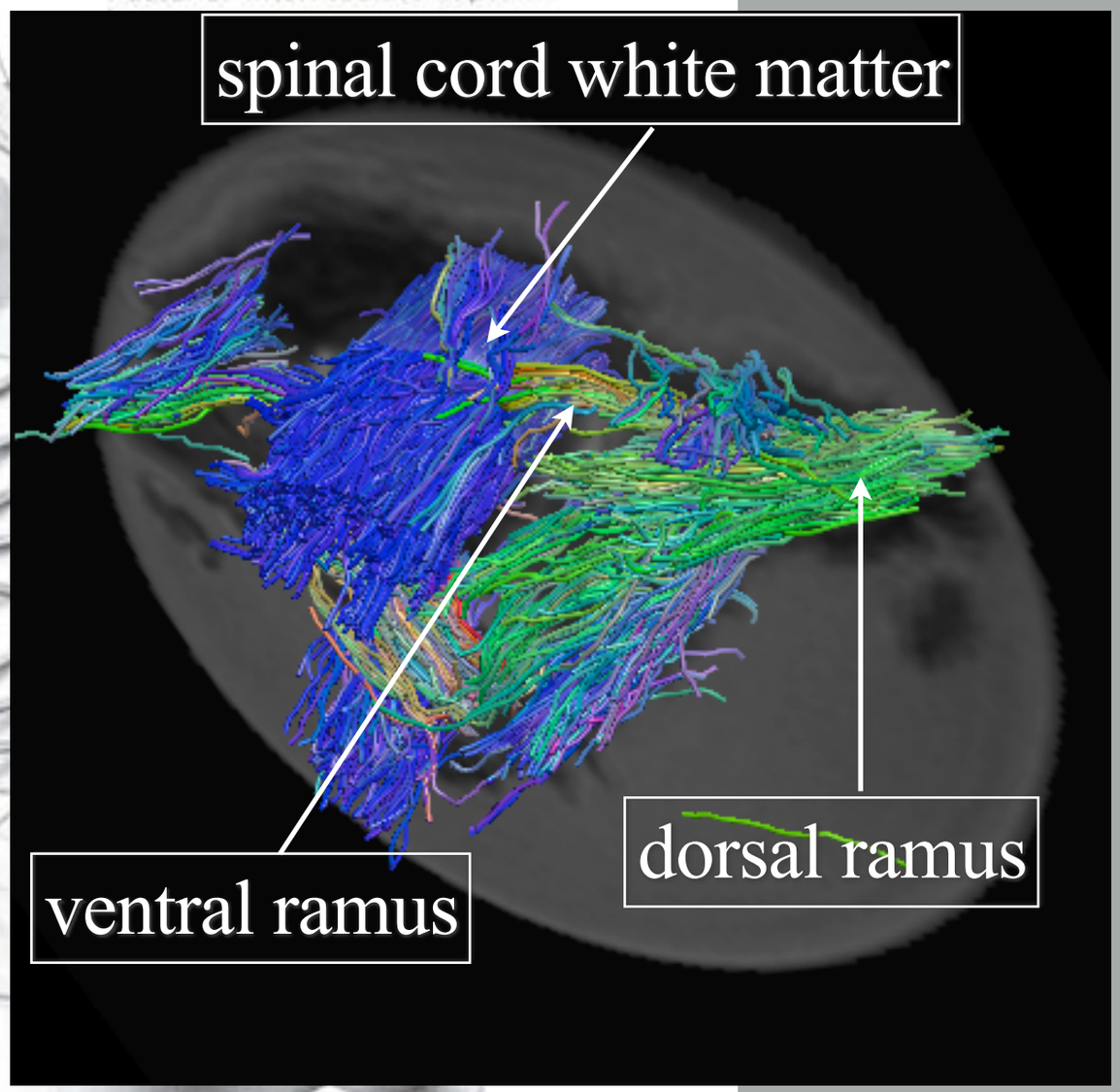

M.D., Ph.D.
Center for Neural Repair
University of California, San Diego

DTI in Muscle

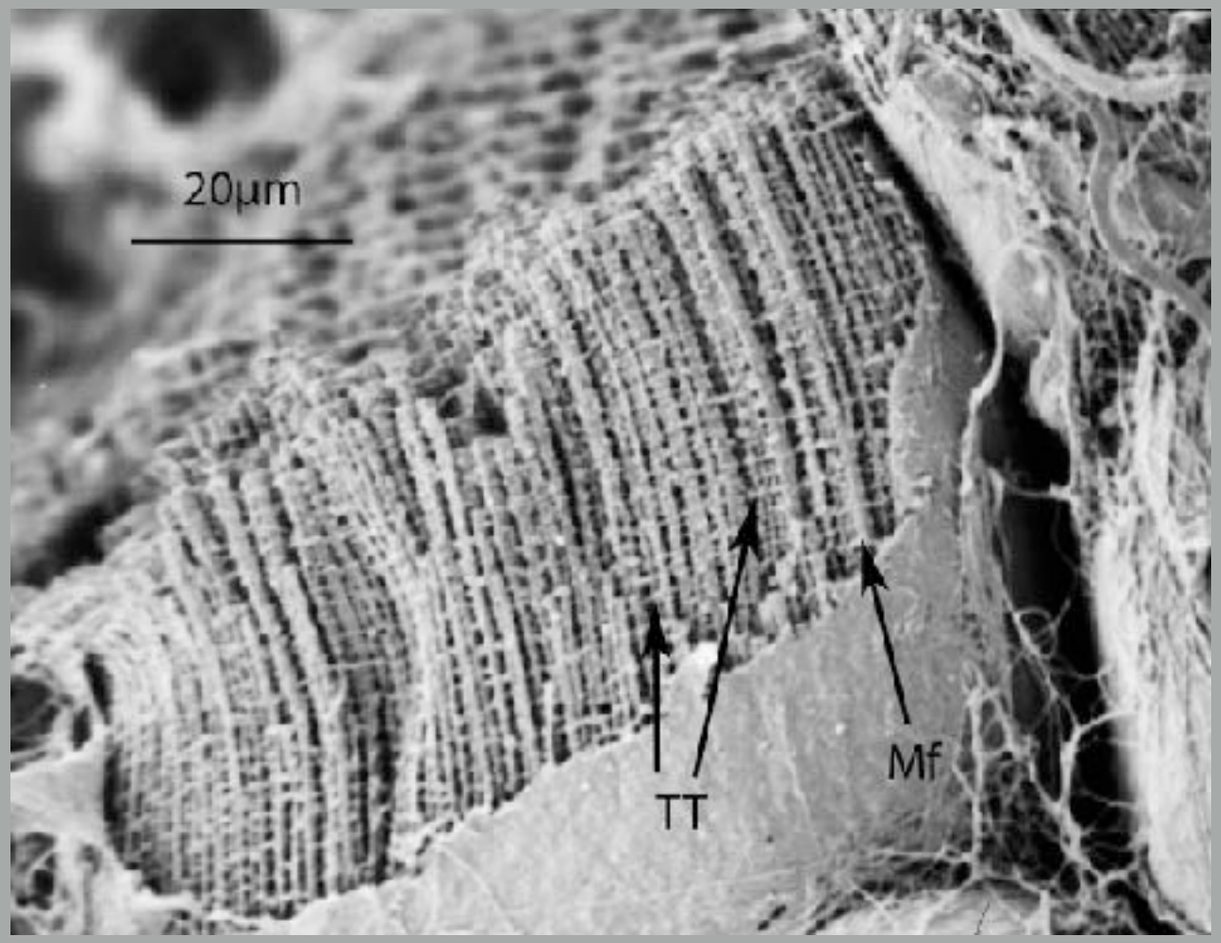

Rabbit skeletal muscle SEM image
leech.smith.edu

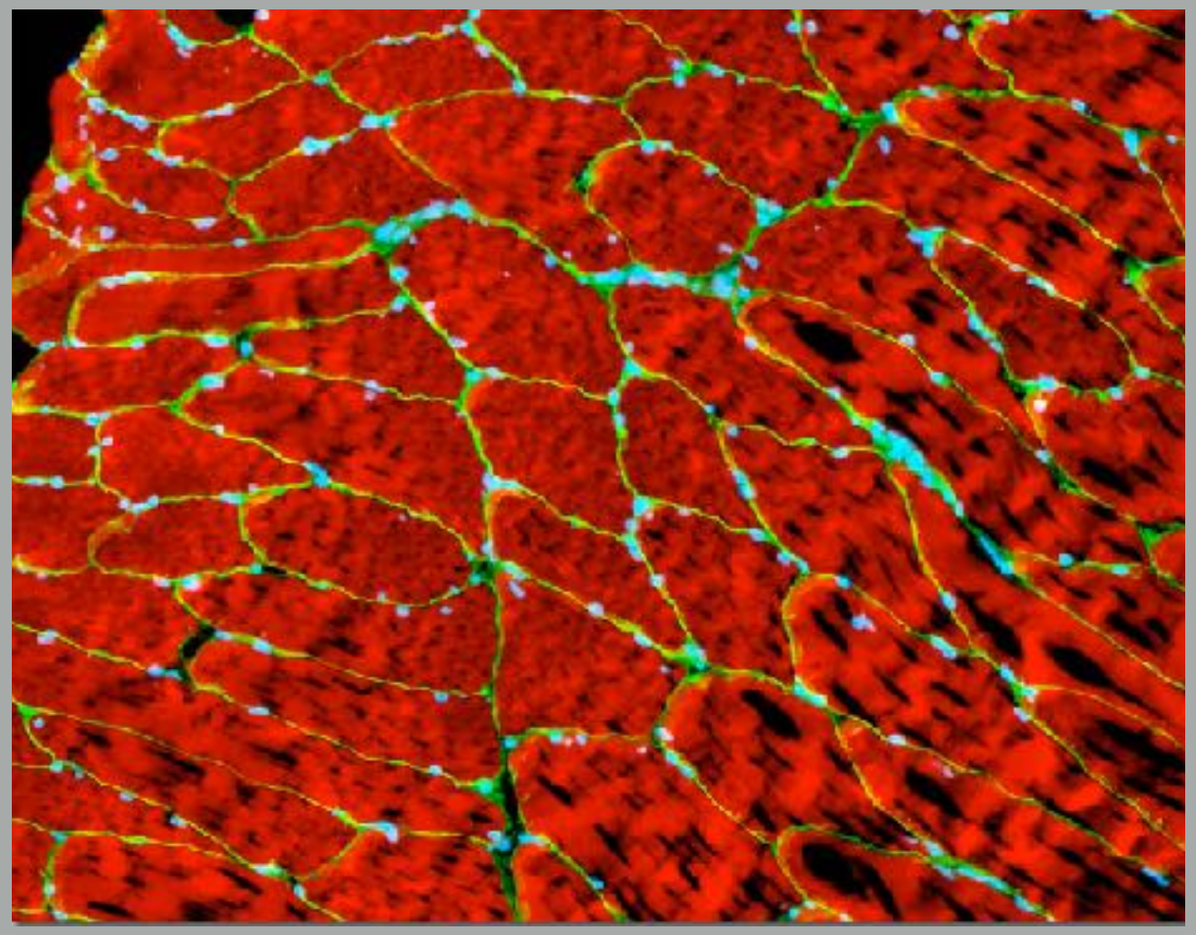

Rat skeletal muscle fluorescence microscopy image
FSU

DTI in Muscle

Magnetic Resonance in Medicine 53:1333–1340 (2005)

Determination of Mouse Skeletal Muscle Architecture Using Three-Dimensional Diffusion Tensor Imaging

Anneriet M. Heemskerk,[1*] Gustav J. Strijkers,[1] Anna Vilanova,[2] Maarten R. Drost,[3] and Klaas Nicolay[1]

DTI in Muscle

a, b = anatomical

c, d = MD

e, f = FA

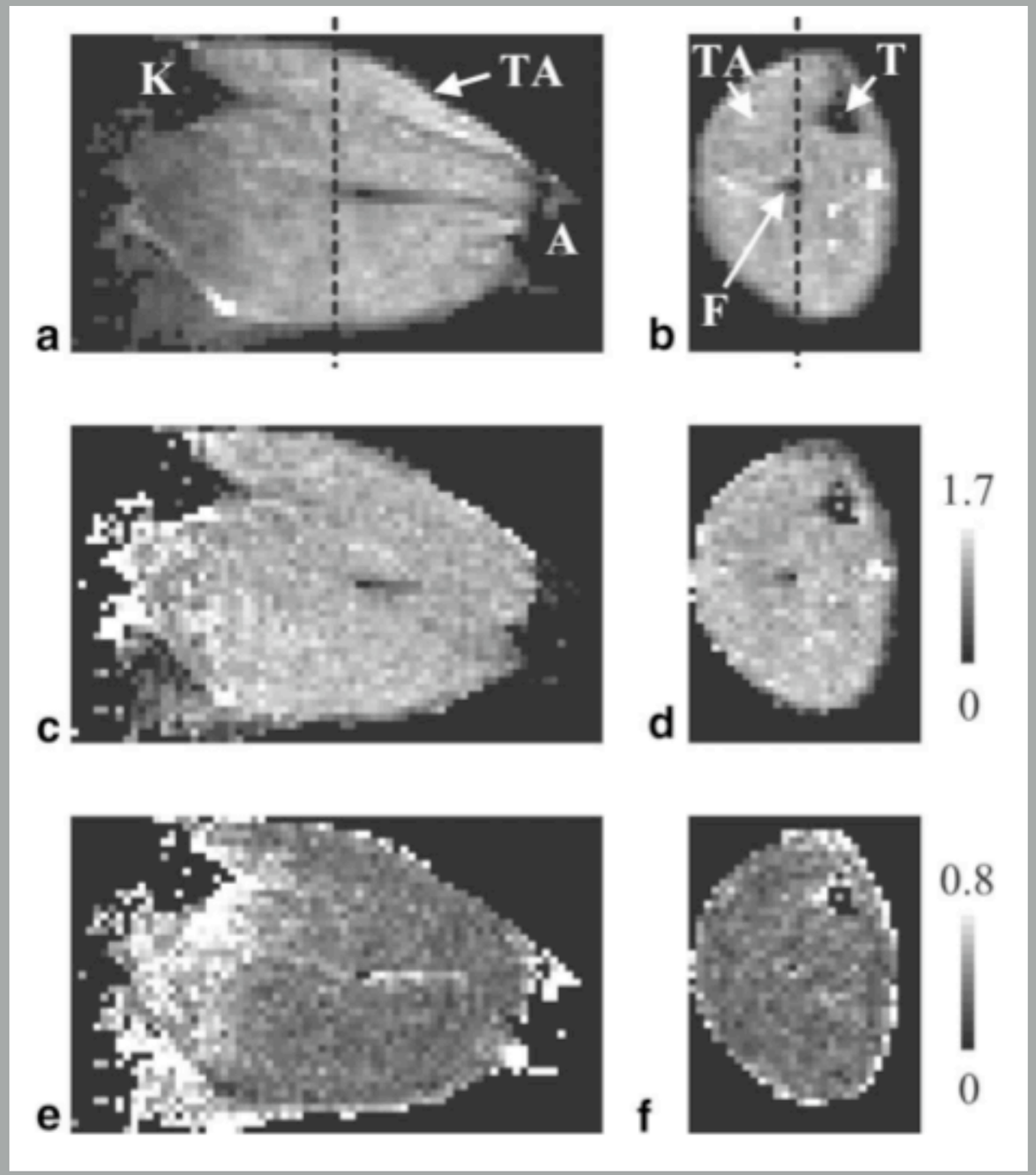

DTI in Muscle

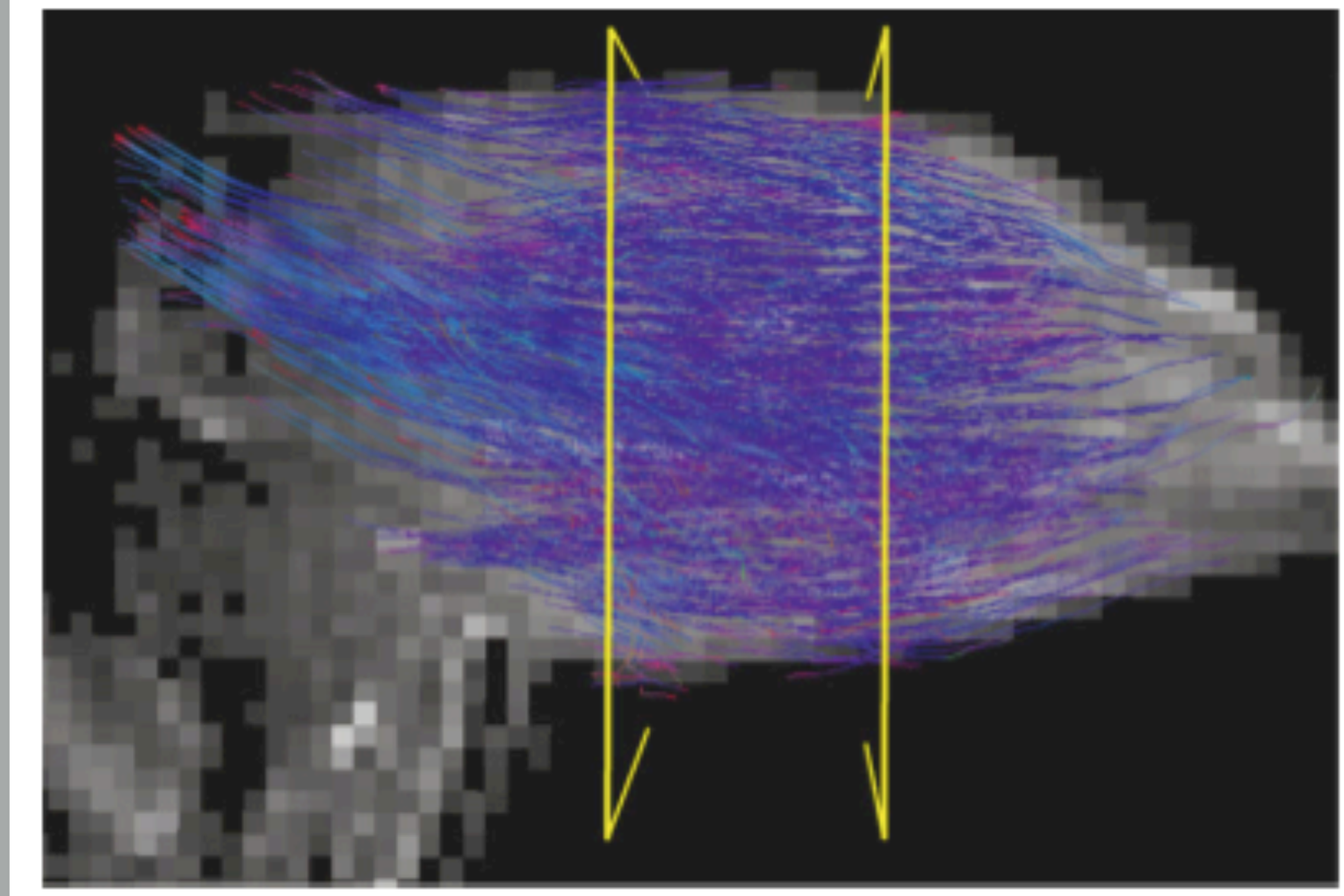

tractography

DTI in Muscle

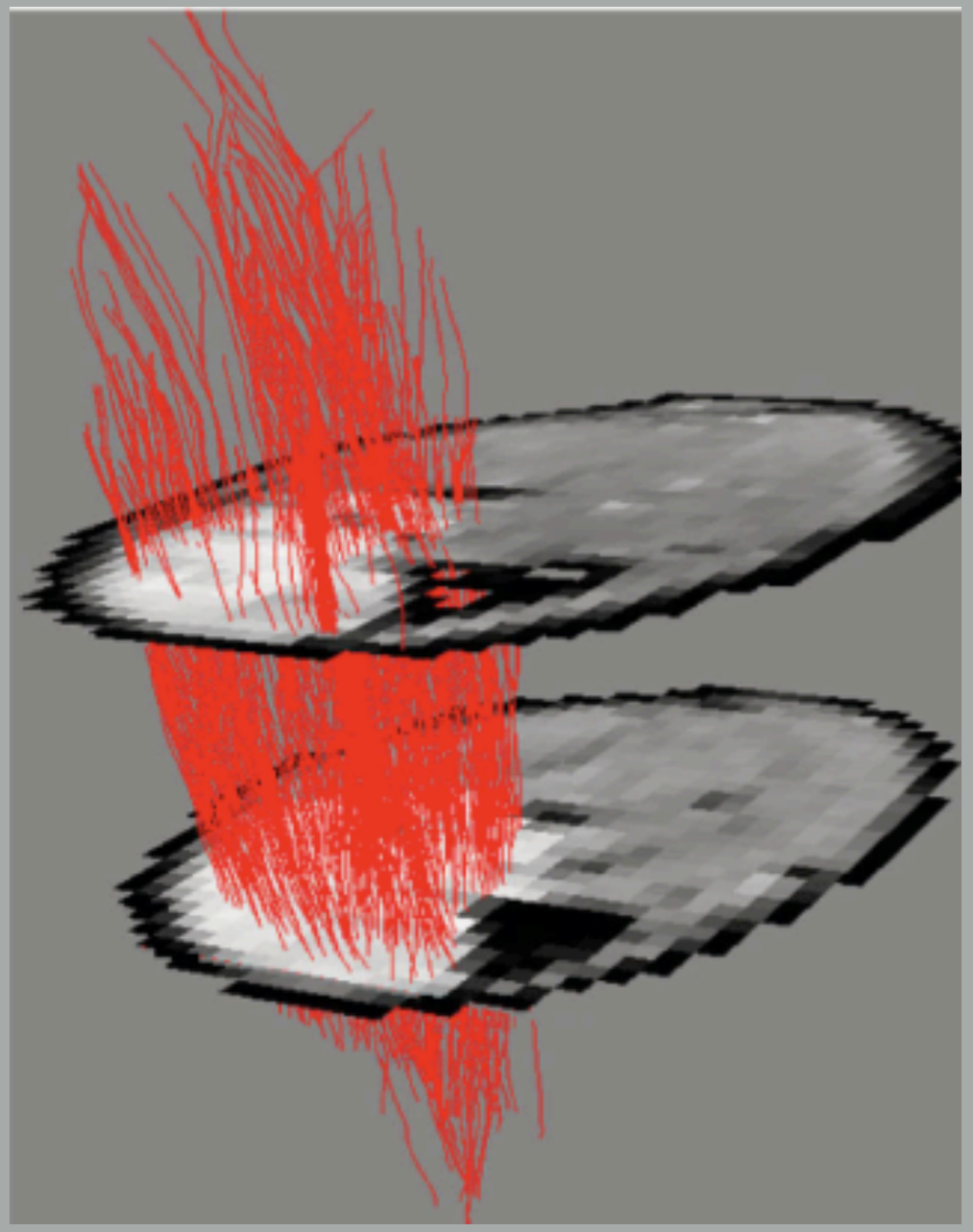

tractography

DTI in Muscle

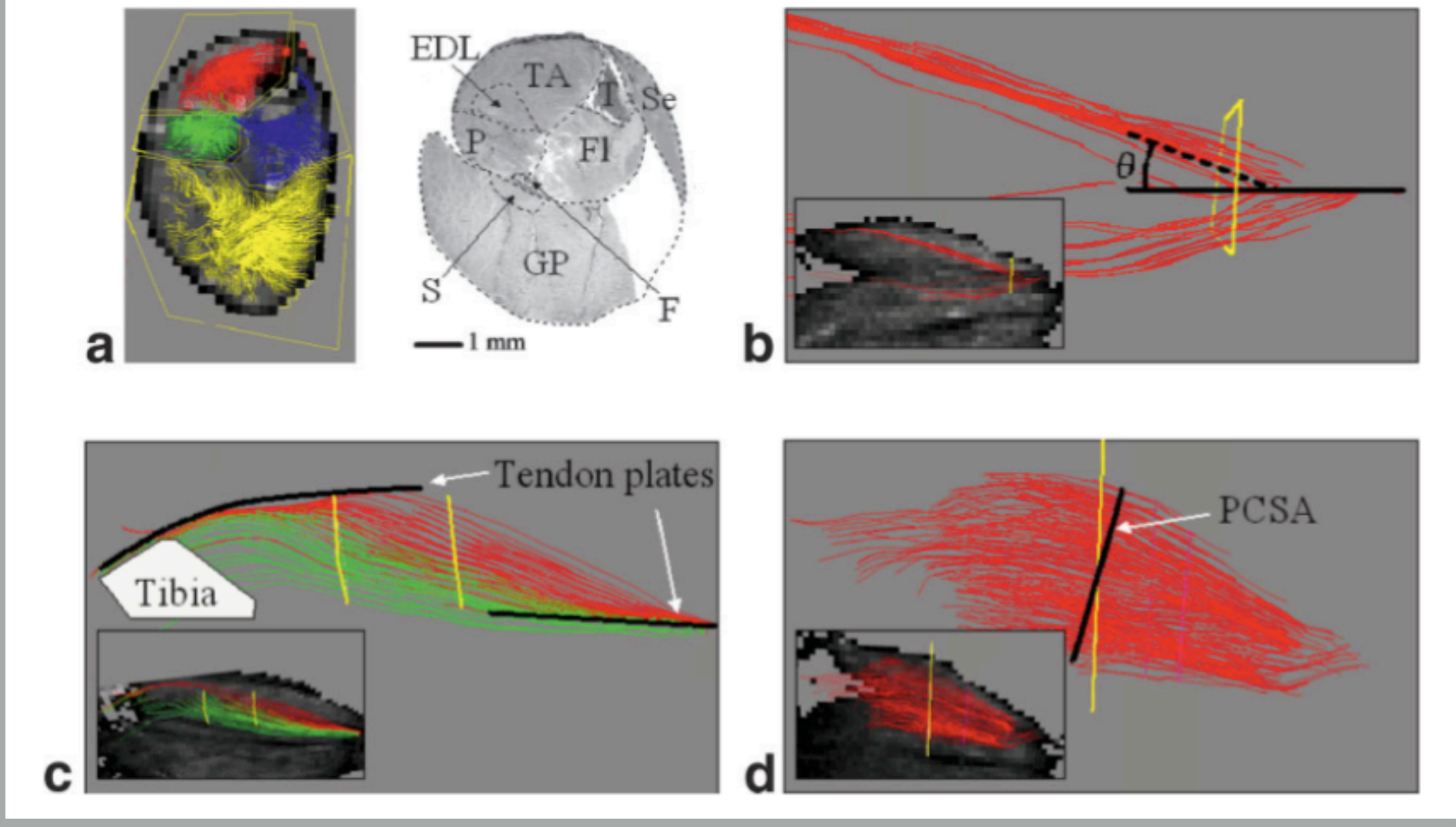

Supraspinatus DTI

Supraspinatus

Anterior

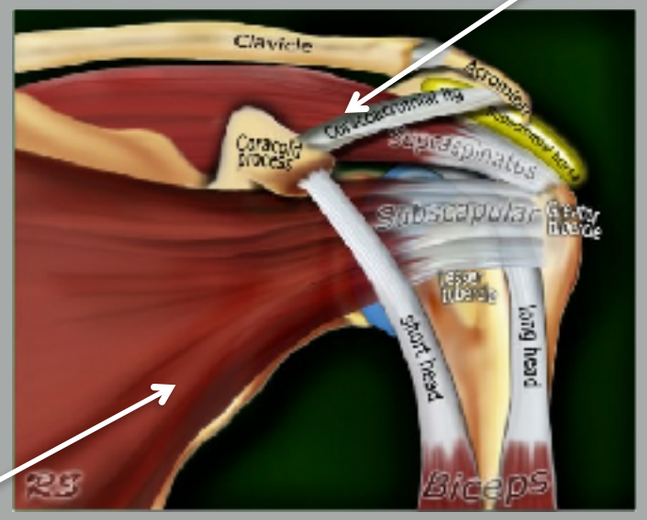

Posterior

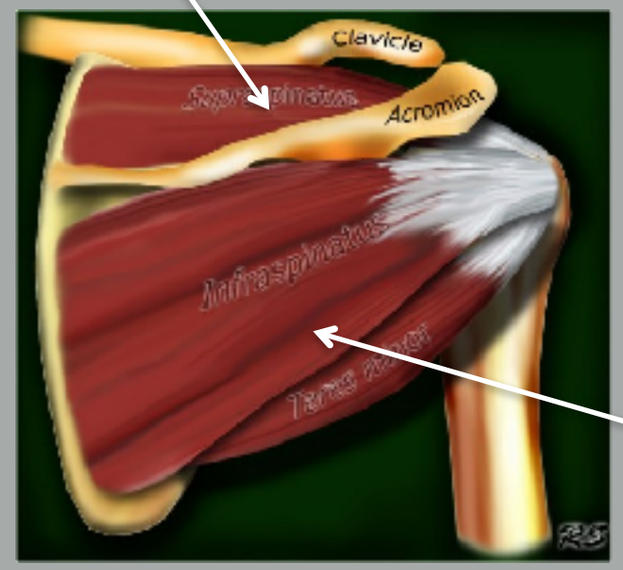

Infraspinatus
+ Teres Minor

Subscapularis

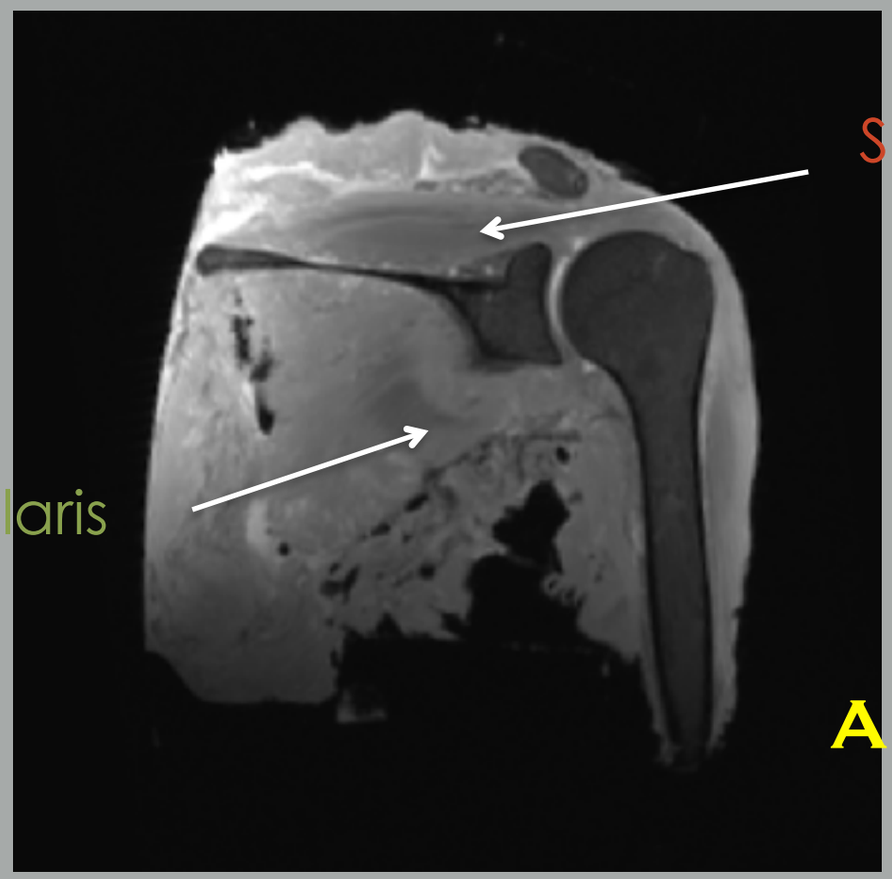

Supraspinatus

Subscapularis

A. Rodrigues-Soto,
Ward group

Supraspinatus Structure in Tractography

15 directions

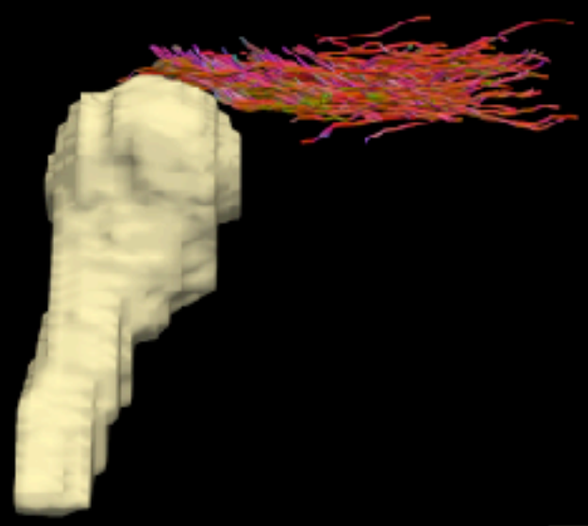

30 directions

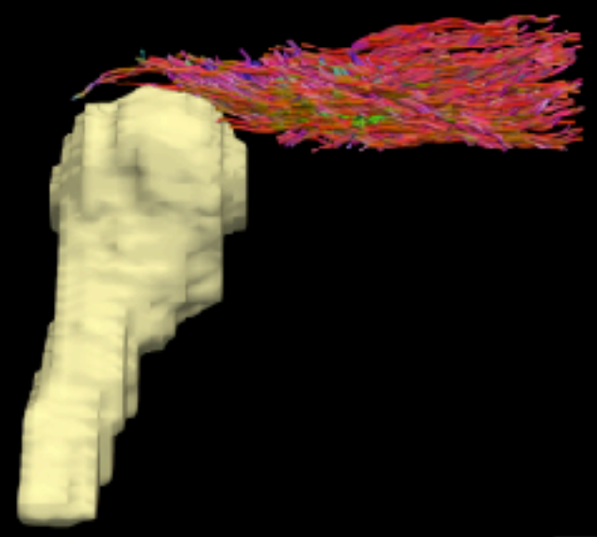

45 directions

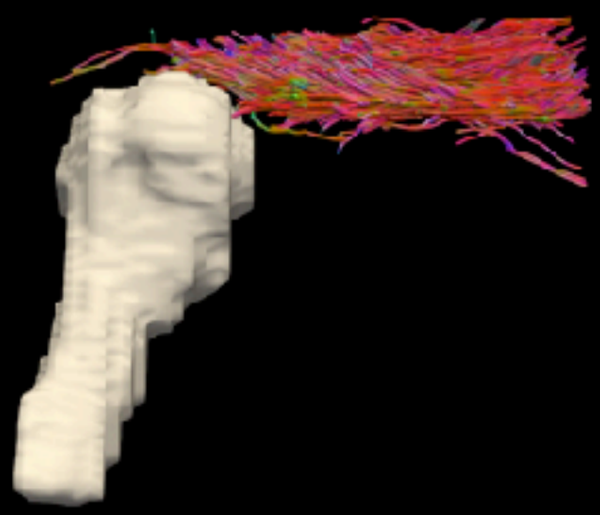

60 directions

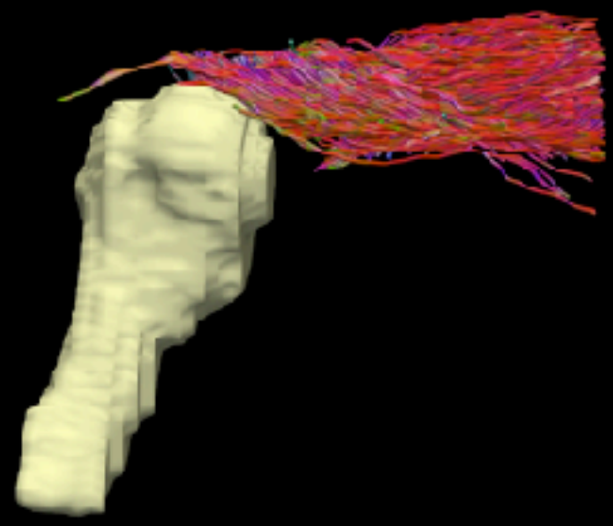

A. Rodrigues-Soto,
Ward group

Supraspinatus DTI

Supraspinatus

Anterior

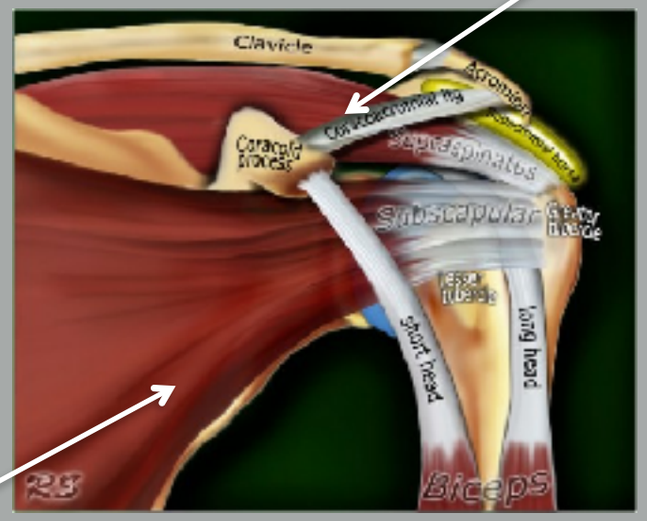

Posterior

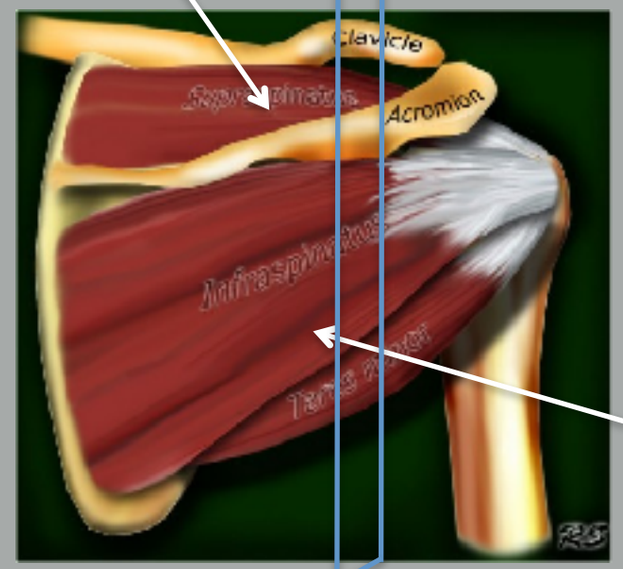

Infraspinatus
+ Teres Minor

Subscapularis

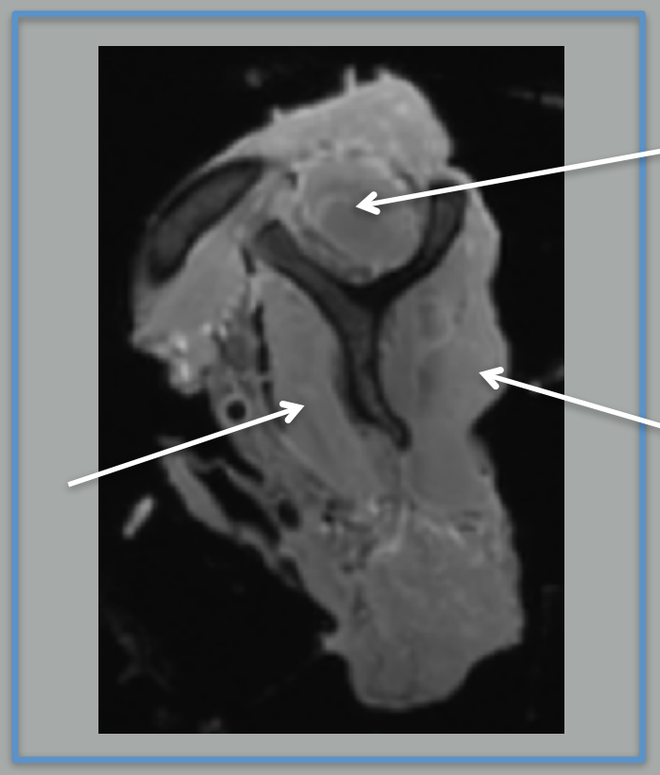

Supraspinatus

Infraspinatus

Subscapularis

A. Rodrigues-Soto,
Ward group

Supraspinatus Tractography @60 directions

A. Rodrigues-Soto,
Ward group

Cardiac Mechanics

There are other organs besides the brain

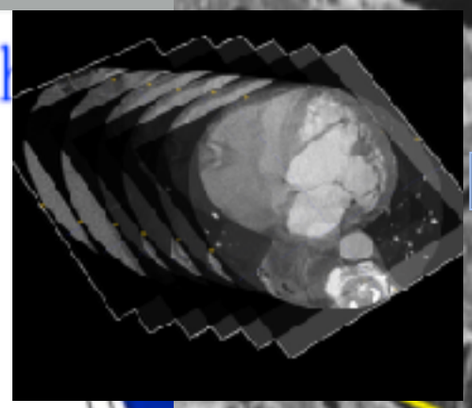

CT/MRI
anatomical data

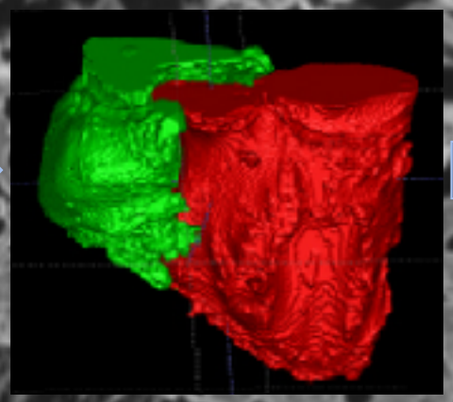

Segmented
geometry

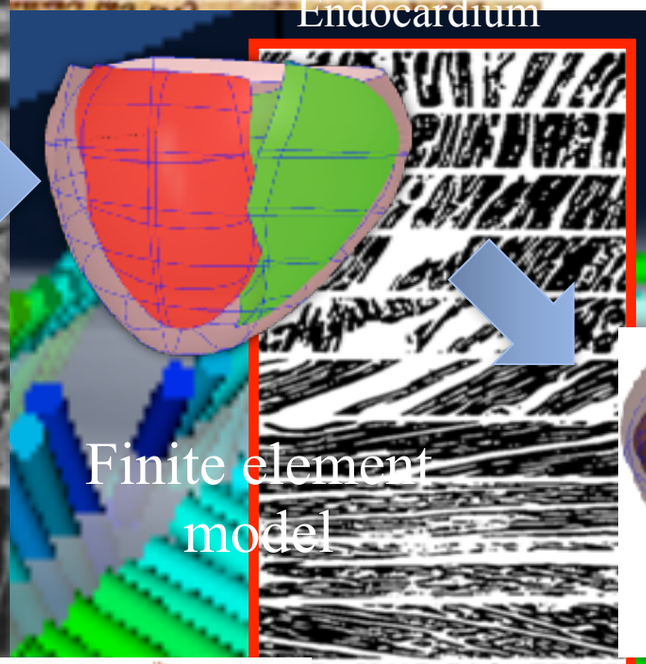

Finite element
model

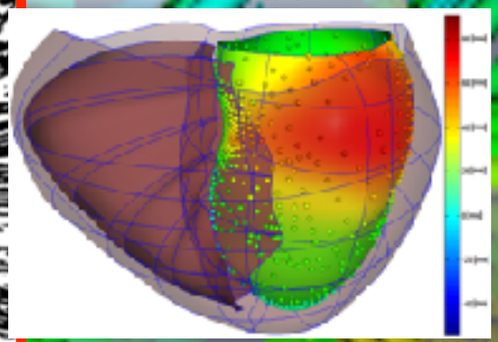

Patient-specific
model

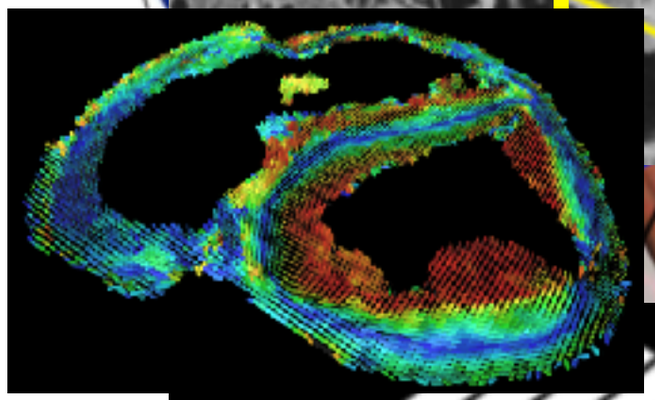

Epi DTMRI data

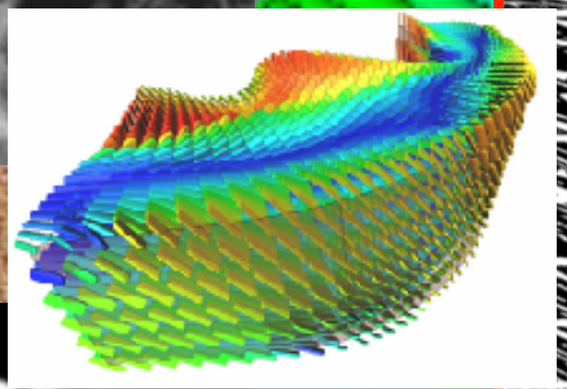

Fiber architecture

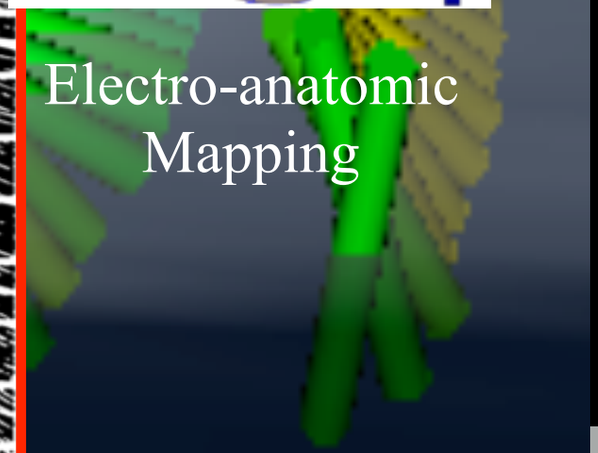

Electro-anatomic
Mapping

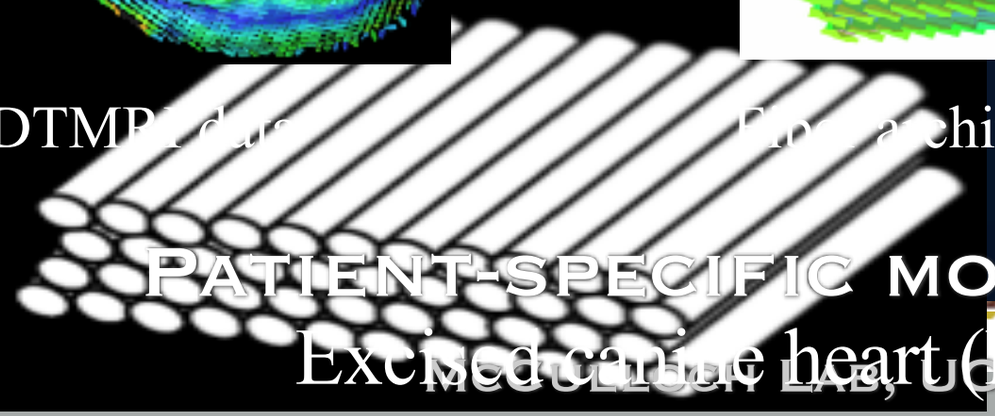

Excised canine heart (

Legrice et al. 1995

3D Spiral FSE DTI sequence (Frank et al. Neuroimage 2010)

Streeter et al. 1969

Our first whole human heart DTI (ex vivo)

Patient-specific modeling of Heart Failure

DTI in Cardiac Biomechanics

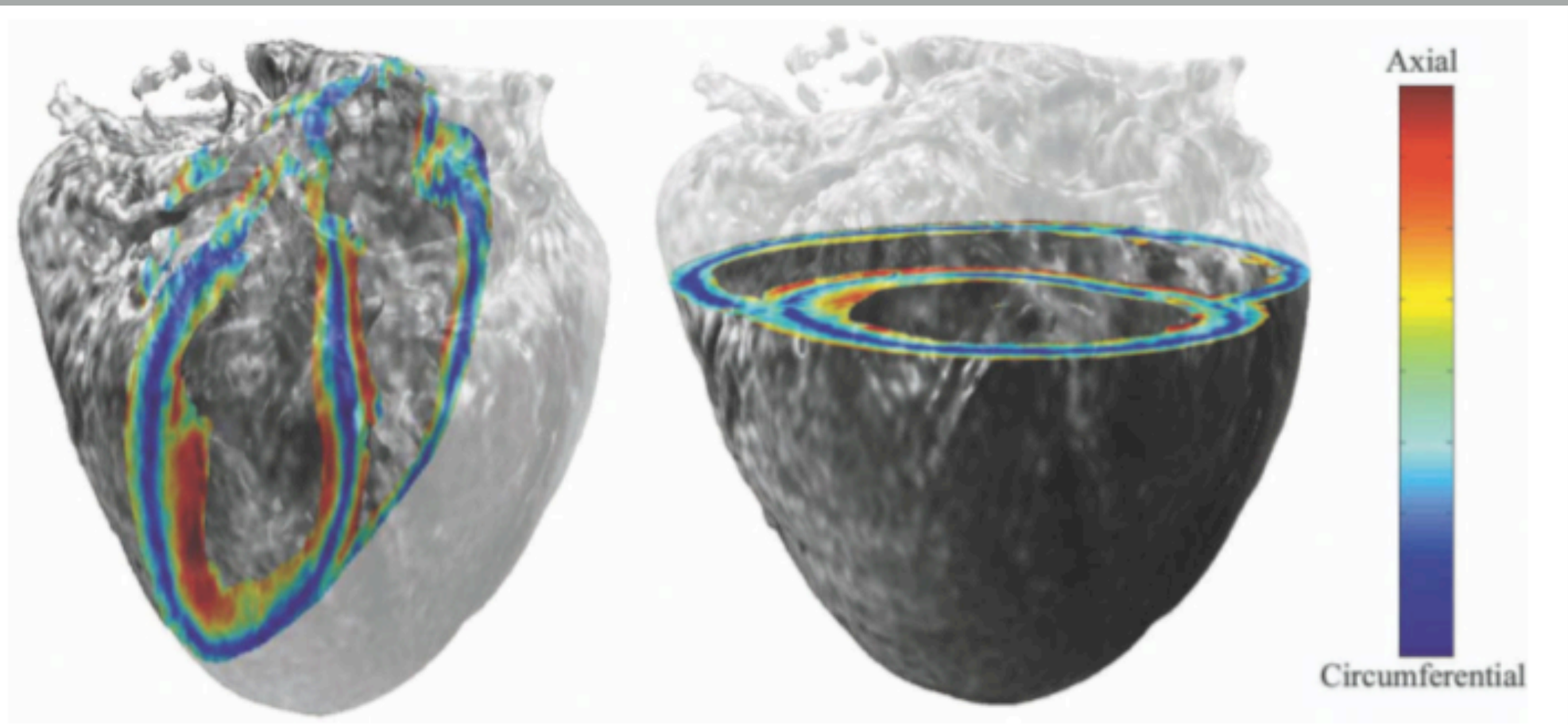

FIG. 4. 3D rendering of the geometry and corresponding fiber structure for one reconstructed heart. The heart is color-coded according to the orientation of the *z*-component of the principle eigenvector. Fibers that run in a circumferential direction are shown in blue, whereas fibers that run in the base–apex direction are colored red.

DTI in Cardiac Biomechanics

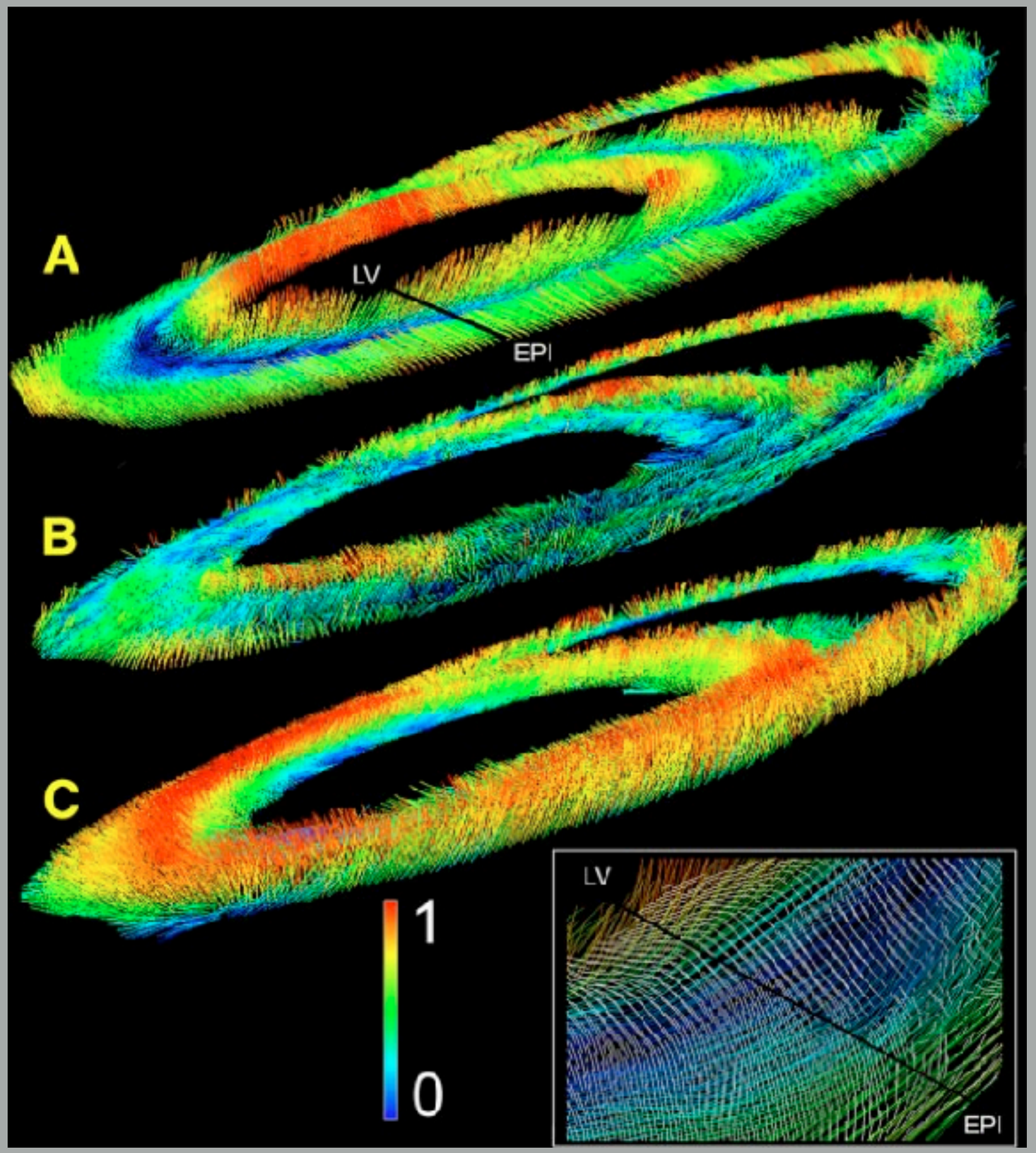

A) Primary, B) Secondary, and C) Tertiary eigenvectors.
Out of plane component shown in color

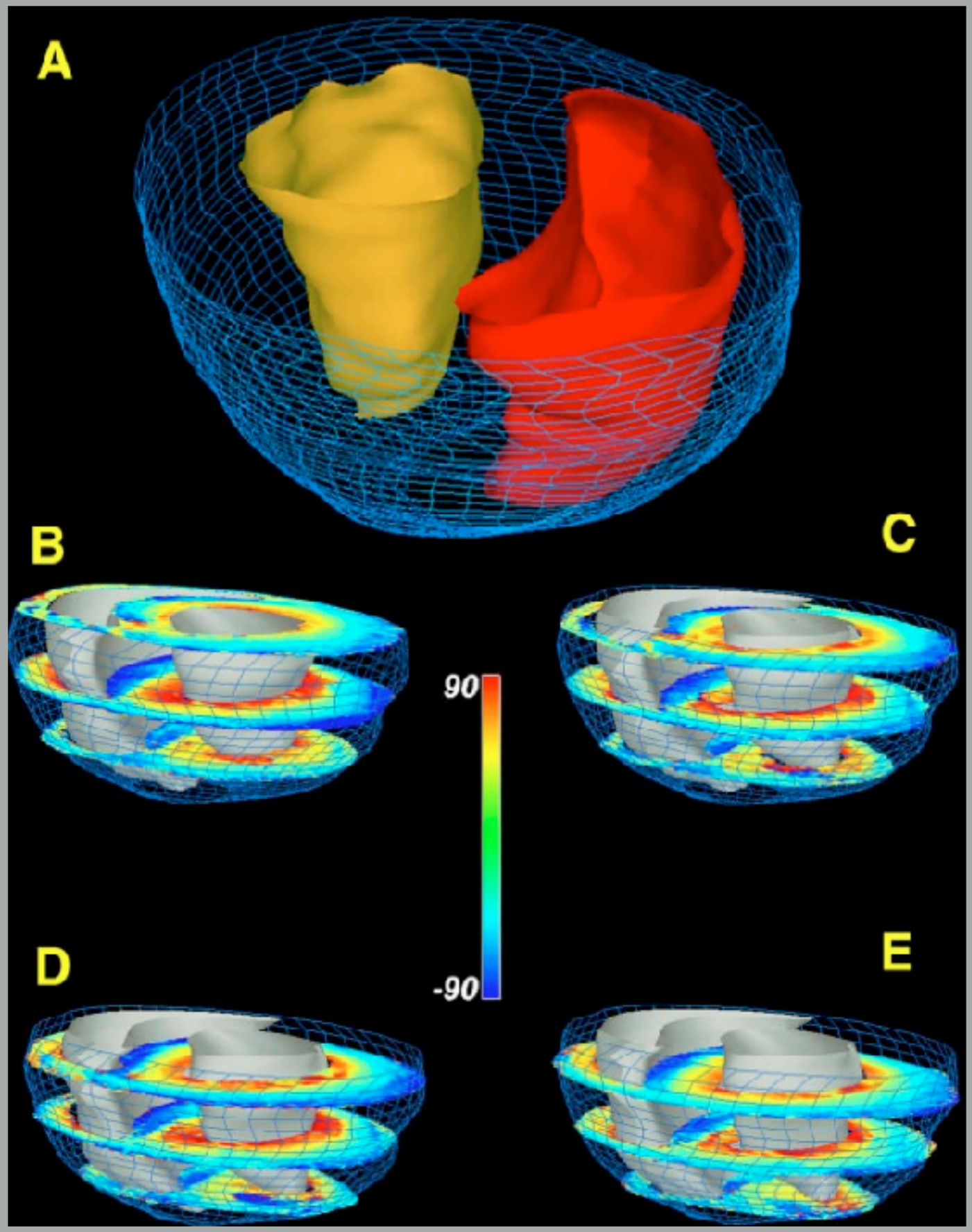

computational modeling

High Resolution MRI of Elasmobranchs

Elasmobranchs have an elaborate sensory system

Brown Smoothhound (Data courtesy JM Tyszka)

Elasmobranchs have an elaborate sensory system

The 7 Senses

Electroreception

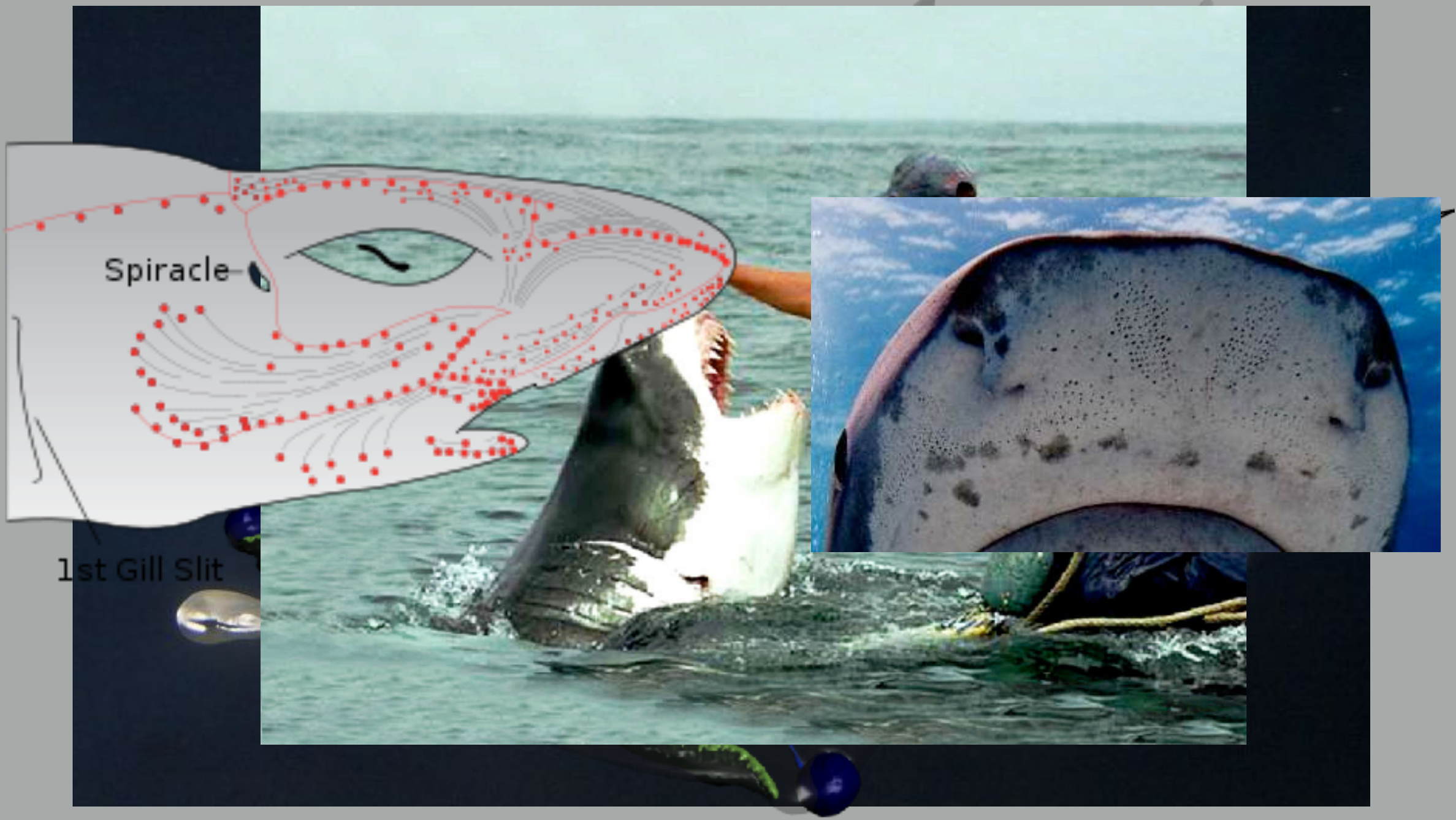

Organization

Teleost

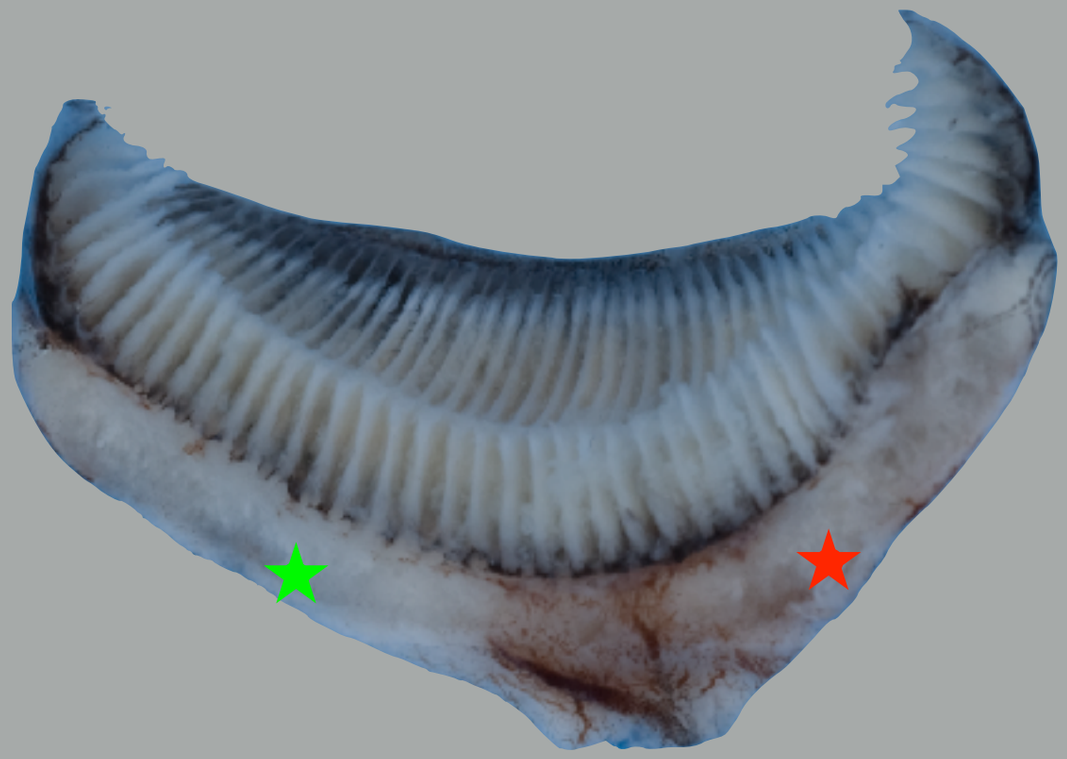

- ORN’s in epithelium project to discrete glomeruli in OB
- Chemotopic arrangement

Stingray

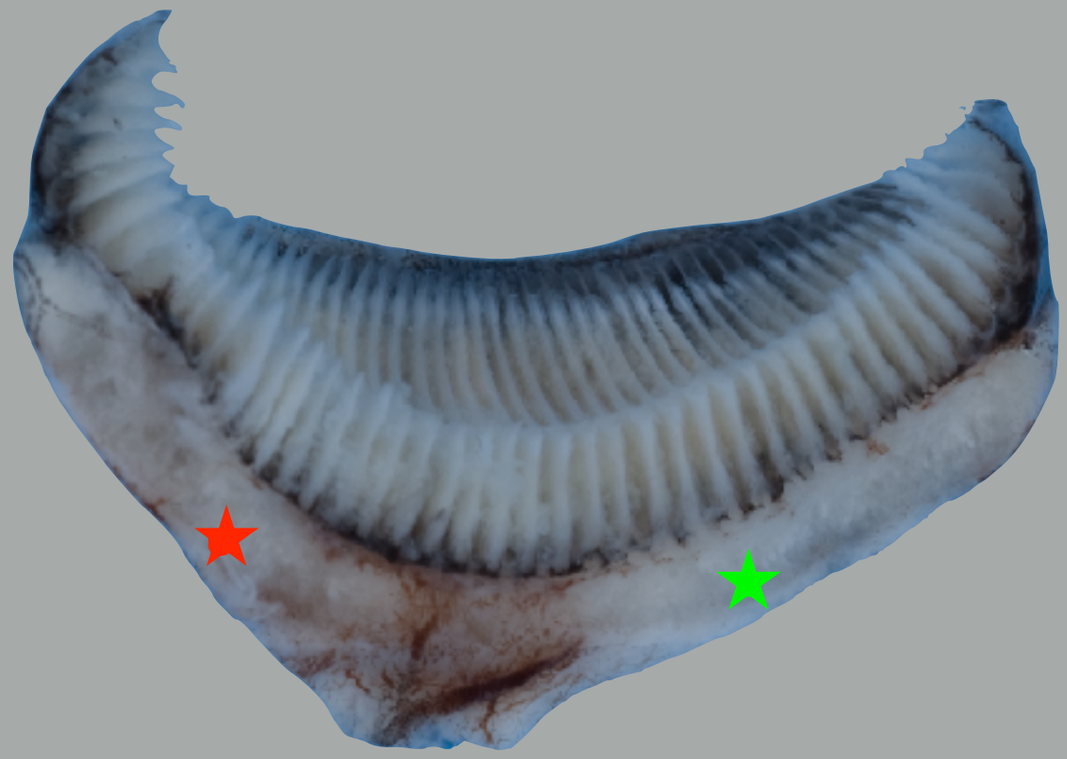

- ORN’s in epithelium project straight back to OB
- Somatotopic arrangement

lamina propria

axon bundles

ORN's

epithelium

100.0µm

Organization

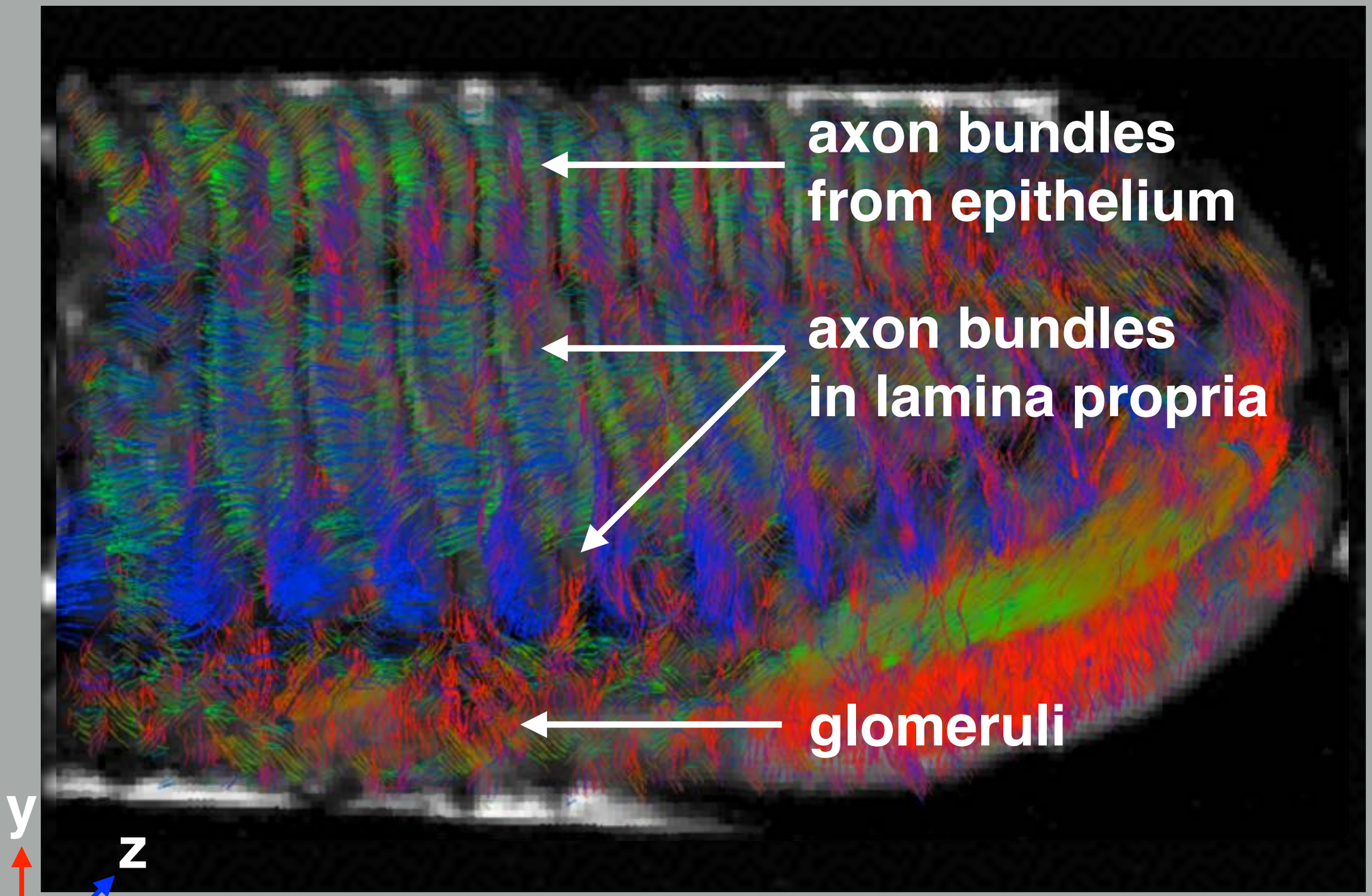

in collaboration with Drs S. Kajiura & T. Meredith, FAU
Drs S. Blackband and M. Hwang, UFL

I

Structure

axon bundles
from epithelium

axon bundles
in lamina propria

glomeruli

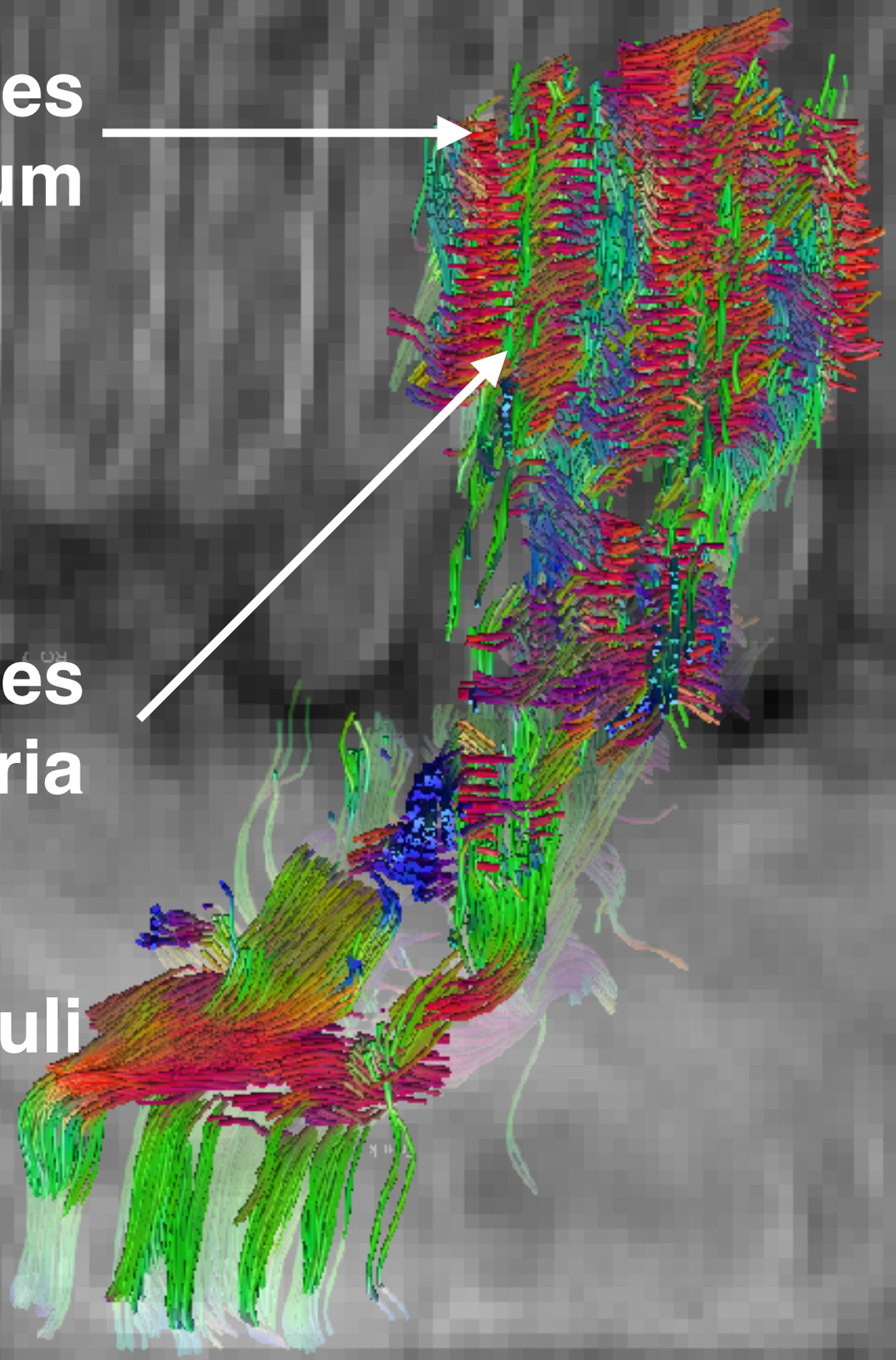

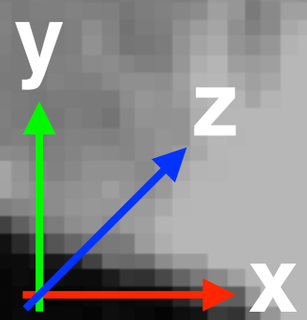

DTI in Alzheimer's

Neurodegenerative conditions of late life (e.g., AD, PD, DLB) involve slowly accruing neuron losses that evolve over some years before symptoms occur

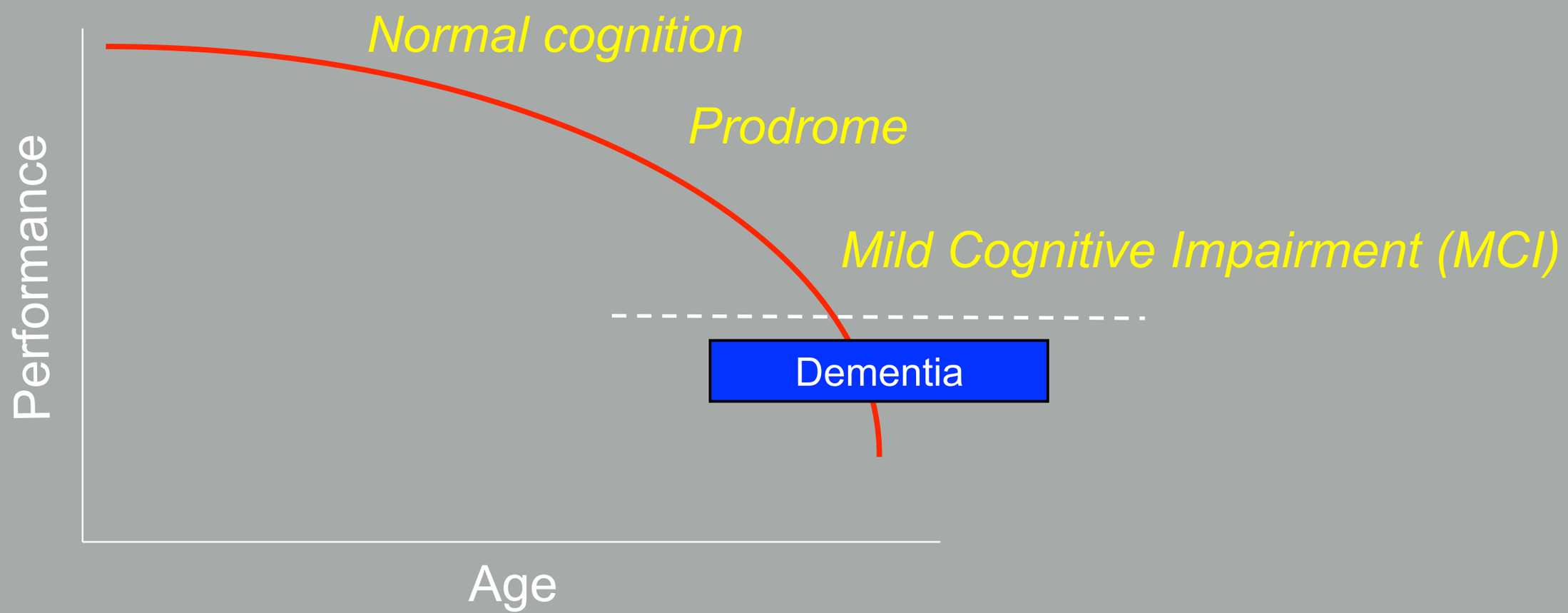

Chronic disease model (Katzman 1976)

Cummings et al. Alzheimer's Research & Therapy 2014, 6:37
http://alzres.com/content/6/4/37

alzheimer's research&therapy

RESEARCH Open Access

Alzheimer's disease drug-development pipeline: few candidates, frequent failures

Jeffrey L Cummings[1*], Travis Morstorf[2] and Kate Zhong[1]

Abstract

Introduction: Alzheimer's disease (AD) is increasing in frequency as the global population ages. Five drugs are approved for treatment of AD, including four cholinesterase inhibitors and an *N*-methyl-D-aspartate (NMDA)-receptor antagonist. We have an urgent need to find new therapies for AD.

Methods: We examined Clinicaltrials.gov, a public website that records ongoing clinical trials. We examined the decade
mecha
phase t

Results
trials, a
of Ame
than U.
improv
disease
numbe
and lor
during

Conclu
therapeutics, considering the magnitude of the problem. The success rate for advancing from one phase to another is low, and the number of compounds progressing to regulatory review is among the lowest found in any therapeutic area. The AD drug-development ecosystem requires support.

ptomatic agents. A very high
d of 0.4% (99.6% failure).
gov database demonstrates th

Neuropathologic Hallmarks Of AD
Evolution of Neurofibrillary Changes

Stages I / II
(pre AD)

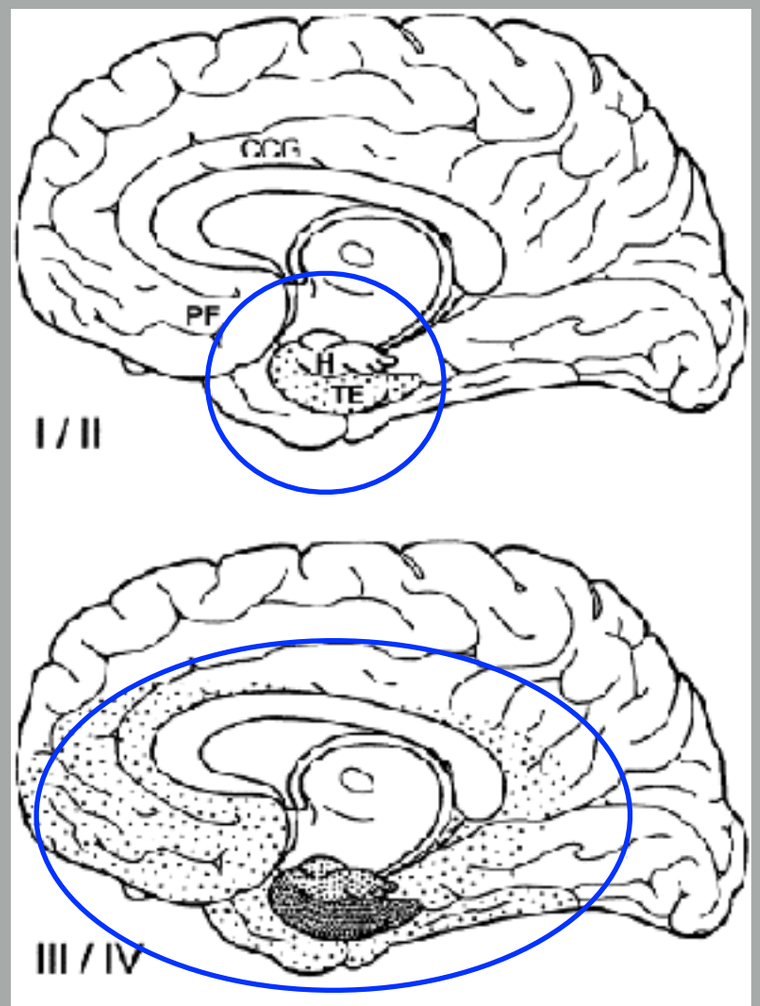

entorhinal and transentorhinal (TE): mild

Stages III / IV
(early AD)

TE: severe
hippocampus: moderate
cortical association areas: mild

Stages V / VI
(clinical AD)

TE: severe
Cortical association areas: severe
hippocampus: severe
primary sensory and motor areas spared

Braak & Braak

Stages of NFT Pathology

Stages I and II

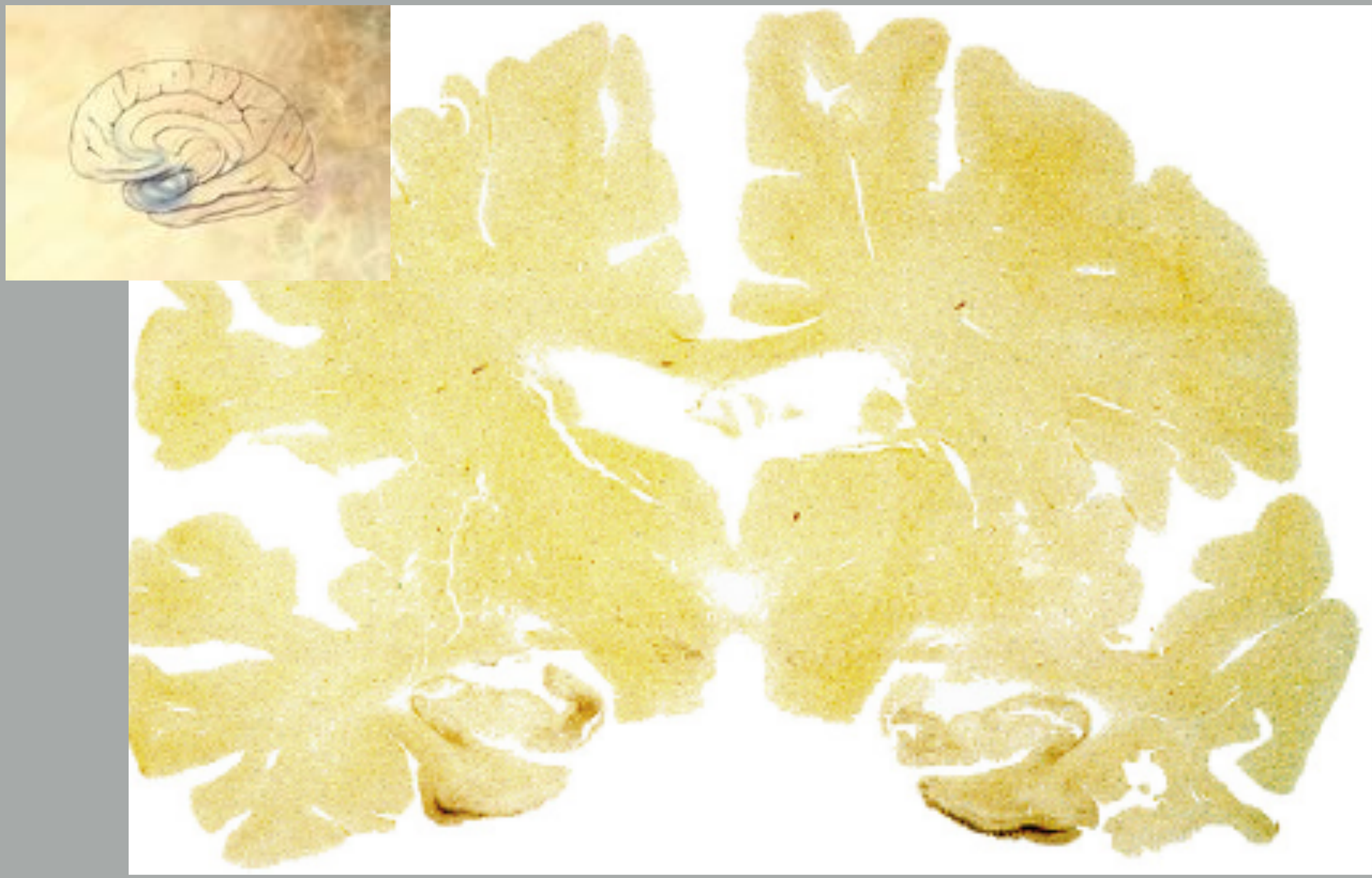

Braak & Del Tredici (2012). *Alz & Dem.*

Stages of NFT Pathology

Stage III

Braak & Del Tredici (2012). *Alz & Dem.*

Stages of NFT Pathology

Stages V and VI

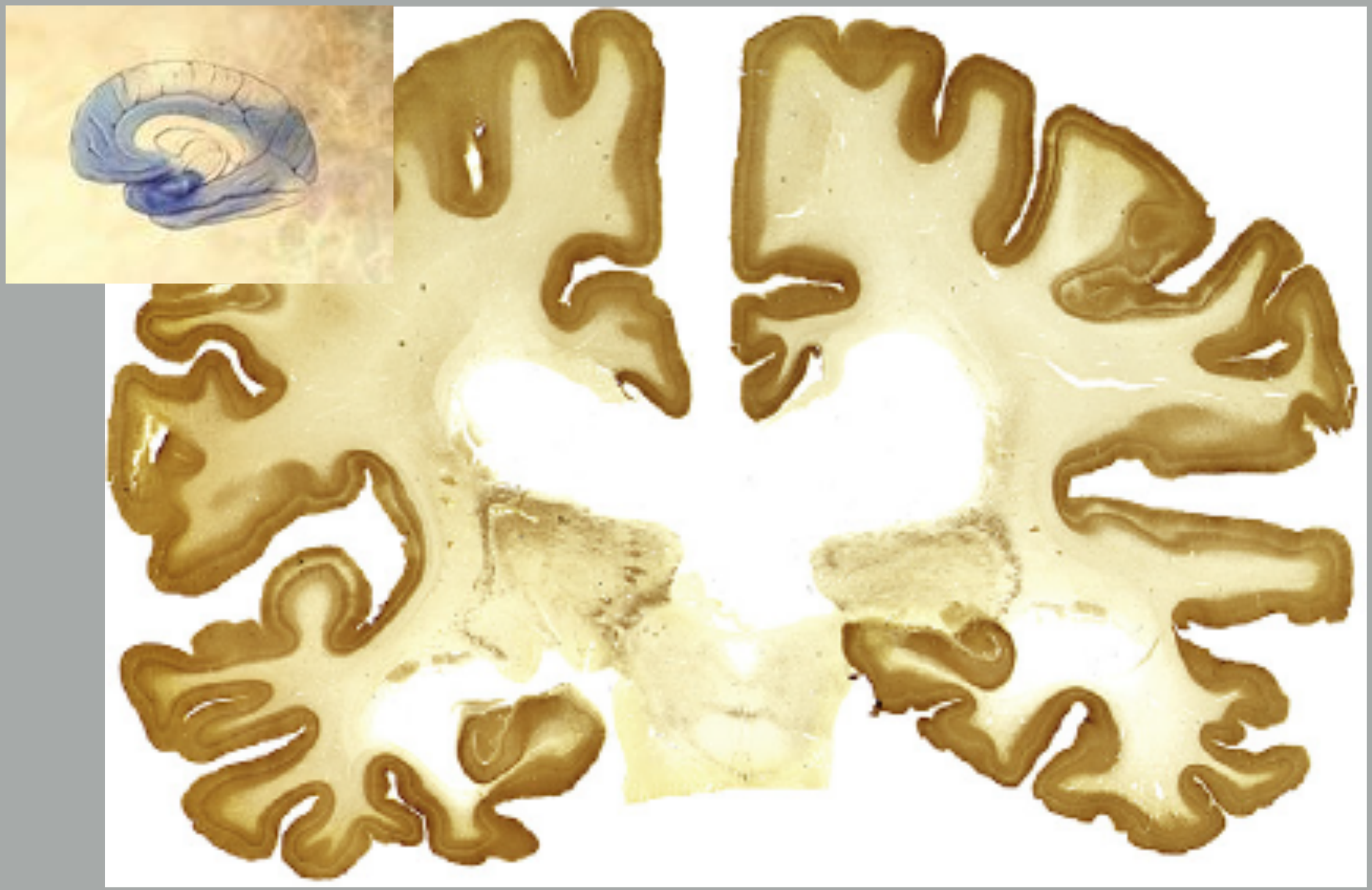

Braak & Del Tredici (2012). *Alz & Dem.*

Cognitive Abilities Affected by AD

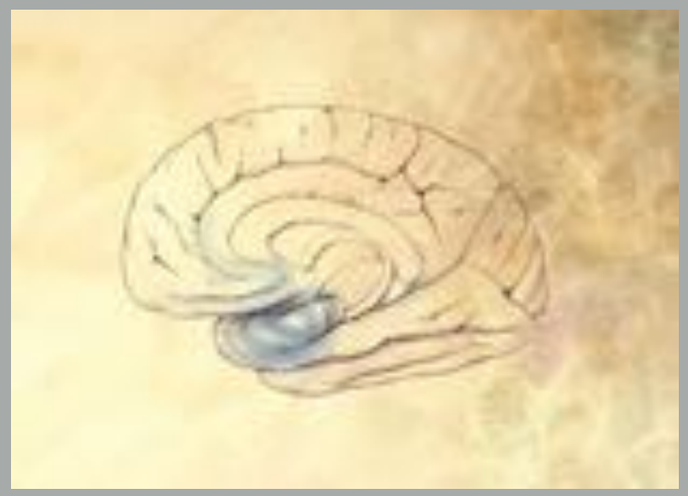

Learning and Memory

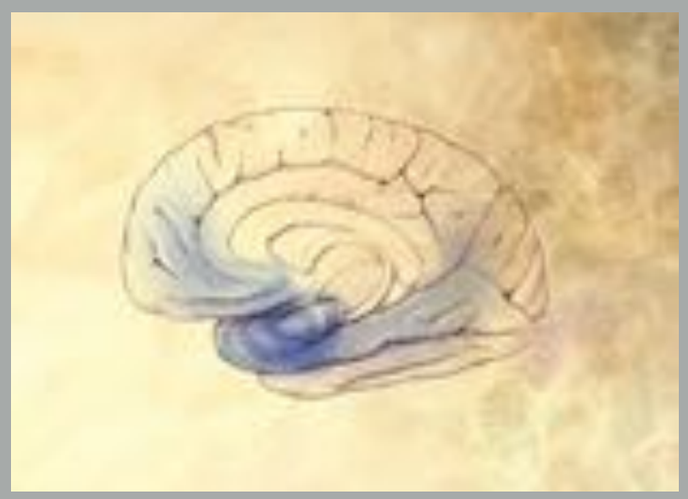

Language and Semantic Memory

Executive Functions / Attention

Visuospatial / Constructional Ability

Morphological Changes

Amnestic MCI group had significantly smaller hippocampal volumes and cortical thinning

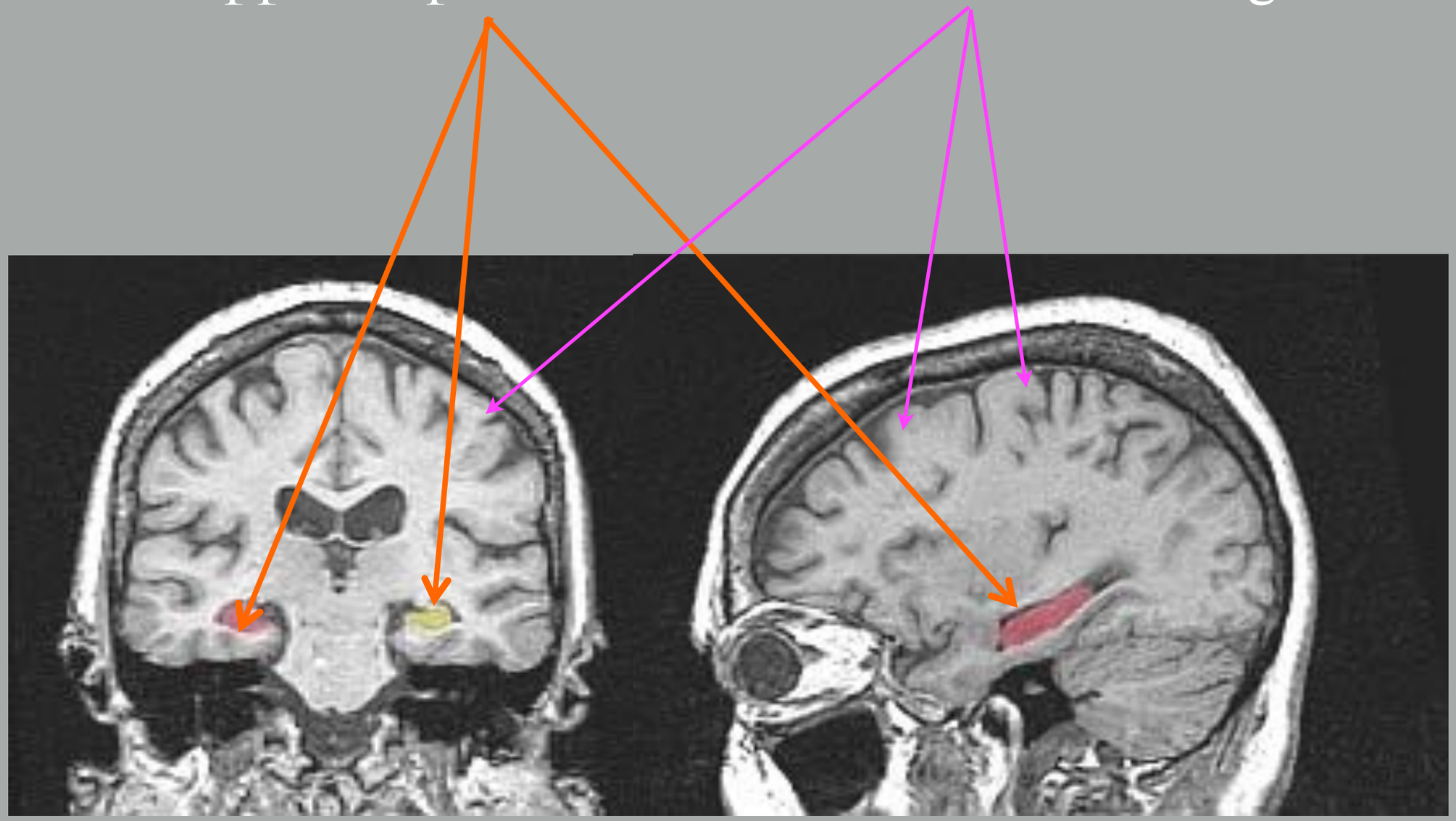

Jak et al. (2009). J Int Neuropsychol Soc.

Alzheimer's

NeuroImage 45 (2009) 10–16

Contents lists available at ScienceDirect

NeuroImage

journal homepage: www.elsevier.com/locate/ynimg

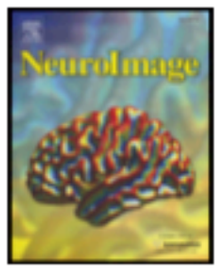

Decreased white matter integrity in late-myelinating fiber pathways in Alzheimer's disease supports retrogenesis

N.H. Stricker [a], B.C. Schweinsburg [b,c], L. Delano-Wood [d,j], C.E. Wierenga [d,j], K.J. Bangen [e], K.Y. Haaland [a,f,g], L.R. Frank [h,j], D.P. Salmon [i], M.W. Bondi [d,j,*]

[a] New Mexico VA Healthcare System, USA
[b] VA Connecticut Healthcare System, USA
[c] Yale University, USA
[d] Department of Psychiatry, University of California San Diego, School of Medicine, USA
[e] San Diego State University/University of California San Diego Joint Doctoral Program in Clinical Psychology, USA
[f] Department of Psychiatry, University of New Mexico, USA
[g] Department of Neurology, University of New Mexico, USA
[h] Department of Radiology, University of California San Diego, USA
[i] Department of Neurosciences, University of California San Diego, School of Medicine, USA
[j] VA San Diego Healthcare System, USA

Alzheimer’s

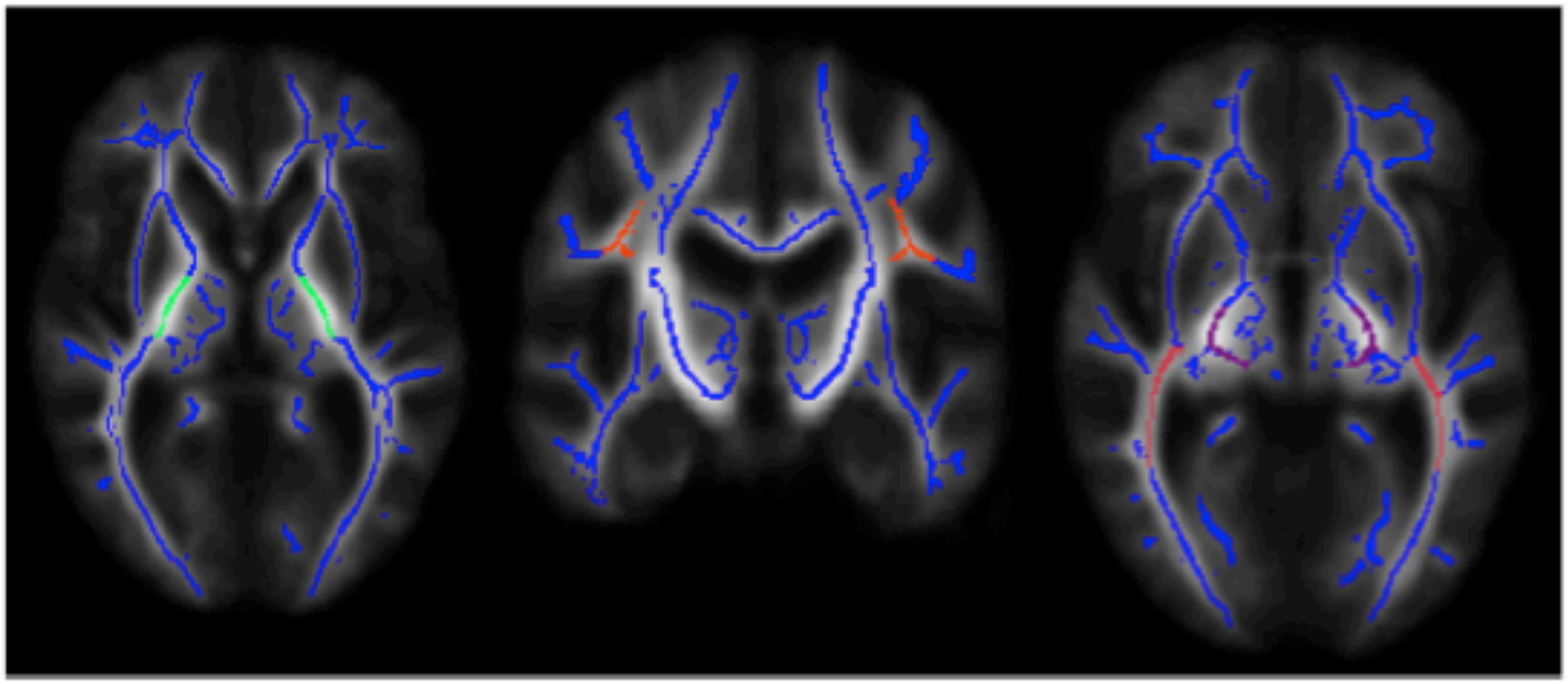

Fig. 1. Regions of interest: posterior limb of the internal capsule (in green), superior longitudinal fasciculus (in orange), cerebral peduncles (in purple), and inferior longitudinal fasciculus (in pink) overlaid on mean FA skeleton (in blue). The left hemisphere of the brain corresponds to the right side of the image.

Alzheimer's

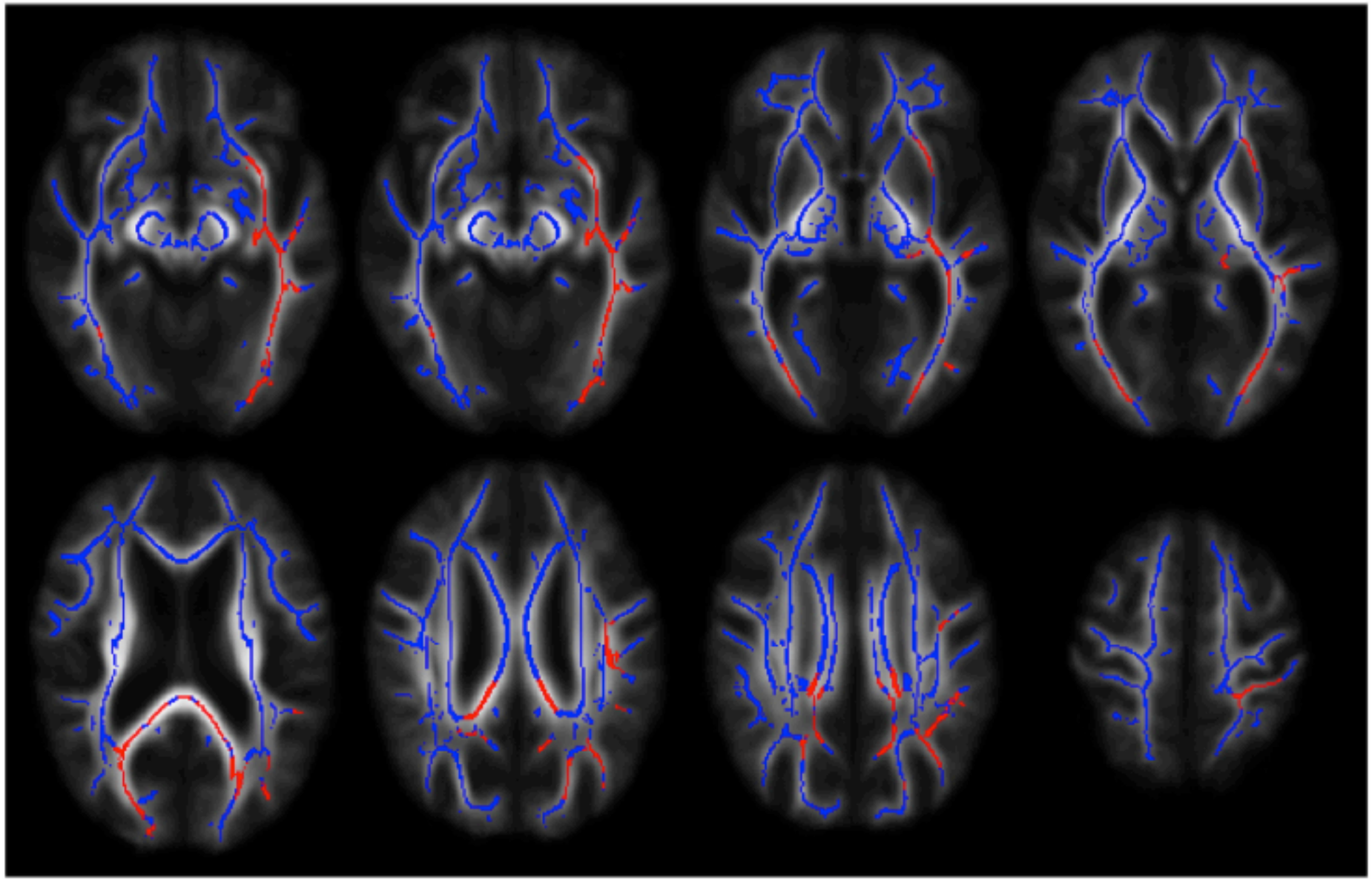

Fig. 2. Voxelwise group differences in the uncinate fasciculus, inferior longitudinal fasciculus, fornix, splenium, cingulum, forceps major and superior longitudinal fasciculus (in red) overlaid on mean FA skeleton (in blue). In all instances, AD patients demonstrated significantly lower fractional anisotropy values in the aforementioned regions. The left hemisphere of the brain corresponds to the right side of the image.

Alzheimer’s

Table 3
Average fractional anisotropy values for Alzheimer's disease (AD) patients and healthy normal control (NC) participants for each region of interest[a]

	NC $n=14$	AD $n=16$	p
Early-myelinating	.644 (.023)	.638 (.031)	.58
CP	.620 (.026)	.617 (.029)	.75
ICp	.667 (.028)	.659 (.039)	.52
Late-myelinating[b]	.435 (.027)	.414 (.028)	.04
SLF	.403 (.027)	.394 (.030)	.40
ILF[b]	.467 (.036)	.434 (.037)	.02

Note. CP=cerebral peduncles, ICp=posterior limb of the internal capsule, SLF=superior longitudinal fasciculus, ILF=inferior longitudinal fasciculus.

[a] Mean (SD).

[b] $p<.05$.

The Locus Ceruleus in AD

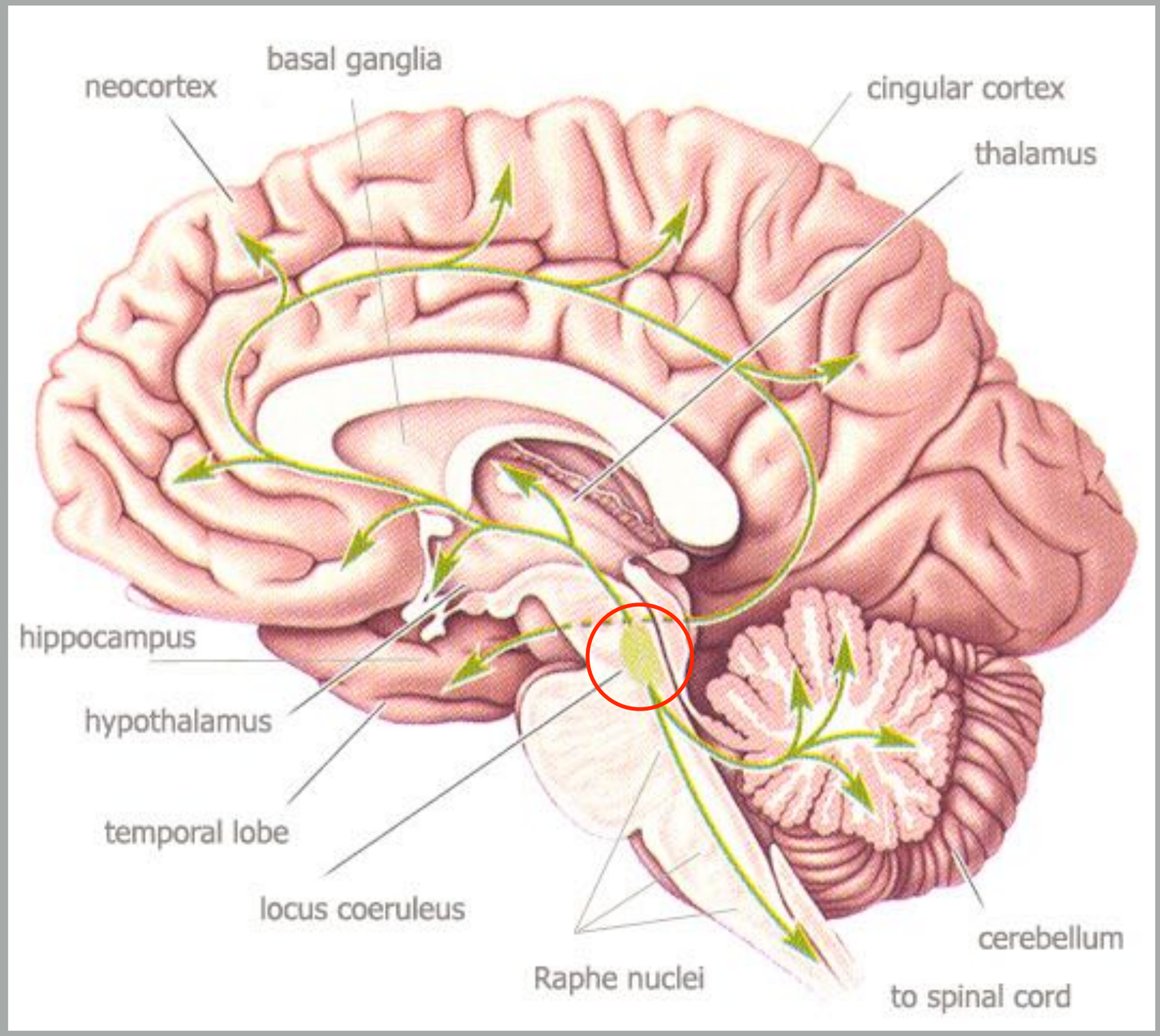

Efferent projections of the LC

Adaptive Gain Model
Locus Coeruleus

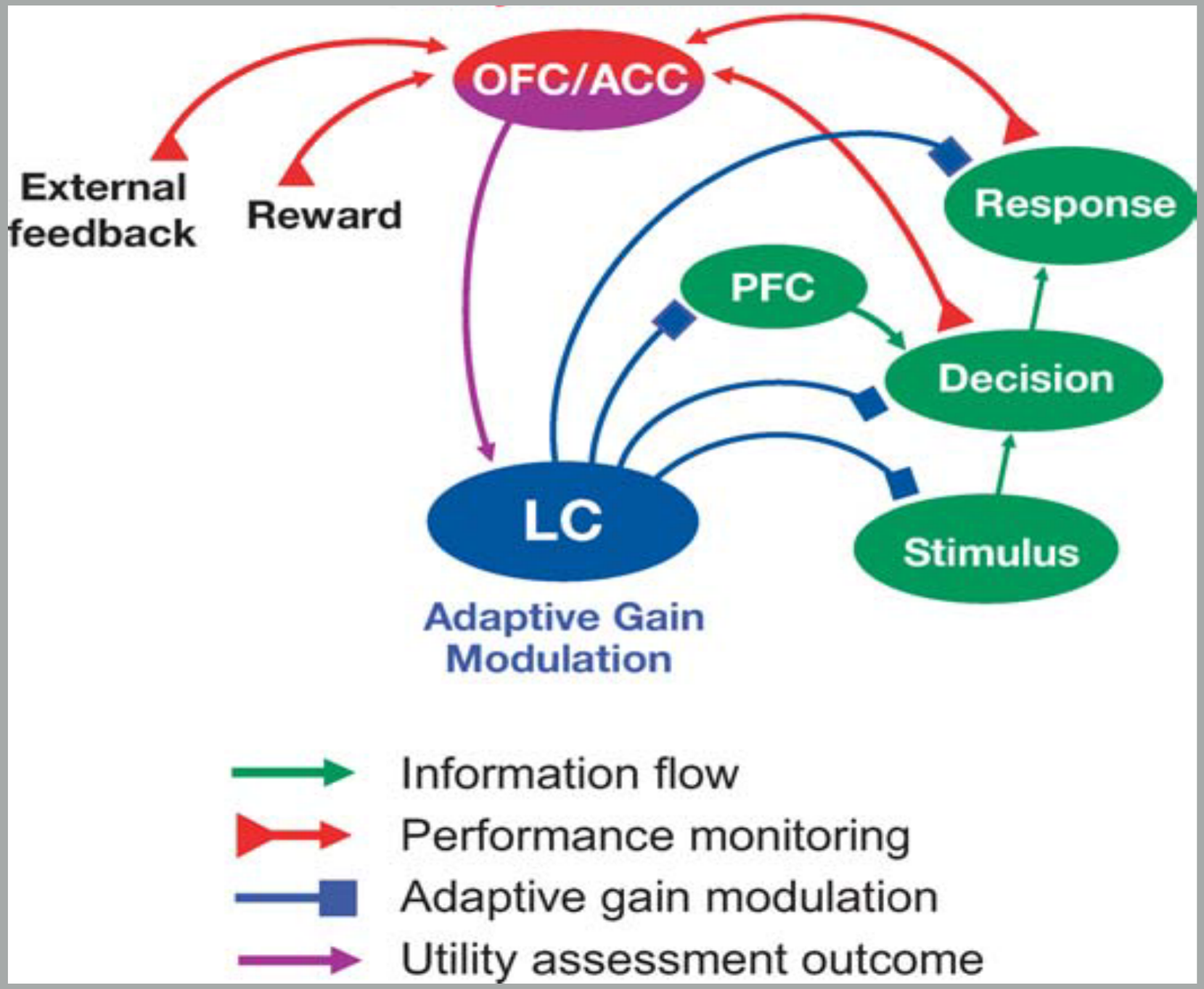

Functional brain networks

Functional networks important in AD

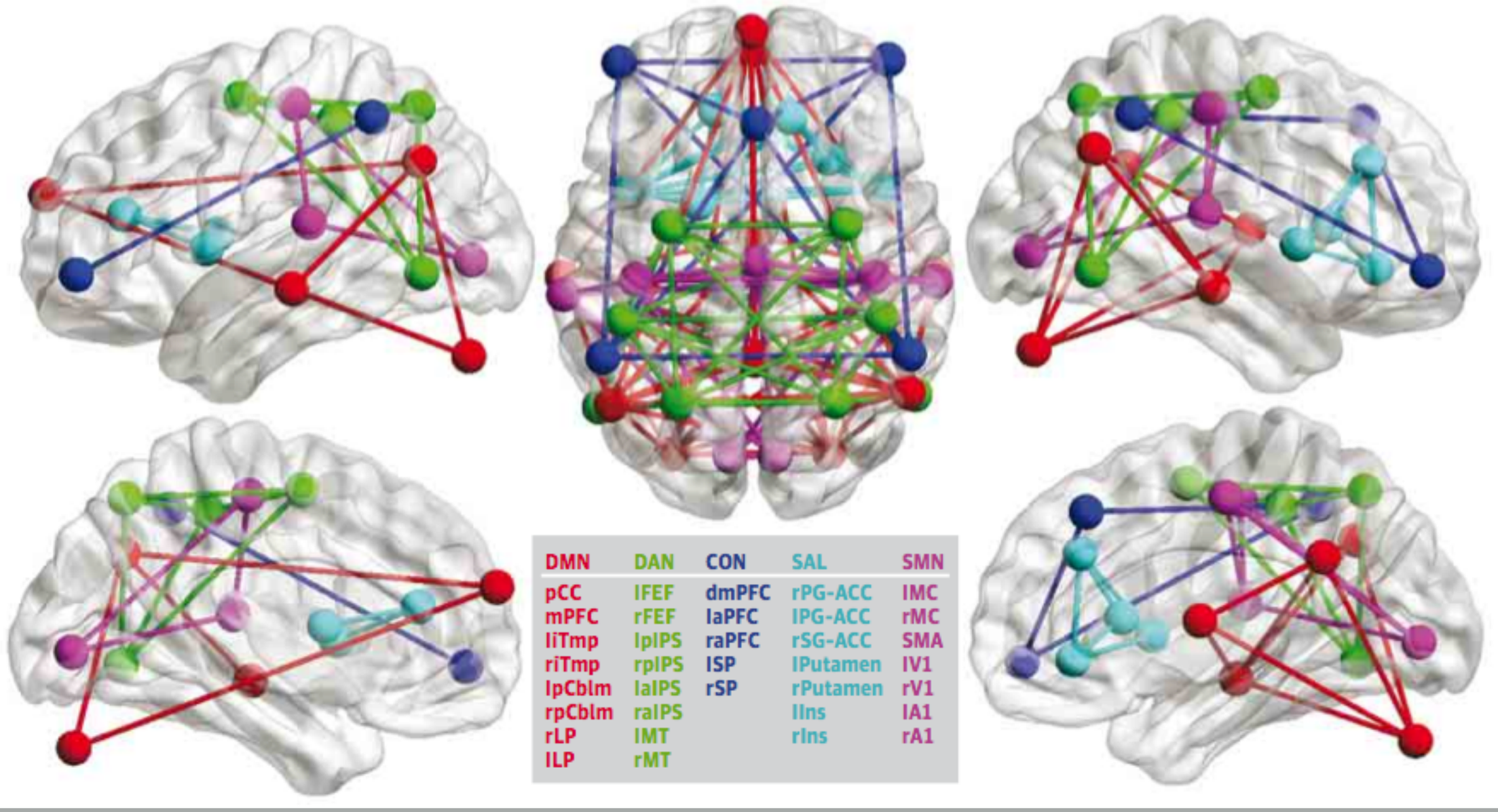

DMN	DAN	CON	SAL	SMN
pCC	lFEF	dmPFC	rPG-ACC	lMC
mPFC	rFEF	laPFC	lPG-ACC	rMC
liTmp	lpIPS	raPFC	rSG-ACC	SMA
riTmp	rpIPS	lSP	lPutamen	lV1
lpCblm	laIPS	rSP	rPutamen	rV1
rpCblm	raIPS		lIns	lA1
rLP	lMT		rIns	rA1
lLP	rMT			

CON: executive control network
DAN: dorsal attention network
DMN: default mode network

SAL: salience network
SMN: sensorimotor network

Thomas, et. al. JAMA Neurol. 2014;71(9):1111-1122

Locus Coeruleus in Alzheimer's Disease

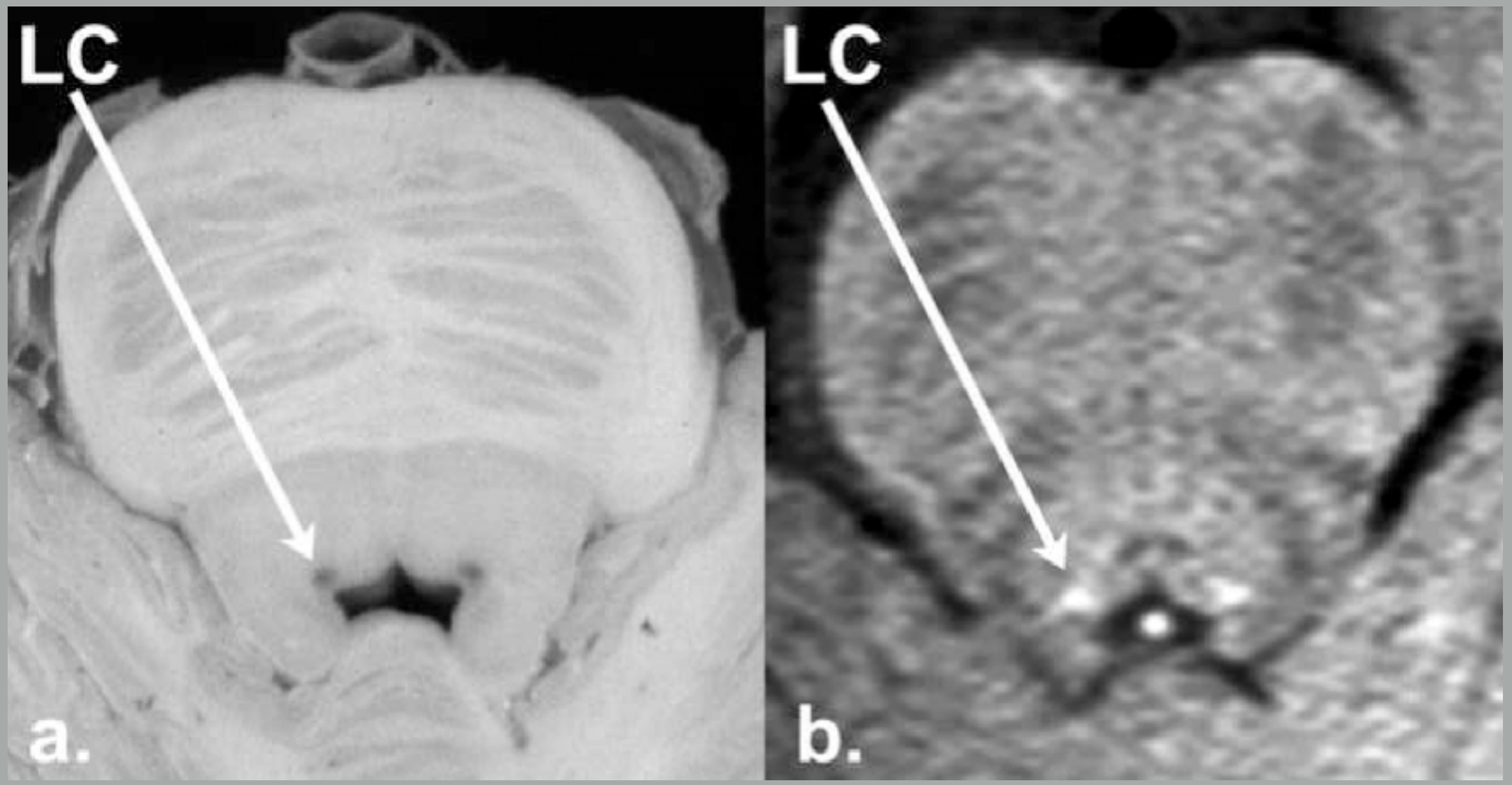

Keren et al. (2009). *NeuroImage.*

Locus Ceruleus Tractography

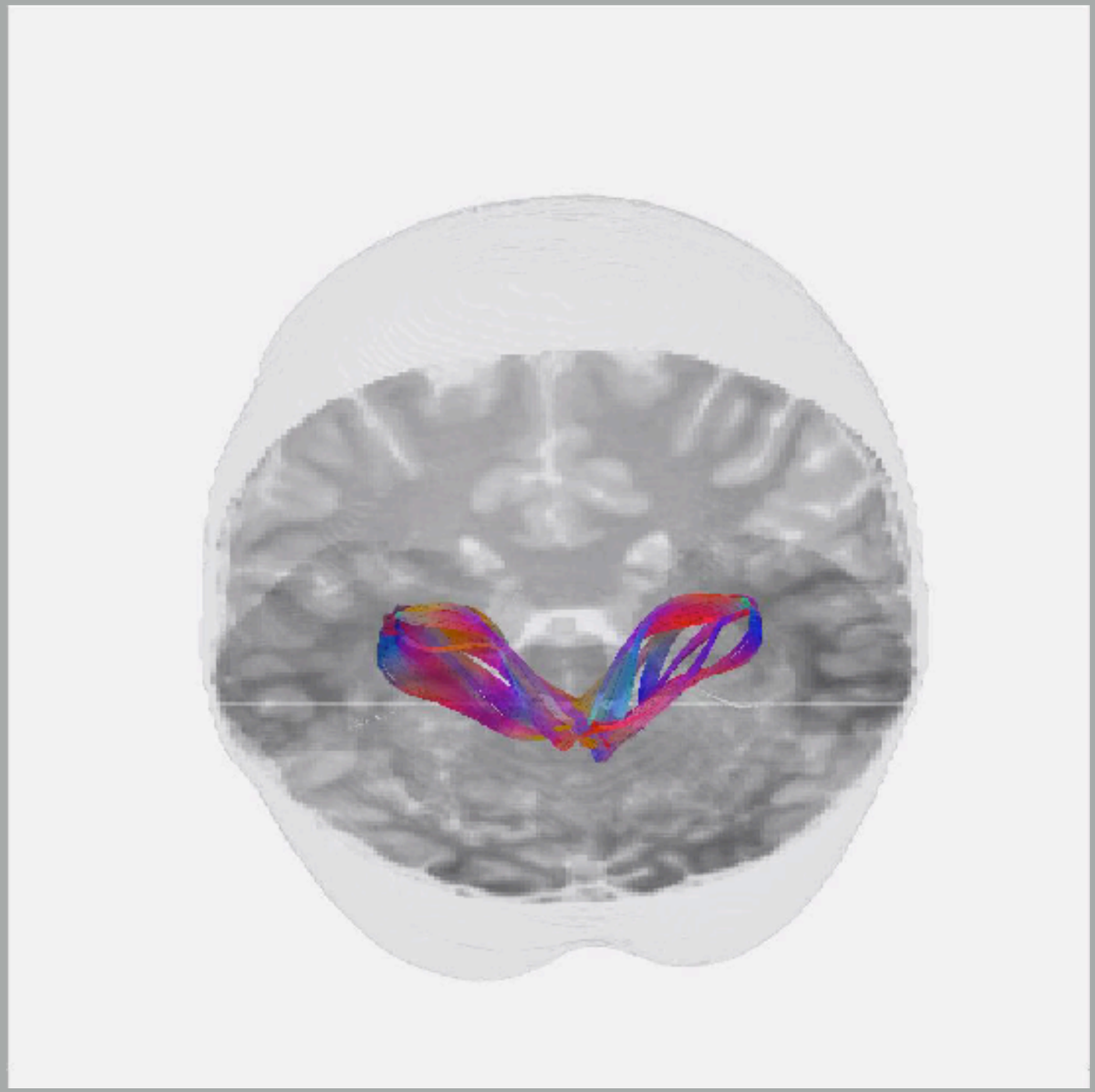

Temporal lobe projections

data from Dr Scott Sorg and Dr Mark Bondi

Locus Ceruleus Tractography

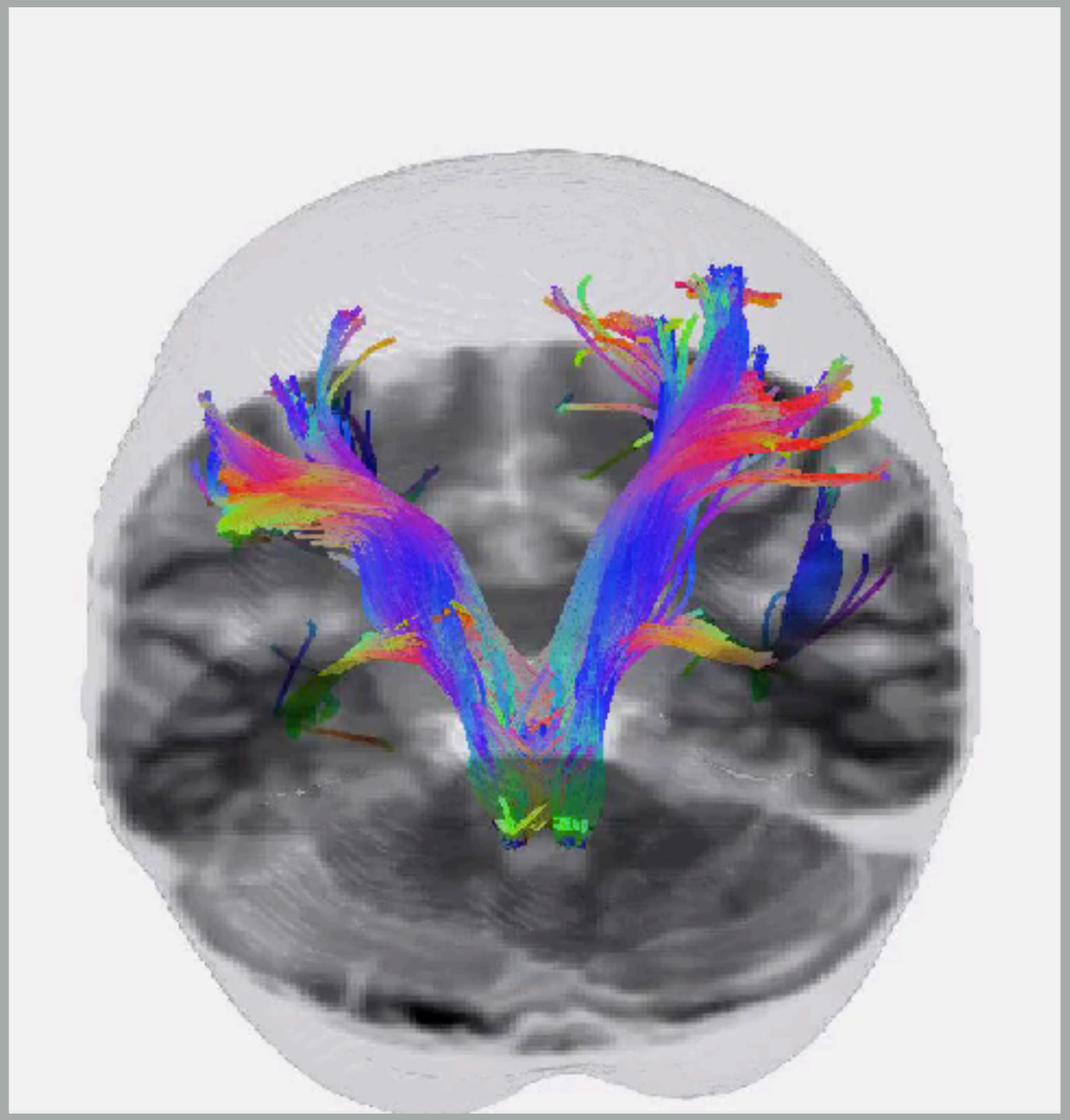

Cortical projections

data from Dr Scott Sorg and Dr Mark Bondi

GO-ESP Tractography and EMI in Locus Coeruleus

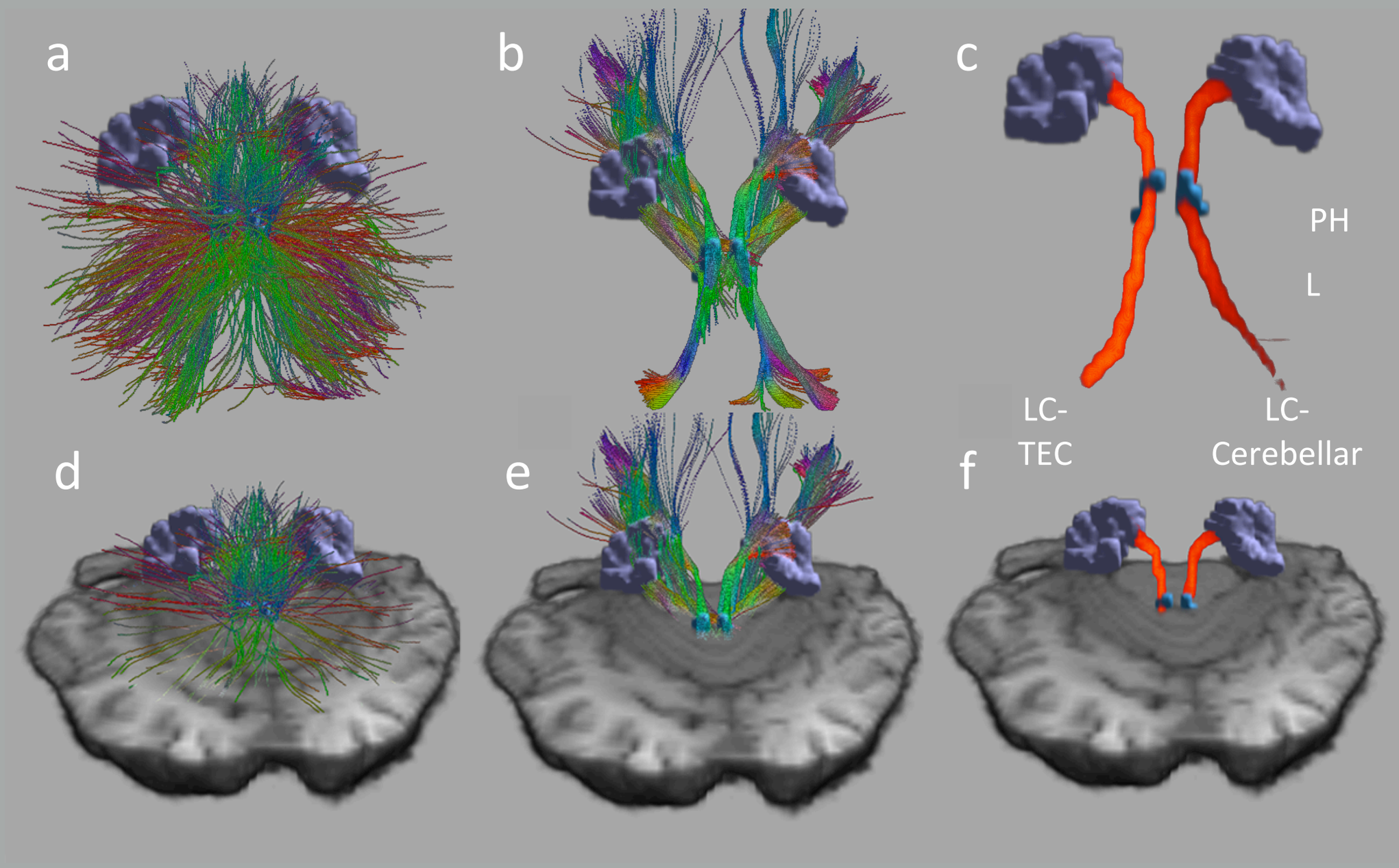

(a,d) Seed in LC, no target regions
(b,e) tracking restricted to LC and transentorhinal cortex (TEC)
(c,f) Highest probability pathway in (b,e)

Application: Alzheimer's Disease
LC tractography

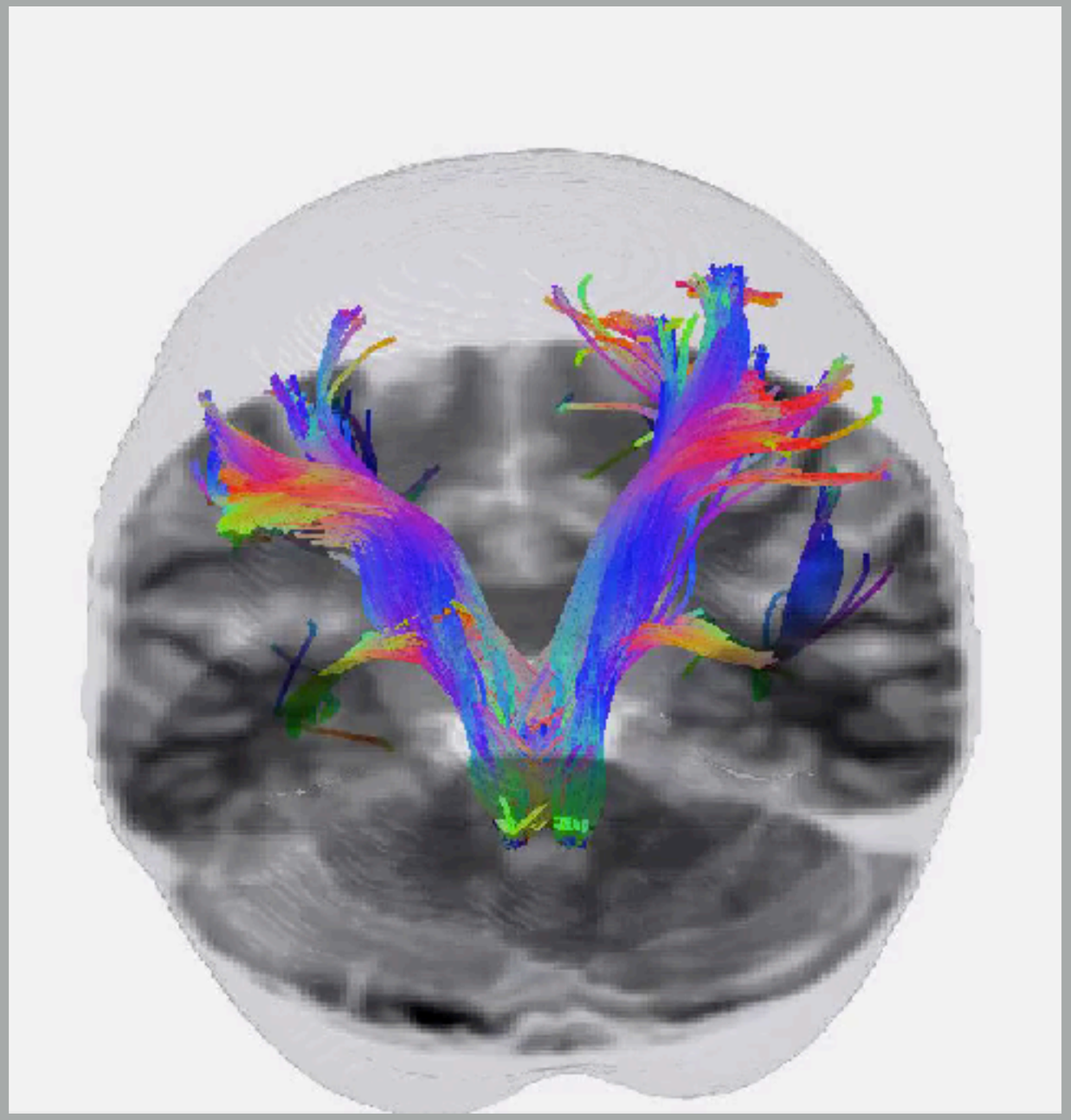

data from Dr Scott Sorg and Dr Mark Bondi

LC tractography

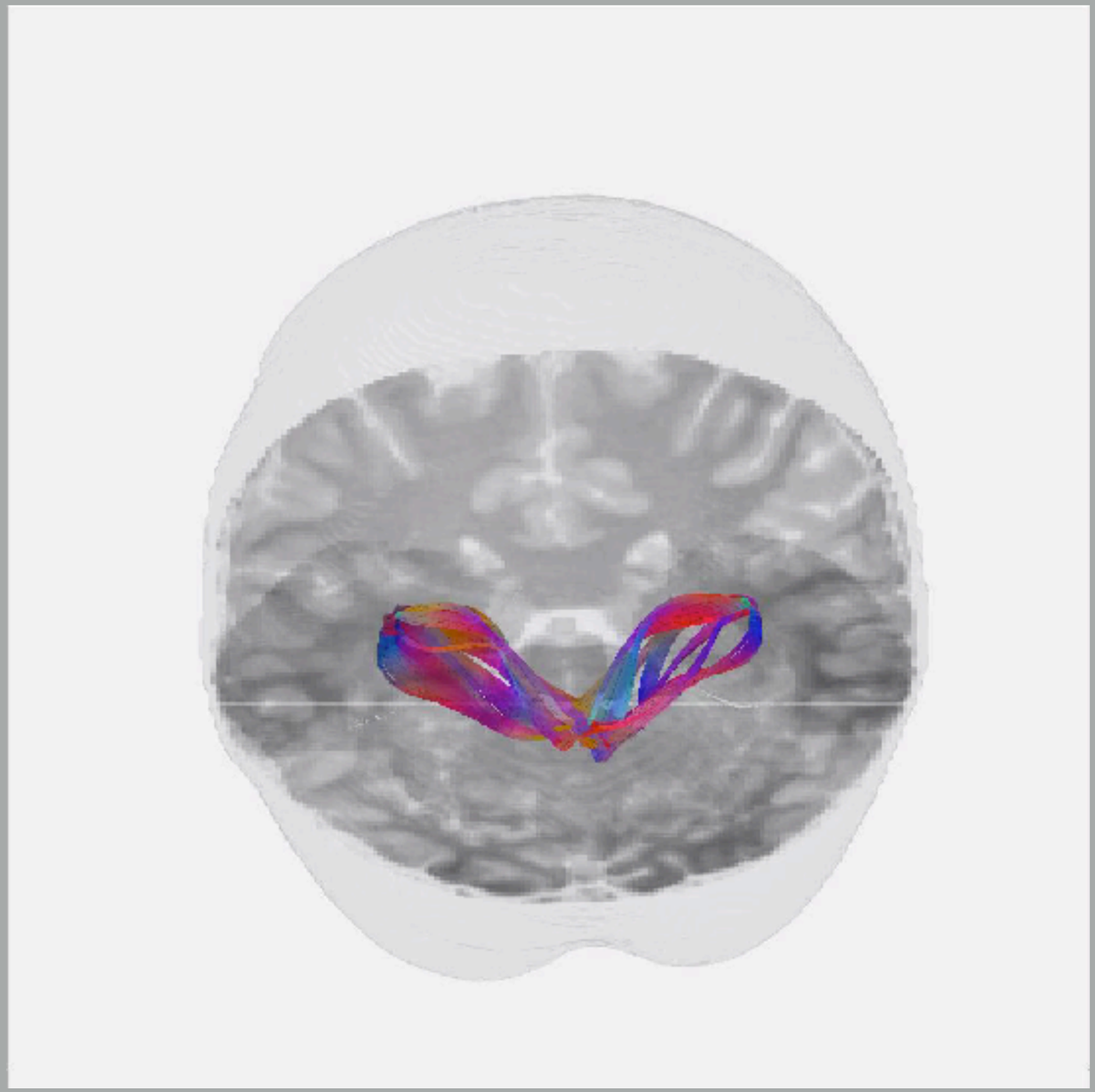

data from Dr Scott Sorg and Dr Mark Bondi